HMGCR Pathway Mediates Cerebral-Vascular Stability and Angiogenesis in Developing Zebrafish

Shahram Eisa-Beygi

Thesis submitted to the
Faculty of Graduate and Postdoctoral Studies
in partial fulfillment of the requirements for the degree of
Doctor of Philosophy in Biology

Ottawa-Carleton Institute of Biology
Faculty of Science
University of Ottawa

"Look at the Perfect One at the Circle's Center:
He Spins and whirls like a Golden Compass,
Beyond all that is rational,
To show this dear world that Everything,
Everything in Existence Does point to God. "

---- Hafez of Persia

This PhD dissertation is humbly dedicated to the loving memory of my grandparents.

Acknowledgements

I would like to extend my gratitude to Dr. Thomas W. Moon and Dr. Marc Ekker, two brilliant and accomplished scientists, for giving me the unique opportunity to study under their guidance and for their constant support and inexorable patience. They both have exerted a profound contribution to my scientific and personal growth and have compelled me to pursue further studies in life-sciences. I would also like to thank my committee members, Drs Carole Yauk, Marie-Andrée Akimenko, and Michael Jonz for their continuous critiques and suggestions, which have indubitably helped me refine this project. The personal friendship and kindness of Andrey Massarsky is appreciated beyond words. This project could not have progressed to this extent if it were not for the constant technical assistance and friendship of Vishal Saxena, Sandra Noble, Bill Fletcher, Gary Hatch, Jamie Holden, Khaled Eid, Rafael Godoy and Raymond W.M. Kwong. I would also like to extend my heartfelt gratitude and love to my parents and my siblings for enriching my life and giving me a sense of purpose and fulfillment. Last but not least, I would like to express my sincere appreciation of my dear friends, Ali Al-Rewashdy and Saud Ayed, with whom I enjoyed our intense but friendly philosophical and existential discourses during our frequent tea breaks. I would also like to acknowledge that this work was supported by grants primarily from NSERC to TM and ME, as well as a grant from Pfizer Pharmaceuticals to TM.

Abstract

Intracerebral hemorrhage (ICH) is a severe form of stroke, with a high mortality rate and often resulting in irreversible neurological deterioration. Although animal studies have provided insight into the etiology of the disease, many of the causative genes and mechanisms implicated in cerebral-vascular malformations are unknown. Treatment options remain ineffective. With the present models, the pathophysiological consequences of ICH can only be assessed *in situ* and after histological analysis. Furthermore, common deficiencies of the current models include the heterogeneity, low expression and low reproducibility of the desired phenotype. Hence, there is a requirement for novel approaches to model ICH pathogenesis. Zebrafish (*Danio rerio*) has gained recognition as a vertebrate model for stroke research.

Through a combination of pharmacological blockers, metabolite rescue, genetic approaches, and confocal imaging analysis, I demonstrate a requirement for the 3-hydroxy-3-methylglutaryl-CoA reductase (HMGCR) pathway in regulating developmental cerebral-vascular stabilization. A transient loss in HMGCR function induces ICH, characterised by progressive dilation of blood vessels, vascular permeability and vessel rupture. These effects are likely due to reduced prenylation of Rho GTPases, evidenced by morpholino-mediated blocking of the prenylation pathway and *in vivo* assessment of endothelial-specific localization of cdc42, a Rho GTPase family protein. These results are in conformity with recent clinical and experimental evidence.

I have further shown that this model consistently replicates common pathoghysiological processes associated with ICH. The hemorrhages are associated with the disruption of the blood-brain barrier, vessel disintegration, hematoma expansion and edema into the adjacent brain regions. Also, enhanced apoptosis, activation of inflammatory mediators in the periphery of the hematoma, enriched heme oxygenase 1 (HO-1) expression and localised thrombosis were observed in these embryos. I show that the patterning and distribution of catecholaminergic neurons, response to sensory stimulus and swimming speed were impaired as a consequence of ICH.

These results suggest that HMGCR contributes to cerebral-vascular stabilisation through Rho GTPase mediated-signalling and that zebrafish can serve as a powerful paradigm for the systemic analysis of the etiological and pathophysiological underpinnings of ICH and can help establish the basis for future studies into screening for putative therapeutics and elucidating mechanisms aiding functional recovery.

Résumé

L'hémorragie intracérébrale (HIC) est une forme grave d'accident cérébro-vasculaire associé à un taux élevé de mortalité et qui cause une détérioration neurologique sévère. Quoique des études sur des modèles animaux nous ont permis de mieux comprendre l'étiologie de cette maladie, plusieurs gènes responsables et les mécanismes sous-jacents aux malformations cérébro-vasculaires sont encore inconnus. Les options thérapeutiques demeurent inefficaces. En utilisant les modèles courants, les conséquences patho-physiologiques des HIC peuvent seulement être examinées *in situ* à l'aide d'analyses histologiques. De plus, un désavantage des modèles courants est le faible taux d'expression de de reproductibilité des phénotypes. Il nous faut donc de nouveaux modèles pour la pathogénèse des HIC. Le poisson-zèbre, *Danio rerio*, a acquis une renommée comme modèle pour l'étude des accidents cérébro-vasculaires.

En utilisant une combinaison d'agents pharmacologiques, de manipulations métaboliques, d'approches génétiques, et d'imagerie confocale, j'ai montré le rôle essentiel joué par la voie métabolique impliquant la 3-hydroxy-3-méthylglutaryl-CoA réductase (HMGCR) dans le contrôle et la stabilisation du système cérébro-vasculaire. Une perte transitoire de la fonction de HMGC induit une HIC caractérisée par la dilatation progressive des vaisseaux sanguins, une perméabilité vasculaire et la rupture des vaisseaux. Ces effets sont attribuables à une prénylation réduite des Rho GTPases, tel que démontré par l'effet de morpholinos dur la voie de prénylation et un examen *in vivo* de la localisation spécifique de cdc42, un membre de la famille des Rho GTPases. Ces résultats sont en accord avec de récentes données cliniques et expérimentales.

J'ai de plus montré que ce modèle reflète fidèlement les processus patho-physiologiques les plus couramment associés à l'HIC. Les hémorragies coïncident avec un dérangement de la barrière hémato-encéphalique, une désintégration des vaisseaux, une expansion des hématomes et de l'oedème dans les régions avoisinantes du cerveau. De plus, une apoptose accrue, l'activation des médiateurs inflammatoires dans la périphérie de l'hématome, une hausse localisée de l'hème oxygénase et une thrombose localisée sont

observées chez ces embryons. J'ai montré que le profil des neurones catécholaminergiques, la réponse à une stimulation tactile et la vitesse natatoire étaient affectées suite à l'HIC.

Ces résultats suggèrent que l'HMGCR contribue à la stabilisation cérébro-vasculaire via la voie de signalisation des Rho GTPases et que le poisson-zèbre constitue un paradigme pertinent pour l'analyse systématique des causes étiologiques et patho-physiologiques de l'HIC . Ce modèle peut contribuer à établir une base pour des études ultérieures visant le criblage de thérapies potentielles ainsi que la découverte de mécanismes facilitant la guérison.

TABLE OF CONTENTS

LIST OF FIGURES

LIST OF ABBREVIATIONS

AMPK: AMP-activated protein kinase
ATV: Atorvastatin
bp: Base pairs
CNS: Central nervous system
CCM: Cerebral cavernous malformation
CVT: Cerivastatin
cDNA: Complementary DNA
dpf: days post fertilisation
DAB: Diaminobenzidine
DA: Dopaminergic
DLAV: Dorsal longitudinal anastomotic vessel
ER: Endoplasmic reticulu
EGFP: Enhanced green fluorescent protein
GGTase I: Geranylgeranyltransferase type 1
GFP: Green fluorescent protein
hpf: hours post fertilisation
HRP: Horseradish peroxidase
HMGCR: 3-hydroxy-3-methylglutaryl-CoA reductase
ICH: Intracerebral hemorrhage
ISV: Intersegmental vessel
LDL: low density lipoprotein
MO: Morpholino oligonucleotides
NO: Nitric oxide
MCeV: Middle cerebral vein
OD: o-Dianisidine
PFA: Paraformaldehyde
PBST: 1X Phosphate Buffered Saline Tween-20
PPrA: Primitive prosencephalic artery
PMBC: Primordial midbrain channel
PrA: Prosencephalic artery
PTU: 1-pheny1-2-thiourea
pak: p21-activated kinase
SCAP: SREBP-cleavage activating protein
SREBP: sterol-regulatory element binding protein
SPARCL: Stroke Prevention by Aggressive Reduction in Cholesterol Levels
ROS: Reactive oxygen species
RT-PCR: Reverse transcriptase polymerase chain reaction
TH: Tyrosine hydroxylase

TH: Tyrosine hydroxylase
VEGF: Vascular endothelial growth factor
VE-cadherin: Vascular endothelial cadherin

Chapter 1

General Introduction

1. Introduction

1.1. Rationale for the study

The 3-hydroxy-3-methylglutaryl-CoA reductase (HMGCR) is a metabolic enzyme, regulating the rate-limiting step in the biosynthesis of cholesterol and isoprenoids. Through an initial small-scale toxicity assay of various pharmaceuticals, I have isolated two structurally distinct pharmacological inhibitors of HMGCR (statins) that induce an intracerebral hemorrhage (ICH) phenotype in zebrafish embryos and larvae. These observations emerged in parallel with recent experimental and clinical studies suggesting a link between inhibition of HMGCR function and ICH pathogenesis. These findings compelled me to elucidate the precise mechanisms and signalling pathways under the control of HMGCR that mediate cerebral-vascular stabilisation.

1.2. The 3-hydroxy-3-methylglutaryl-CoA reductase (HMGCR) pathway

The enzyme, 3-hydroxy-3-methylglutaryl coenzyme A reductase (HMGCR; E.C. 1.1.1.88), is an endoplasmic reticulum (ER)-bound, polytopic glycoprotein with eight trans-membrane helices located at the N-terminus, and a catalytic domain at the C-terminal, which projects into the cytosol (Gil et al., 1985). Although HMGCR expression is highly enriched in liver cells (hepatocytes) (Hwa et al., 1992), it is also expressed in extra-hepatic tissues, including the heart (Laufs et al., 2002), and the brain (Thelen et al., 2005; Michalak and Wender, 1996).

The trans-membrane domain of HMGCR anchors the protein to the ER and the trans-membrane domain contains the residues required for the binding of regulatory proteins to the enzyme (DeBose-Boyd et al., 2008). The soluble C-terminal domain

catalyzes the rate-limiting step in the *de novo* synthesis of mevalonate, the precursor for the biosynthesis of cholesterol and bile acids, as well as several non-sterol isoprenoid metabolites, including Farnesyl-pyrophosphate (FPP) and Geranyl-geranyl pyrophosphate (GGPP) (**Fig. 1.1**) (Goldstein and Brown, 1990). This rate-limiting step involves the conversion of acetyl-CoA-derived HMGCoA to mevalonate through a reductive de-acetylation reaction, in the presence of two molecules of NADPH (Goldstein and Brown, 1990). This metabolic reaction is summarised below:

HMG-CoA + 2NADPH + $2H^+$ → Mevalonate + $NADP^+$ + S-CoA

1.2.1 Regulation of HMGCR activity

A complex feedback mechanism, involving both steroidal and non-steroidal mediated pathways, is involved in the regulation of HMGCR activity (Brown and Goldstein, 1997; Nakanishi et al., 1988; Omkumar et al., 1994; DeBose-Boyd, 2008). The enzyme is subjected to sterol-induced ubiquitination and degradation through specific residues in the trans-membrane domain, which anchors the protein to the ER and contains the necessary residues required for the binding of regulatory proteins to the enzyme (Gil et al., 1985; Skalnik et al., 1988). This is further evidenced by that fact that several point-mutations in the trans-membrane domain of HMGCR impair sterol-induced degradation (Lee et al., 2006).

The transcription of the HMGCR gene is controlled through the sterol-regulatory element binding protein (SREBP), a family of membrane-bound transcription factors (Brown and Goldstein, 1999). Under diminished cellular cholesterol levels, SREBP

Figure 1.1: The HMGCR-dependent mevalonate pathway. HMGCR-mediated lipid biosynthesis, showing the rate-limiting step of mevalonate generation (HMGCR), along with the synthesis of farnesyl-pyrophosphate (FPP) and geranylgeranyl-pyrophosphate (GGPP), all of which are derivatives of mevalonate**.**

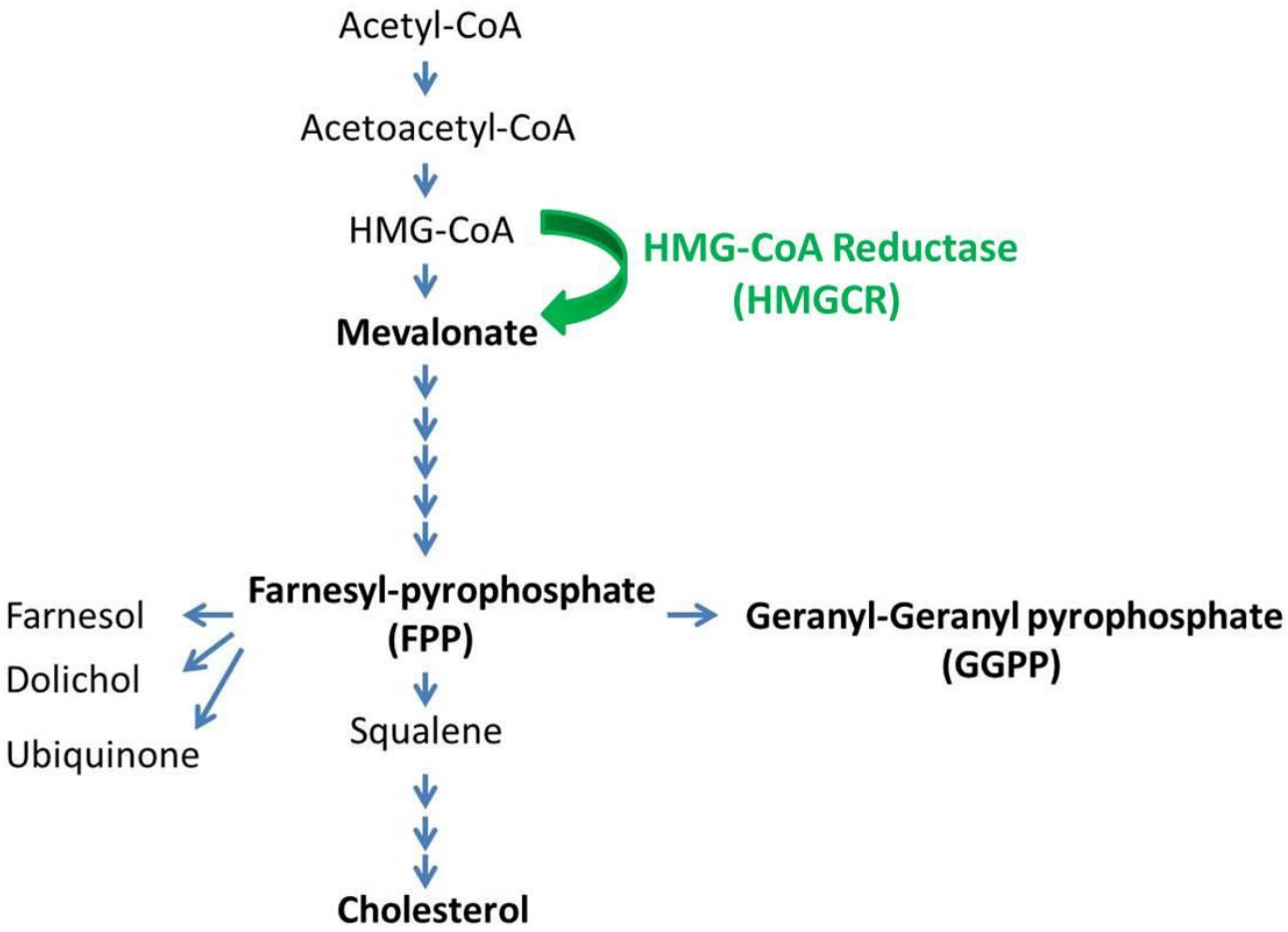
Acetyl-CoA
Acetoacetyl-CoA
HMG-CoA
HMG-CoA Reductase
(HMGCR)
Mevalonate
Farnesyl-pyrophosphate
(FPP)
Farnesol
Dolichol
Ubiquinone
Geranyl-Geranyl pyrophosphate
(GGPP)
Squalene
Cholesterol

interacts with the SREBP-cleavage activating protein (SCAP), which facilitates sequential cleavage of SREBP by S1P, a serine protease belonging to the subtilisin/kexin family, and S2P, a zinc metalloprotease. After this sequential processing in the Golgi apparatus, the water-soluble and transcriptionally active N-terminal fragment of SREBP, of approximately 480 amino acids, is translocated to the nucleus (Ye et al., 2000).

Upon translocation to the nucleus, this SREBP fragment binds to the 'Sterol regulatory element', which flanks the low density lipoprotein (LDL) receptor gene and other genes involved in the HMGCR pathway. This enhances the uptake and synthesis of extracellular cholesterol by activating the transcription of target genes encoding HMGCR and other cholesterol biosynthetic enzymes, including the LDL-receptor gene (Brown and Goldstein, 1999). As such, pharmacological inhibition of cholesterol biosynthesis triggers SREBP-mediated up-regulation of HMGCR gene expression, evidenced by both *in vitro* and *in vivo* studies (Brown and Goldstein, 1999; Krycer et al., 2009; Mammen et al., 2011).

Early kinetic experiments performed on microsomes isolated from the rat liver showed that HMGCR kinetics could also be regulated at the level of phosphorylation, where ATP would serve as a phosphate donor (Gibson, 1985). It was shown that the catalytic activity of HMGCR could be inhibited, in a dose-dependent fashion, when microsomes were incubated in a solution of ATP, Mg^{2+}, and a cytosolic fraction isolated from rat liver (Clarke and Hardie, 1990). In subsequent experiments, it was demonstrated that HMGCR is phosphorylated at Ser-871, near the C-terminus of the protein, by AMP-activated protein kinase (AMPK) (Hardie, 1992). It was further reported that this phosphorylation event reduced HMGCR activities by approximately 80% (Hardie, 1992).

Over-expression of a cDNA construct encoding a mutant form of hamster HMGCR, where Alanine is substituted for Serine at residue 871, further verified that phosphorylation of the Serine-871 residue is a critical regulator of HMGCR enzyme activity and that this process is mediated by AMPK (Sato et al., 1993). Furthermore, the Serine→Alanine substitution, through site-directed mutagenesis, failed to prevent the post-transcriptional regulation of HMGCR activity by mevalonate, cholesterol or LDL (Sato et al., 1993). It was further established that incubation of rat hepatocytes with fructose resulted in a surge in cellular AMP levels and that this was followed by activation of the AMPK, which resulted in reduced HMGCR activities (Gillespie and Hardie, 1992). Similarly, phosphorylation of Serine-871 was shown to decrease the activity of HMGCR in humans (Clarke and Hardie, 1990). In terms of the specific mechanism, it is predicted that phosphorylation of Ser-817 reduced the activities of the enzyme by reducing its affinity for NADPH, thereby preventing the synthesis of mevalonate (Sato et al., 1993; Omkumar et al., 1994).

The HMGCR-mediated lipid biosynthesis is also regulated through ubiquitin-mediated proteoloysis of the enzyme HMGCR. This involves the attachment of ubiquitin, thus marking HMGCR for degradation and recycling. This process is catalyzed by Ufd1, an adaptor protein residing in the ER. As such, cells expressing higher levels of Ufd1 tend to exhibit reduced HMGCR activity. Hence, *de-novo* synthesis of cholesterol is significantly reduced due to the ubiquitination (Cao et al., 2007).

Recent evidence points towards alternative splicing of *HMGCR* pre-mRNA as contributing to inter-individual variations in enzyme activity in response to treatments with pharmacological inhibitors (Medina et al., 2008; Medina and Krauss, 2009). This

splicing event gives rise to a variant transcript that is shorter in length when compared with the wild-type isoform. Although it does not disrupt the open-reading-frame, this alternative splicing event generates an isoform in which exon-13 is deleted, which otherwise codes for a part of the catalytic domain of HMGCR (exons 11-20) (Medina and Krauss, 2009). In addition, it was speculated that deletion of exon-13 would reduce enzyme activity due to loss of critical residues and truncation of the L-domain, which contains part of the substrate-binding region (Medina et al., 2010).

1.2.2 HMGCR pathway and pharmacology of statins

As a result of the direct effects the endogenous levels of cholesterol, HMGCR-mediated lipid biosynthesis and its mechanism of regulation are exploited by human pharmaceuticals that selectively bind, in a reversible manner, to the active site of HMGCR and render it less active. As such, statins (both naturally-derived and synthetic statins) are known as agonists of the natural substrate, HMG-CoA, since they compete for the active site on the enzyme (Istvan and Deisenhofer, 2001). Sequence alignment of the partial catalytic sites of the HMGCR proteins indicates that the statin-binding residues (Istvan and Deisenhofer, 2001) on the C-terminus site of the enzyme are identical in both of the HMGCR paralogs identified in zebrafish, *Danio rerio* (**Fig. 1.2**) (Please refer to Chapter 2 for more information).

In addition to effectively lowering the rate at which HMGCR can produce cholesterol, statins also curtail the biosynthesis of other metabolites downstream of mevalonate, namely isoprenoid intermediates, which serve as essential lipid attachments for heterotrimeric G proteins and the Rho/Ras GTPase family of proteins (Liao, 2002).

This post-translational modification ensures that the prenylated complexes are localised to the cell membrane, which facilitates their activation and mediation of their signalling (Berzat et al., 2006).

Statins are primarily prescribed to inhibit cholesterol biosynthesis in the liver, since liver is the major organ where *de novo* cholesterol synthesis takes place. In addition, liver is where cholesterol is converted into bile salts, and where lipoproteins involved in transporting cholesterol are synthesised and exported (Lennernas and Fager, 1997). The high efficacy of statins in the treatment of hypercholesterolemia has been extensively demonstrated through the use of animal models and through clinical studies (Johnston et al., 2001; Dubuc et al., 2004; Wu et al., 2005; Versmissen et al., 2008). Statin-induced depletion of intracellular cholesterol biosynthesis stimulates the up-regulation of the HMGCR pathway, through transcription, by the SREBP-mediated feedback mechanisms noted above (Brown and Goldstein, 2004). This, in turn, increases the rate of lipoprotein uptake from the circulation through the cytoplasmic membrane of hepatocytes, by increasing the transcription of LDL-receptor gene. Once delivered to the interior of the cell by the newly synthesised LDL-receptors, the LDL molecules are then digested and the cholesterol is used for metabolic processes or storage (Goldstein et al., 1975). Therefore, statin treatment decreases both *de novo* cholesterol synthesis and serum cholesterol levels, while maintaining a steady level of cholesterol in the liver (Brown and Goldstein, 2004).

The statin family of pharmaceuticals can be classified on the basis of whether they are naturally-derived or synthetic (Weitz-Schmidt, 2002). All statins share the common HMG-CoA-like moiety (dihydroxy heptanoic acid), in an either closed (lactone)

Figure 1.2: Zebrafish possess two paralogous genes encoding functional HMGCR proteins with conserved inhibitor-binding residues. Amino acid sequence alignment of the partial catalytic (C-terminus) sites of human HMGCR and zebrafish orthologs is shown. Numbers denote amino acid positions. Identical amino acids are highlighted in grey. Amino acid residues thought to be critical for statin interaction are highlighted in green.

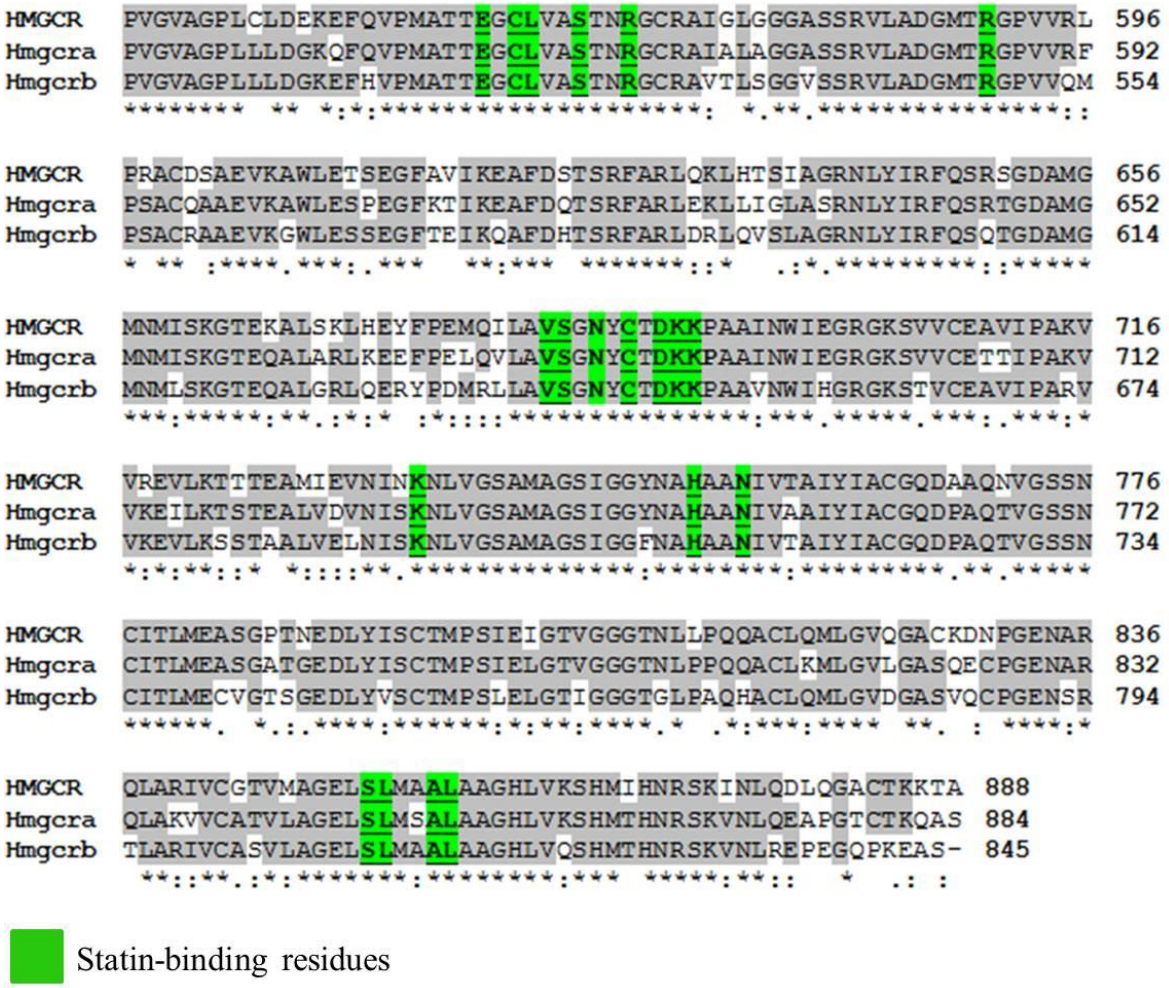
HMGCR PVGVAGPLCLDEKEFQVPMATTEGCLVASTNRGCRAIGLGGGASSRVLADGMTRGPVVRL 596
Hmgcra PVGVAGPLLLDGKQFQVPMATTEGCLVASTNRGCRAIALAGGASSRVLADGMTRGPVVRF 592
Hmgcrb PVGVAGPLLLDGKEFHVPMATTEGCLVASTNRGCRAVTLSGGVSSRVLADGMTRGPVVQM 554
HMGCR PRACDSAEVKAWLETSEGFAVIKEAFDSTSRFARLQKLHTSIAGRNLYIRFQSRSGDAMG 656
Hmgcra PSACQAAEVKAWLESPEGFKTIKEAFDQTSRFARLEKLLIGLASRNLYIRFQSRTGDAMG 652
Hmgcrb PSACRAAEVKGWLESSEGFTEIKQAFDHTSRFARLDRLQVSLAGRNLYIRFQSQTGDAMG 614
HMGCR MNMISKGTEKALSKLHEYFPEMQILAVSGNYCTDKKPAAINWIEGRGKSVVCEAVIPAKV 716
Hmgcra MNMISKGTEQALARLKEEFPELQVLAVSGNYCTDKKPAAINWIEGRGKSVVCETTIPAKV 712
Hmgcrb MNMLSKGTEQALGRLQERYPDMRLLAVSGNYCTDKKPAAVNWIHGRGKSTVCEAVIPARV 674
HMGCR VREVLKTTTEAMIEVNINKNLVGSAMAGSIGGYNAHAANIVTAIYIACGQDAAQNVGSSN 776
Hmgcra VKEILKTSTEALVDVNISKNLVGSAMAGSIGGYNAHAANIVAAIYIACGQDPAQTVGSSN 772
Hmgcrb VKEVLKSSTAALVELNISKNLVGSAMAGSIGGFNAHAANIVTAIYIACGQDPAQTVGSSN 734
HMGCR CITLMEASGPTNEDLYISCTMPSIEIGTVGGGTNLLPQQACLQMLGVQGACKDNPGENAR 836
Hmgcra CITLMEASGATGEDLYISCTMPSIELGTVGGGTNLPPQQACLKMLGVLGASQECPGENAR 832
Hmgcrb CITLMECVGTSGEDLYVSCTMPSLELGTIGGGTGLPAQHACLQMLGVDGASVQCPGENSR 794
HMGCR QLARIVCGTVMAGELSLMAALAAGHLVKSHMIHNRSKINLQDLQGACTKKTA 888
Hmgcra QLAKVVCATVLAGELSLMSALAAGHLVKSHMTHNRSKVNLQEAPGTCTKQAS 884
Hmgcrb TLARIVCASVLAGELSLMAALAAGHLVQSHMTHNRSKVNLREPEGQPKEAS- 845
Statin-binding residues

or opened (acid) ring confirmation (**Fig. 1.3**). Once delivered to the serum, the lactone form of the statin is activated (hydrolyzed) by a family of serine esterases known as carboxylesterases. This modification allows statins to bind as an intermediate analogue to the active site of HMGCR (Fukami et al., 2010). Statins have a higher affinity for the active site of HMGCR than the natural substrate HMG-CoA (Istvan and Deisenhofer, 2001). However, despite their identical mode of function, statins display variation with respect to their chemical structure, hepato-selectivity, molecular weight, pharmacokinetic profiles, biochemical metabolism, and affinity for the active site of HMGCR, half-life, and excretory pathways (Igel et al., 2001). All of these parameters can affect the efficiency with which statins can reduce serum LDL and total cholesterol levels. Furthermore, both animal and human studies have attested to the efficacy of statins to reduce serum cholesterol levels through inhibition of HMGCR pathway (Johnston et al., 2001; Dubuc et al., 2004; Wu et al., 2005; Versmissen et al., 2008).

Lipophilic statins are less hepato-selective, as they can passively diffuse through cell membranes, whereas hydrophilic statins display minimal perfusion to other tissues, since they require specific membrane interactive transport mechanism, making them more hepato-selective (Sirtori, 1993). Hence, hydrophilic statins, due to lower distal tissue absorption, are more tolerated in patients and with less reported side-effects or non-specific toxicity (Sirtori, 1993, Hemant et al., 1999; Liao and Laufs, 2005). The two synthetic and lipophilic statins I have used in this project are atorvastatin (ATV) and cerivastatin (CVT) (**Fig. 1.4**).

Figure 1.3: Chemical structure of the HMG-CoA moiety (dihydroxy heptanoic acid) in statins. The statin HMG-CoA moiety can exist as either a 3-hydroxy lactone ring (closed conformation) (A) or as an opened dihydroxy acid (opened conformation) (B).

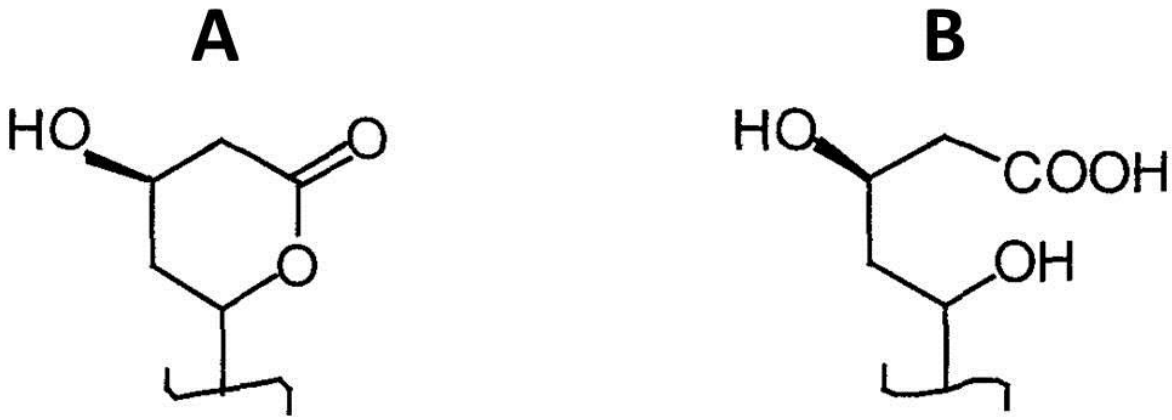

Figure 1.4: Basic properties of atorvastatin (ATV) and cerivastatin (CTV) are presented.

	Cerivastatin	Atorvastatin
Structure:	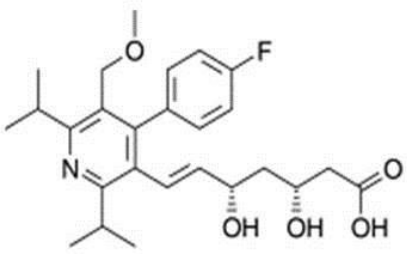	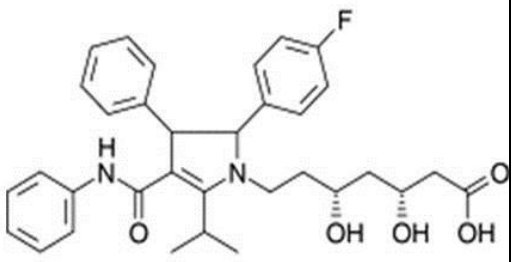
Brand name:	Lipobay, Baycol	Lipitor
Derivation:	Synthetic	Synthetic
Chemical formula:	$C_{26}H_{34}FNO_5$	$C_{33}H_{35}FN_2O_5$
Weight:	459.5503	558.6398

1.2.3 HMGCR pathway and embryonic development

Gene-expression analysis in chick tissues, *Drosophila*, zebrafish and murine models demonstrate that HMGCR transcripts are enriched during embryonic development (Alejandre et al., 1981; Gertler et al., 1988; Thisse and Thisse, 2004; Brewer et al., 1993) reflecting a developmental requirement for products of HMGCR-mediated metabolism. However, the specific developmental processes that require mevalonate-derived products have only been explored recently. Toxicology experiments to assess the possible teratogenicity of statins, using rats and rabbits, have reported that at high doses, statins could induce developmental and maternal toxicity, affecting parameters such as body weight and levels of food consumption (Dostal et al., 1994). Preliminary experiments in pregnant rats showed that exposure to high dose mevinolin (a fungal-derived/natural inhibitor of HMGCR), resulted in fetuses with malformed vertebrae and ribs, along with failure of the abdominal wall to close resulting in protrusion of the stomach and intestine to the outside (gastroschisis) (Minsker et al., 1983).

In subsequent studies, targeted disruption of the HMGCR pathway in mice was achieved through sequence replacement gene-targeting technology in order to prevent translation of the entire carboxyl-terminus of the enzyme (Ohashi et al., 2003). The *Hmgcr–/–* mice experienced embryonic lethality prior to reaching the implantation stage (Ohashi et al., 2003). These results highlight the crucial function that HMGCR-mediated metabolism and downstream signalling events play during mammalian development.

More recent work in *Drosophila* and zebrafish suggested that deficiencies in HMGCR activity during development were implicated in prenylation-dependent germ

cell migration delays and misguidance, hence affecting developmental patterns (Van Doren et al., 1998; Santos and Lehmann, 2004; Deshpande and Schedl, 2005). Studies in *Drosophila* showed that down-regulation of the HMGCR pathway induced congenital heart defects (Yi et al., 2006). Consistently, a point mutation was identified at base-pair (bp) position 1575 of *hmgcrb* (G to A transition), the maternally derived *hmgcr* paralog in zebrafish, resulting in an amino acid change from Glycine (Gly) to Aspartic acid (Asp) at codon 497 (D'amico et al., 2007). In these embryos, loss of *hmgcrb* function was associated with defective myocardial epithelial migration and fusion and defective heart-tube formation and pericardial edema. This was attributed to impaired prenylation of target proteins that would otherwise activate Rho-dependent signalling (D'amico et al., 2007). Moreover, the *hmgcrb–/–* zebrafish embryos did not survive (D'amico et al., 2007).

However, the entire suite of developmental processes that require adequate amounts of mevalonate-derived metabolites are poorly understood by virtue of the mortalities associated with the null mutations of the HMGCR gene.

An important avenue that needed to be further explored, hence a motivation for my PhD thesis, was whether transient or partial reductions in the HMGCR activity, through a reverse genetics approach or by exposure to specific pharmacological inhibitors, could affect additional developmental processes, in particular CNS circulation and angiogenesis. My particular focus was cerebral-vascular development. The reason for this focus was that preliminary drug-screening experiments showed that statin treatment of zebrafish embryos gave rise to a distinct CNS hemorrhage phenotype, which warranted further studies**.**

1.2.4 The HMGCR pathway and angiogenesis

Angiogenesis is a complex physiological process by which new capillary networks are established from pre-existing ones through a series of morphogenic events involving differentiation, proliferation, migration, and maturation of endothelial cells (ECs). It is followed by formation of cell-to-cell junctions through adhesion molecules and formation of network-like structures, lumenisation of vessels and deposition of a new basement membrane (Adams and Alitalo, 2007).

After undergoing proliferation, the endothelial tip cells, which are analogous to neuronal growth cones, extend and retract their long filopodia-like processes in a dynamic protrusive fashion to exert a pulling force and to form sprouts into adjacent tissues, as well as to form connections with other vessels (Zelzer and Shilo, 2000). Earlier evidence suggested that these filopodia extend and protrude to navigate the path of growth in proportion with the relative abundance of guidance cues (Benjamin et al., 1999). Subsequent studies have concluded that the activation of endothelial tip cells as well as the protrusion of filopodia is induced by over-expression of vascular-endothelial growth factor (VEGF). This was evidenced by the fact that inhibition of VEGF-signalling led to loss of sprouting which was supported by *in vitro* analysis (Gerhardt et al., 2003). Further evidence in support of a requirement for VEGF gradients guiding endothelial tip migration was documented in vertebrates, including zebrafish (Gerhardt et al., 2003; Habeck et al., 2002).

Angiogenic mechanisms are significantly up-regulated during embryonic development (Breier et al., 1992), wound healing (Wu et al., 2007), as well as regenerative processes (Bayliss et al., 2006). However, aberrant angiogenesis has also

been implicated in many diverse pathological conditions including tumor metastasis (Strieter et al., 2006), atherosclerosis (Sluimer and Daemen, 2009), diabetic retinopathy (Crawford et al., 2009), chronic inflammation (Costa et al., 2007), chronic kidney disease (Futrakul et al., 2008), and rheumatoid arthritis (Paleolog, 2002).

Variations in HMGCR activity are shown to exert effects on angiogenesis, as suggested by early *in vitro* and *in vivo* studies. Evidence obtained *in vitro* demonstrated that high dose statin exposure induced anti-angiogenic effects by provoking EC apoptosis, delaying EC migration, reducing endothelial VEGF2 release and decreasing the total VEGF2-receptor levels in primary human adult dermal microvascular ECs (HMVECs) (Weiss et al., 2002). These anti-angiogenic effects were attributed to curtailment in prenyl biosynthesis, which are metabolites required for post-translational modification of Rho GTPases (Weiss et al., 2002). Similarly, hydrophobic statins were shown to induce apoptosis in rat pulmonary vein ECs (PVECs) due, in part, to mis-localisation of RhoA to the plasma membrane (Kaneta et al., 2003). Likewise, the inhibition of geranylgeranylation and RhoA-mediated pathways is linked with apoptosis in human-derived ECs (Hippenstiel et al., 2002). More recently, it was shown that statin treatment of human liver sinusoidal ECs (HLSECs) resulted in apoptosis through inhibition of isoprenoid-dependent signalling pathways (Acquevella et al., 2010). HMGCR inhibitors were also shown to induce apoptosis in vascular smooth muscle cells (mural cells) in culture, which otherwise contribute to the elasticity and physical integrity of blood-vessels and regulation of blood flow (Guijarro et al., 1999). This suggests that HMGCR inhibitors could affect vascular smooth muscle cell interactions with ECs, hence raising the possibility that statins may interfere with vascular stabilisation *in vivo*.

The anti-angiogenic effects of statins were further substantiated through *in vivo* observations. At high doses, statin treatment inhibited capillary growth in chick chorioallantoic membranes and mouse corneas (Park et al., 2002). More substantial *in vivo* evidence was reported in studies using zebrafish, where a high dose statin exposure (10 μM) resulted in incomplete or defective anterior to posterior sprouting/migration of intersegmental vessels (ISV) from the dorsal aorta (DA), thereby severely restricting circulation in the developing organism (Choi et al., 2011). Overall, the endothelial-specific consequences of statin exposure are shown to be due to their cholesterol-independent or pleiotropic effects, through reduction of prenyl biosynthesis. Collectively, these studies support an anti-angiogenic effect associated with the inhibition of HMGCR function, with potential therapeutic implications. Of clinical relevance is the fact that preliminary studies exploiting the anti-angiogenic properties of statins have provided encouraging data regarding their efficacy to decrease tumor vascularisation, volume, and mass (Hindler et al., 2006; Wang et al., 2010).

However, an outstanding question that will be addressed in this thesis was whether products of HMGCR-mediated metabolism are required for cerebral-vascular development and stabilisation, and, if so, through what mechanisms? Another question that necessitated inquiry was the pathophysiological consequences of statin-induced interference with angiogenesis and vascular stabilisation during embryonic development.

1.2.5 The HMGCR pathway and stroke

By virtue of the association between high serum cholesterol levels and the pathogenesis of coronary artery disease (Hutter et al., 2004), statins were considered ideal

to ameliorate the risk of stroke. Nevertheless, more recent evidence does not support a strong relationship between the risk of stroke and serum cholesterol levels. Yet, studies have attested to the effectiveness of statins in reducing the risk of acute ischemic complications and atherosclerosis, through their effectiveness to reduce the serum cholesterol levels (Borghi et al., 2000; Elahi et al., 2008). The efficacy of statins has also been attributed to their non-cholesterol dependent or pleiotropic effects that lead to plaque stabilisation, reduction of reactive oxygen species (ROS), and enhanced endothelial function by increased nitric oxide (NO) synthesis (Vaughan et al., 1999).

Furthermore, a recent study uncovered a G→T single nucleotide polymorphism (SNP) in the HMGCR gene, which, based upon pyrosequencing data derived from more than 23,000 participants, was found to be associated with an elevated risk for stroke, which was independent of high blood pressure (Freitas et al., 2010).

However, of direct relevance and importance to my thesis are the conclusions of a large-scale, randomised clinical study conducted by The Stroke Prevention by Aggressive Reduction in Cholesterol Levels (SPARCL) Investigators. The results suggested that while statin treatment significantly attenuated the risk of ischemic stroke in patients, there was a slight, but significant risk for intracerebral hemorrhage (ICH) in these same individuals (Amarenco et al., 2006). Although the study was aimed at addressing whether statins could reduce the risk of stroke in individuals with prior history of stroke or transient ischemic attack, the unexpected result that statins are associated with ICH has raised tremendous interest as it has paved the way for follow-up clinical studies most of which were based on meta-analysis of randomised controlled trials.

Subsequent studies further evaluated the association between statin use and the risk for ICH, and led to contentious results with some reporting no observable risk for ICH (Hackam et al., 2012; Spence, 2012; McKinney and Kostis, 2012) to other studies suggesting complete avoidance of statins in order to mitigate the risk for ICH (Arboix et al., 2010; Westover et al., 2011). Of clinical importance is whether this unanticipated adverse outcome of ICH, as suggested by at least some of the aforementioned studies, could be outweighed by the potential cardiovascular benefits of statins. There has been no reproducible etiological or angio-structural analysis in the context of animal models to further investigate this possibility or the mechanism(s) of statin-induced ICH. However, some of these clinical studies led us to the hypothesis that statins may interfere with the integrity of vascular endothelium, thus resulting in hemorrhage. This could be especially relevant in individuals with a weaker vascular endothelium, such as those with high blood pressure, in a developing organism or in individuals with genetic vascular dysplasia resulting from mutations in cerebral cavernous malformation (CCM) genes and those with previous history of stroke.

In sharp contrast with the mounting clinical evidence, it has been reported, in at least one study that in mice with a genetic predisposition for cerebral-vascular permeability defect resulting from a heterozygous mutation of *CCM2*, treatment with statins effectively restores the endothelial barrier function by inhibiting Rho GTPase activation (Whitehead et al., 2009). These findings raised the possibility for statin treatment as a therapeutic for CCM-like pathologies and to prevent cerebral hemorrhage (Whitehead et al., 2009).

Coincidently, these clinical and animal studies, which highlighted a link between the HMGCR pathway and cerebral-vascular integrity, emerged in parallel with the progress of my PhD project, which was geared towards dissecting the mechanisms of statin-induced ICH in zebrafish. Hence, I reasoned that the development of a robust animal model (zebrafish) for statin-induced cerebral-vascular disorders may assist to address the discrepancies highlighted by clinical and animal studies**.** There exists considerable overlap between the genes and mechanisms implicated in vascular morphogenesis in zebrafish and mammals (Gore et al., 2012). Therefore, it is my prediction that the findings of this project can contribute to our understanding of some of the molecular and cellular mechanisms leading to stroke in humans, as it highlights a metabolic contribution to cerebral-vascular stabilisation.

1.3. Cerebral-vascular stabilisation during development

Vascular stabilisation is a crucial process required to establish and maintain a barrier function so as to ensure the integrity of nascent vessels that are formed through either angiogenesis or vasculogenesis (Mizuguchi et al., 2004; Loeys et al., 2005). Once the newly formed vessels stop the process of re-modelling, attain their adequate size and form vascular tubes, they must be stabilised to prevent rupture and subsequent hemorrhage into the interstitial spaces. The establishment of a functional vasculature requires cessation of angiogenesis, followed by ECs entering a quiescent state.

Timely and rapid stabilisation of new vessels, through establishment of endothelial cell-to-cell contacts and interactions of the endothelium with support (mural) cells, is particularly crucial during development, since these vessels are particularly

fragile and prone to hemorrhage (Jain, 2003). Such is also the case during cancer metastasis, as the nascent vasculature supplying oxygen and nutrients to the newly formed tumors tends be highly permeable, since these vessels lack adequate investment by mural cells, making them fragile and disorganised (Abramsson et al., 2002). Moreover, several genetic defects underlying disruption of cell-cell junctions and detachment of ECs from the vessel wall have been identified and characterised in mice and, more recently, in zebrafish (Clatterbuck et al., 2001; Bergers and Song, 2005; Butler et al., 2011).

Although the mechanisms and signalling pathways regulating angiogenesis and vasculogenesis have been examined in great detail through both *in vitro* and *in vivo* experiments, the endogenous signalling pathways involved in developmental vascular stabilisation remain underexplored (Adams and Alitalo, 2007). Endothelial cell-cell contacts are established and maintained by trans-membrane adhesion molecules that are anchored to cytoskeletal elements. The intra-endothelial cell communication is mediated through gap junctions, whereas the adhesion molecules that confer structural support and contribute to vascular stability include adherens junctions (AJ) and tight junctions (TJ) (Dejana et al., 1995; Gumbiner et al., 2000; Tsukita et al., 2001). Nonetheless, the genetic and mechanistic bases that regulate junction assembly for a functional cerebral-vascular system, particularly in the context of zebrafish development, are not yet elucidated.

Gene expression and functional analysis have led to the identification and characterisation of several EC-specific and trans-membrane adhesion molecules involved in the maintenance of endothelial barrier integrity. These include vascular endothelial (VE)-cadherin, claudin-5, filamin-A, and β-catenin (Feng et al., 2006; Gavard and

Gutkind, 2008; Das et al., 2011; Glading and Ginsburg, 2010). Targeted inactivation of VE-cadherin and truncation of the β-catenin-binding cytosolic domain of VE-cadherin induces EC-specific apoptosis, along with defective remodelling and maturation of the vasculature and early lethality(Carmeliet et al., 1999). Endothelial-specific conditional deletion of β-catenin, a protein interacting with the cytoplasmic tail of VE-cadherin, is associated with altered vascular patterning (Caveda et al., 1996), defective lumenisation and frequent hemorrhage *in vivo*, as well as decreased intricacy of endothelial cell-cell junctions *in vitro*, based on studies on mice(Cattelino et al., 2003). Similarly, a vascular-specific defect associated with morpholino-induced partial and transient loss of VE-cadherin was developed in the zebrafish (Montero-Balaguer et al., 2009). Morpholino oligonucleotide-induced depletion of VE-cadherin in zebrafish resulted in vascular instability, defective lumenisation, as well as frequent cerebral hemorrhage, predominantly at 52 hpf (hour post-fertilisation) (Montero-Balaguer et al., 2009). More complete depletion of VE-cadherin, through higher doses of morpholinos, resulted in more profound defects including total inhibition of EC sprouting activity and mortality (Montero-Balaguer et al., 2009). Functional analysis of claudin-5, another trans-membrane tight junction protein, in both murine and zebrafish models, has highlighted a functional role for this protein in maintaining the integrity of the endothelial blood–brain barrier function, thus assigning for it a role in brain morphogenesis (Xie et al., 2010).

In addition to endothelial cell-cell contacts, vascular integrity is also maintained through ECs interacting with perivascular mural/support cells. These mural cells include smooth muscle cells, astrocytes, neuroepithelial cells, and pericytes (McCarty et al., 2002). Whereas ECs establish a monolayer and line the inner surface of a vessel, mural

cells wrap around the outside of the vascular tube and assist in regulating blood flow. The components of the signalling pathways involved in recruitment of mural cells to the vascular endothelium have been identified and characterised (Kumar and Owens, 2003; Larsson et al., 2001; Ballabh, 2009). Such close interactions between the endothelium and mural cells are essential for the development and maintenance of the blood-brain barrier and regulation of blood flow by controlling the contractility/elasticity of the vessels. At the ultra-structural level, disruption of the focal contact between mural cells and the endothelium is associated with cerebral hemorrhage (McCarty et al., 2002; Ballabh, 2009).

Several loss-of-function mutations associated with the disruption of endothelial-mural cell junction proteins have been reported in humans. These vascular-specific disorders, which follow an autosomal-dominant pattern of inheritance, are collectively referred to as cerebral cavernous malformations (CCMs). The CCM phenotype is characterised by dilated, leaky central nervous system (CNS) blood-vessels lacking adequate coverage by smooth muscle cells, and frequent hemorrhage into the brain parenchyma (Clatterbuck et al., 2001). Thus far, three genes, which participate in a signalling pathway involving Rho GTPase signalling, namely *CCM1* (*KRIT1*), *CCM2* (*MGC4607*) and *CCM3* (*PDCD10*), have been identified (Sahoo et al., 1999; Denier et al., 2004; Bergametti et al., 2005).

However the mechanism by which CCM gene products interact with Rho GTPase signalling and how reductions in the expression of these structurally diverse gene products can contribute to the pathogenesis of the CCM phenotype is still a subject of intense research. Many studies have attempted to functionally characterise these genes

using murine models (Plummer et al., 2004; Whitehead et al., 2009; Louvi et al., 2011) and, more recently, developing zebrafish (Gore et al., 2008; Yoruk et al., 2012). These studies have greatly contributed to our understanding of the etiology and angio-structural basis underpinning CCM pathogenesis.

One unique advantage of the zebrafish, which is particularly manifest during their development, is their optical transparency which facilitates easy visualisation of cerebral hemorrhage through the use of bright-field microscopy (**Fig. 1.5**). Another advantage of the zebrafish is that it is highly prolific. As a result, the amenability of this fish to large-scale chemical mutagenesis screening has allowed for the isolation of numerous mutations that impact on the cardiovascular system and, as it relates to my project, identification of mutations affecting developmental cerebral-vascular stabilisation (Stainier et al., 1996). In this large-scale mutagenesis screening of the zebrafish genome, the mutant *bubble-head* (*bbh*) was identified, which exhibited cranial hemorrhage and ventricular edema, hence illustrative of weakened cerebral-vessel walls (Stainier et al., 1996). Other mutations affecting cerebral-vascular stabilisation, the viability of ECs, and caudal circulation were also identified in this study. These mutations were referred to as *gridlock* (*gdl*), *m413* and *m521*, and *migraine* (*mig*). All of these genetic defects were associated with frequent hemorrhage and various degrees of vascular disintegration at the same developmental stage in zebrafish (Stainier et al., 1996). Of these lines, the *gridlock* (*gdl*) mutation was later characterised (Weinstein et al., 1995; Zhong et al., 2000; Peterson et al., 2004). However, until recently, neither genetic nor functional characterisations of the other mutations associated with ICH have been reported.

Characterisation of the vascular-specific *bubblehead* (*bbh*) mutation was carried out through positional cloning, *in situ* hybridisation, reverse genetics and high resolution imaging (Liu et al., 2007). Positional cloning of *bbh* revealed a hypomorphic mutation in the βPix gene, which otherwise encodes a p21-activated kinase (Pak)-interacting exchange factor (Pix). βPix is a guanine exchange factor (GEF) which functions to stimulate the exchange of Rho GTPase-bound GDP with cytosolic GTP thus activating the Rho GTPases, Rac and CDC42 (Bagrodia et al., 1998; Manser et al., 1998). A single-nucleotide mutation (G → A) results in alternative splicing and exclusion of exon 14, thus introducing a premature stop codon that gives rise to a truncated βPix protein. The mutation results in an ICH phenotype, accompanied by hydrocephalus in zebrafish embryos at 48 hpf. At the ultra-structural level, the hemorrhage arises due to defective association between mural cells and ECs. Since *βPix* encodes a GEF that activates Rho GTPase proteins by stimulating the exchange of GDP for GTP, it was speculated that a mutation in the *βPix* would be associated with reduced levels of activated Rho GTPases (Etienne-Manneville and Hall, 2002, Liu et al., 2007). Given that the Rho GTPase signalling regulates a wide array of biological processes including mediation of cytoskeletal organisation, cell motility, wound healing, apoptosis and immune function, it would be expected that down-regulation of *βPix* expression would affect these parameters.

Figure 1.5: The optical transparency of zebrafish facilitates easy evaluation of ICH during development. Representative bright-field photomicrographs of 36 hpf zebrafish embryos. The black *arrows* denote the sites of blood extravasation in the forebrain, midbrain and hindbrain regions of embryos treated continuously with 0.5 mg/L of atorvastatin at 2 hpf and imaged at 33 hpf. Anterior is to the left and dorsal to the top. Scale bar = 200 μm.

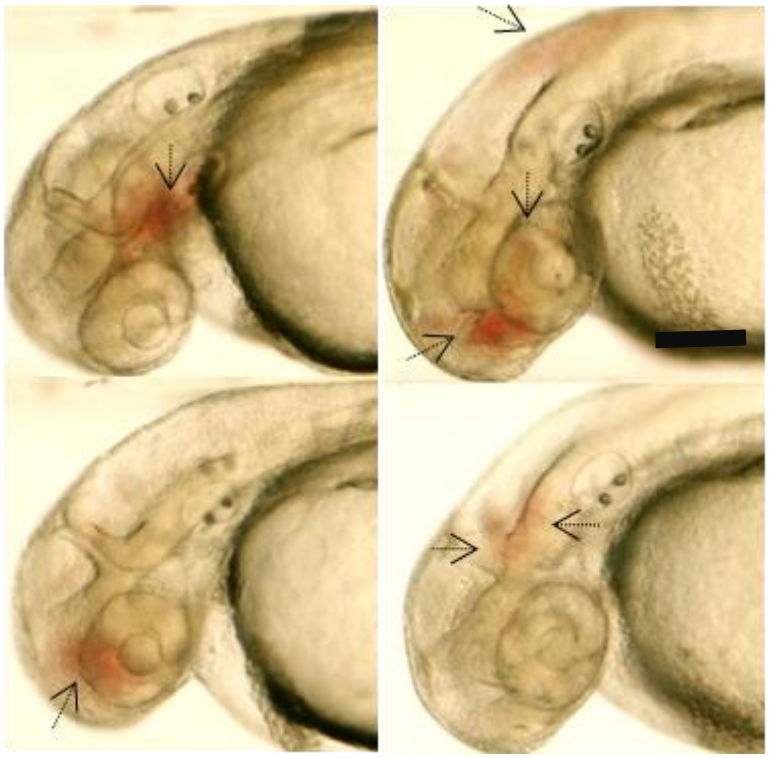

In parallel with the characterisation of the *bbh* mutation, a separate study characterised a recessive zebrafish mutant termed *redhead*, which displayed a similar ICH phenotype at the same developmental stage (Buchner et al., 2007). Interestingly, this vascular defect was mapped to a mutation in *p21-activated kinase 2a* (*pak2a*), a member of the p21-activated kinase gene family and a binding partner for *βPix*. Pak proteins are serine/threonine kinases that act downstream of Rho GTPase signalling and are involved in the transduction of this pathway (Hofmann et al., 2004).

In both *redhead* and *bubblehead* zebrafish embryos, these mutations were mapped to genes that are involved in the activation and transduction of Rho GTPase-mediated signalling pathways, which synergistically participate in the development of vascular networks (Gore et al., 2008). In both mutant strains, the structural basis for the hemorrhage phenotype stems from defective stabilisation and maturation of nascent vessels (Buchner et al., 2007; Liu et al., 2007).

Of noteworthy relevance to my thesis project is that the activation of Rho GTPase signalling is mediated, in part by a mevalonate-derived metabolite, geranylgeranyl-pyrophosphate (GGPP), a 20-carbon lipid molecule (Bishop and Hall, 2000). GGPP serves as an end-product for the lipidation and subcellular localisation of Rho GTPases to the plasma membrane. This process is critical for the activation and function of CAAX-proteins (Bishop and Hall, 2000) (**Fig. 1.6**). This is evidenced by the fact that depleted GGPP levels reduce the GTP-binding capacity of Rho GTPases, rendering them cytosolic and inactive, which would target them for degradation in the cytoplasm (Hirai et al., 1997). On this premise, one can deduce that inhibition of HMGCR activity would reduce Rho GTPase signalling, thus leading to an ICH

phenotype. This assertion is contrary to evidence from murine models where down-regulation of Rho GTPase signalling, by statin treatment, is shown to reverse/prevent the ICH phenotype in mice. Evidently, a clear discrepancy exists between the two models (zebrafish and mice) in terms of requirements for Rho signalling in cerebral-vascular stabilisation.

1.4. Utility of zebrafish as a model for the etiology and pathophysiology of ICH

The zebrafish continues to gain recognition as an excellent vertebrate model for the study of vascular development. The mechanisms and gene signalling pathways mediating the formation and patterning of vessels were found to be similar to those documented in other vertebrates (Gore et al., 2012). The optical transparency and external development of embryos enables easy visualisation of active circulation and organ development and makes them amenable to chemical screening and genetic manipulation.

Blood-vessel morphogenesis, immune response and thrombosis can be assayed in real-time using stable transgenic embryos expressing fluorescently labeled blood-vessels, macrophages, leukocytes, erythrocytes, and thrombocytes. Vascular permeability can be assessed using high-resolution confocal microscopy and micro-angiography. Protein function can be determined rapidly and efficiently through microinjection of morpholino oligonucleotides which reduce gene expression in a dose-dependent fashion. All of these features make the zebrafish an ideal system to study the morphogenesis of cerebral-vascular system.

1.5. Research Objectives

My PhD thesis focuses on expanding our present knowledge regarding the signalling pathways contributing to developmental cerebral-vascular stabilisation in vertebrates. Cerebral-vascular disorders including ICH are associated with high mortality and morbidity (Counsell et al., 1995; Qureshi et al., 2005). Even though considerable research has been conducted in the field of vascular development, the genetic and mechanistic underpinnings behind ICH pathogenesis are still not well characterised. The results of several randomised clinical studies have suggested a significant risk for ICH in patients taking statin drugs. However, these studies are limited in that no follow-up animal studies have to this point been conducted to independently verify and dissect the mechanism(s) involved. Furthermore, a number of convincing studies in zebrafish have suggested that inhibition of Rho GTPase signalling can potentiate ICH in developing vertebrates. This information, coupled with *in vitro* evidence that HMGCR activity is required for both endothelial and mural cell viability, prompted me to characterise the function of HMGCR in zebrafish with a particular interest in cerebral-vascular development. I hypothesise that HMGCR regulates cerebral-vascular stabilisation through GGPP-dependent signalling. As such my results will have clinical relevance in terms of addressing part of the etiology and pathophysiology of human vascular instability disorders, particularly in the case of spontaneous ICH. My research objectives are:

Objective 1:

Establish whether HMGCR activity is required for developmental cerebral-vascular stabilisation.

Objective 2:

Determine the mechanism(s) whereby HMGCR activity regulates cerebral-vascular stabilisation.

Objective 3:

Characterise the pathophysiological and neurological processes underlying ICH pathogenesis.

Figure 1.6: HMGCR-mediated regulation of Rho GTPase activity. The process of geranylgeranylation, catalysed by GGTase I, regulates Rho GTPase function by promoting their translocation to the plasma membrane. Prenylated Rho GTPases function as molecular switches and they alternate between a GDP-bound state (inactive) and a GTP-bound state (active). Guanine exchange factors (GEFs) function as activators of Rho GTPases by stimulating GDP release and increasing enzyme affinity for GTP. GTPase activating proteins (GAPs) work by accelerating GTP hydrolysis. Statins work by inhibiting mevalonate production and thus geranylgeranyl pyrophosphate (GGPP) production and ultimately protein prenylation, which inhibits membrane association of RhoGTPases.

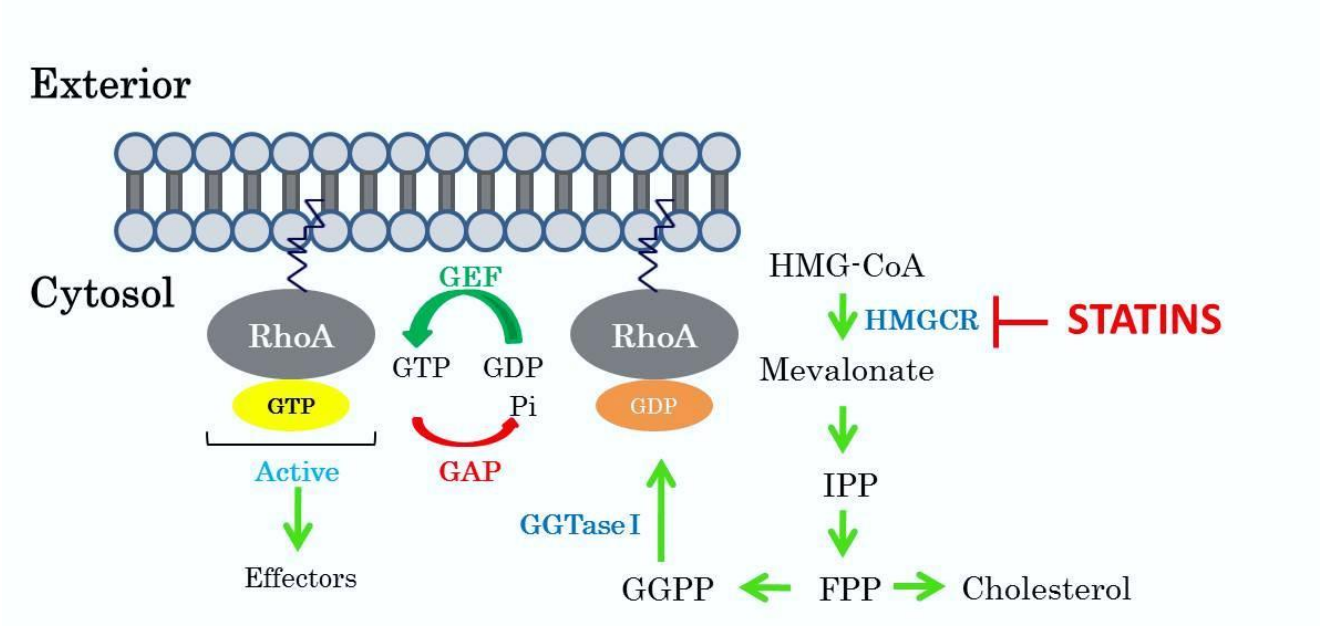
Exterior
Cytosol
RhoA
GTP
GEF
GTP
GDP
Pi
GAP
RhoA
GDP
Active
Effectors
GGTase I
HMG-CoA
HMGCR
STATINS
Mevalonate
IPP
GGPP
FPP
Cholesterol

Chapter 2

The 3-hydroxy-3-methylglutaryl-CoA reductase (HMGCR) pathway regulates developmental cerebral-vascular stabilisation by a prenylation-dependent signalling pathway

The data presented in this chapter have been published in the following manuscript. However, supplementary figures and textual alterations and additional information have been added to this chapter:

- **Eisa-Beygi, S**., Hatch, G., Noble, S., Ekker, M., Moon, T.W. (2013). The 3-hydroxy-3-methylglutaryl-CoA reductase (HMGCR) pathway regulates developmental cerebral-vascular stability via prenylation-dependent signalling pathway. ***Dev. Biol***. 373, 258-266.

Author contributions:

Mr. Gary Hatch replicated the drug-exposure and rescue experiments to ensure consistency of results. Ms. Sandra Noble was instrumental in training me for the use of confocal microscopy and helping me prepare and process embryos for imaging. Dr. Thomas W. Moon and Dr. Marc Ekker helped me design the experiments and assisted me in writing and revising this chapter to ensure that the content is scientifically sound and the style is in accordance with the FGPS requirements. I am profoundly grateful for the assistance of the aforementioned individuals, without whom this chapter would not have been completed.

Shahram Eisa-Beygi

April 20, 2013

2.1 Abstract

Intracerebral hemorrhage (ICH) is a debilitating form of stroke, with the highest mortality rate of all stroke subtypes and, often, precipitating irreversible neurological deterioration. Although recent studies have gained insight into the etiology of the disease, many of the causative genes and mechanisms implicated in developmental cerebral-vascular malformations underlying ICH pathogenesis are unknown. Recent evidence derived from *in vitro* and *in vivo* studies in murine models have shown inhibition of the 3-hydroxy-3-methylglutaryl-CoA reductase (HMGCR) pathway to be effective in stabilizing cranial vessels. Through a combination of pharmacological and genetic approaches to specifically inhibit the HMGCR pathway in zebrafish (*Danio rerio*), we demonstrate contrary to the work in murine models, a requirement for the HMGCR-mediated metabolic pathway in developmental vascular stabilisation within the head. Here we report that inhibition of HMGCR function in embryonic zebrafish disrupts cerebral-vascular stability, resulting in progressive dilation of blood vessels, followed by vessel rupture and hemorrhage into the brain parenchyma, mimicking cerebral cavernous malformation (CCM)-like lesions in humans and murine models. These vascular defects are rescued by prior exogenous supplementation with geranylgeranyl pyrophosphate (GGPP), a 20-carbon metabolite of the HMGCR pathway, required for the membrane localisation and activation of Rho GTPases. Consistent with this observation, morpholino-induced depletion of the β-subunit of geranylgeranyltransferase I (GGTase I), an enzyme that facilitates the post-translational transfer of the GGPP moiety to the C-terminus of Rho family of GTPases, mimics the cerebral hemorrhage-induced by the

pharmacological and genetic ablation of HMGCR. In embryos with cerebral hemorrhage, the endothelial-specific expression of cdc42, a highly-conserved Rho GTPase involved in the regulation of vascular permeability, was significantly attenuated. Taken together, our data reveal a metabolic contribution to the stabilisation of nascent cranial vessels during embryogenesis, requiring protein geranylgeranylation acting downstream of the HMGCR enzyme within the mevalonate pathway.

2.2 Introduction

3-Hydroxy-3-methylglutaryl-CoA reductase (HMGCR) is an endoplasmic reticulum (ER)-bound enzyme that catalyzes the rate-limiting step within the mevalonate pathway that converts acetyl-CoA derived HMGCoA to mevalonate, giving rise to mevalonate-derived molecules, including cholesterol and isoprenoids (Goldstein and Brown, 1990; see Chapter 1). A complex feedback mechanism, involving both steroidal and non-steroidal mediated pathways, is involved in the regulation of HMGCR activity through transcription, translation, phosphorylation, and degradation of the enzyme (Brown and Goldstein, 1997; Nakanishi et al., 1988, Omkumar et al, 1994; DeBose-Boyd, 2008). Statins, competitive inhibitors of HMGCR, are pharmaceuticals that bind part of the HMG-binding residues of the enzyme and inhibit its activity through competitive inhibition (Istvan and Deisenhofer, 2001). In addition to reducing *de novo* cholesterol synthesis and total plasma LDL cholesterol levels, statins also curtail the biosynthesis of other lipids, namely isoprenoids, which otherwise serve as essential lipid attachments for the Rho family of GTPases (Bishop and Hall, 2000).

As such, an efficient way to elucidate HMGCR gene function during development is achieved through the use of statin molecules for which the biochemical mode of action is well characterised. Reduced HMGCR activities during development are implicated in prenylation-dependent germ cell migration delay and misguidance in both *Drosophila* and zebrafish (*Danio rerio*) models (Santos and Lehmann, 2004; Thorpe et al., 2004). A point mutation identified at position 1575 of *hmgcrb*, the maternally-expressed *hmgcr* paralog in zebrafish, results in defective heart-tube formation due to impaired post-translational prenylation of small GTPases (D'amico et al., 2007). In contrast, targeted disruption of *hmgcr* in mice results in early embryonic lethality which is suggestive of the crucial function that HMGCR-mediated metabolism and downstream signalling events play during mammalian development (Ohashi et al., 2003). Presently, the developmental processes that are dependent upon HMGCR-derived products have not been thoroughly identified.

Pharmacological inhibition of the HMGCR pathway has been shown to exert both angiostatic and angiogenic effects *in vitro* and *in vivo* (Lu et al., 2004; Khaidakov, 2009; Weis, 2002; Kaneta, 2003; Li et al., 2002; Acquavella, 2009; Wang et al., 2010; Choi et al., 2011). An outstanding question that needed to be addressed was whether perturbations of the HMGCR pathway would disrupt the stabilisation of nascent vessels and overall vascular morphogenesis *in vivo*, and, if so, what would be the pathophysiological consequences of interference with these processes during a period of rapid angiogenesis.

Zebrafish have recently gained recognition as a suitable model to dissect the etiology of cerebral cavernous malformation (CCM) (Kleaveland, 2009; Hogan et al.,

2008; Yoruk et al., 2012). Moreover, recent work in zebrafish demonstrated that proteins involved in the activation and transduction of Rho GTPase-mediated signalling pathways synergistically participate in the development of the vascular network in zebrafish. Deficiencies within this pathway impair the stabilisation and maturation of nascent vessels by preventing the association of mural cells with endothelial cells, giving rise to multiple hemorrhages in the brain (Buchner et al., 2007; Liu et al., 2007; Gore et al., 2008), along with more pronounced defects in vascular morphogenesis (Epting et al., 2010). It is known that the mevalonate-derived metabolite, geranylgeranyl-pyrophosphate (GGPP) serves as an end-product for the lipidation and subcellular localisation of Rho GTPases to the plasma membrane, which is critical for the activation and function of these Rho GTPases (Bishop and Hall, 2000). Hence, depleted GGPP levels reduce the GTP-binding capacity of Rho GTPases, rendering them cytosolic and inactive. Although the Rho GTPase pathway has been implicated in CCM pathology, there remains a major discrepancy between the mechanisms in mouse and zebrafish. More specifically, recent studies in mice show that global inhibition of Rho GTPase prenylation through statin-mediated inhibition of HMGCR within the mevalonate pathway restores endothelial barrier integrity, thus reversing the vascular permeability dysfunction in mice that are genetically predisposed to CCM (Whitehead et al., 2009). Consistent with this observation, transcript levels of the Rho GTPases, RhoA, Rac and cdc42, were significantly elevated in lesions of a mouse model of CCM (Louvi et al., 2011).

Hence, in mice, statin-mediated inhibition of Rho GTPase signalling, through decreased GGPP biosynthesis, is reported to be an effective treatment to attenuate vascular permeability (Li and Whitehead, 2010), whereas in zebrafish, mutation and

morpholino-induced loss of function of proteins that participate in the activation and transduction of Rho GTPase signalling heightens vascular permeability (Buchner et al., 2007; Liu et al., 2007). To what shall we attribute these divergent outcomes even though the mechanism of statin inhibition is the same? One of the major motives behind this project was to address this inconsistency.

Therefore, to investigate this discrepancy, we subjected developing zebrafish to two structurally different statin molecules (atorvastatin or cerivastatin) and two morpholino oligonucleotides (splice MO or ATG MO) with non-overlapping sequences to inhibit HMGCR function. Our pharmacological and genetic approach consistently resulted in grossly dilated vessels, followed by progressive loss of vascular stability in the brain at specific developmental stages during which nascent cranial vessels are more prone to rupture. Prior supplementation with exogenous mevalonate or GGPP, two of the metabolites downstream of the HMGCR enzyme, are sufficient to rescue the cerebral hemorrhage phenotype. Furthermore, morpholino-mediated specific disruption of the GGTase I-mediated prenylation pathway mimics the cerebral hemorrhages attributed to the inhibition of the HMGCR enzyme. Interestingly, in embryos with cerebral hemorrhage, the vascular-specific expression of cdc42, a Rho GTPase implicated in the mediation of endothelial barrier function (Kouklis et al., 2003; Broman et al., 2006; Ramchandran et al., 2008; Spindler et al., 2010) and highly enriched on the vacuole membranes (Eitzen et al., 2001; Isgandarova et al., 2007), was noticeably reduced in the head and the trunk vasculature, as early as 24 hpf. Our results highlight a requirement for HMGCR activities, through direct effects on GGPP biosynthesis, on the establishment of cerebral-vascular stability during zebrafish development, a process likely mediated by

CAAX proteins that require geranylgeranylation for their subcellular localisation and activation.

2.3 Materials and Methods

2.3.1 Zebrafish husbandry and transgenic lines

Adult wild-type and transgenic zebrafish were maintained under a constant temperature of 28°C and a 14 h light:10 h dark photoperiod in the University of Ottawa Aquatic Care Facility. Embryos were obtained through natural breeding of adult zebrafish and were kept at 28.5°C in embryo medium (5 mmol/L NaCl, 0.17 mmol/L KCl, 0.33 mmol/L $CaCl_2$, 0.33 mmol/L $MgSO_4$). The double transgenic Tg(*fli1:EGFP*);(*gata-1:DsRed*) zebrafish line was kindly provided by Dr. Beth Roman (University of Pittsburgh, Pennsylvania). The Tg(*fli1:EGFP-cdc42wt*)^{y48} was kindly provided by Dr. Brant Weinstein (National Institute of Child Health and Human Development, Maryland). All experiments were carried out in accordance with a protocol approved by the University of Ottawa Protocol Review Committee and conform to the published guidelines of the Canadian Council on Animal Care for the use of animals in research and teaching.

2.3.2 Drug treatment and metabolite rescue experiments

For pharmacological inhibition of HMGCR, zebrafish embryos (1-2 hours post fertilisation; hpf) were treated with Atorvastatin (ATV; Pfizer Inc., Connecticut USA) or Cerivastatin (CVT; Sequoia Research Products Ltd. Pangbourne, UK) in a single-exposure manner in embryo medium. ATV was dissolved in DMSO, whereas CVT was dissolved in sterile/distilled water. All solutions were aliquoted and kept at -20°C until

used. Embryos for the dose-response experiments were placed in final concentrations of 0.3, 0.5 or 1 mg/L ATV; CVT was administered at 0.15 mg/L. For mevalonate rescue experiments, similar numbers of embryos were placed in embryo medium containing 0.5 mg/L ATV and 1, 1.6, 3.2 or 4.4 μmol/L mevalonic acid (Sigma-Aldrich) or DMSO as vehicle control. Each treatment group consisted of more than 70 embryos and all exposure experiments were repeated at least 8 times. GGPP rescue experiments were performed by administering 0.5 mg/L ATV and 0.5, 2 or 4 mg/L GGPP (Sigma-Aldrich) dissolved in DMSO/methanol or DMSO/methanol, as vehicle control.

2.3.3 Whole-mount o-Dianisidine (OD) staining and cryosectioning

Zebrafish embryos at various developmental stages were fixed in 4% PFA/1X Phosphate Buffered Saline Tween-20 (PBST) overnight and subsequently stained for hemoglobin using o-Dianisidine (OD), a sensitive marker of hemoglobin. Briefly, unfixed embryos were dechorionated and stained with a solution of OD (0.6 mg/mL) (Sigma-Aldrich) containing 0.01 M sodium acetate (pH 4.5), 0.65% hydrogen peroxide, and 40% (v/v) ethanol in the dark for 15 min. Treated embryos were visualised using a Nikon NBZ 1500 dissecting microscope and photographed with a Nikon DXM 1200 C digital camera, and stored in 50% glycerol at 4°C. For cryosectioning, whole-mounted embryos previously stained with OD were equilibrated to 30% sucrose/1X PBST overnight. The next day, the samples were mounted in tissue freezing medium (Triangle Biomedical Sciences). Transverse sections of ~10 μm thickness were cut on a Leica CM1850 standard cryostat (Leica Microsystems) at -20 °C.

2.3.4 Confocal microscopy

For confocal microscopy, 48-52 hpf Tg(*flk1:EGFP;gata1:dsRED*) embryos previously treated with ATV or DMSO were embedded in 1% low melting agarose in embryo medium and tricaine mesylate (ethyl 3-aminobenzoate methanesulfonate; Sigma-Aldrich). A rendered Z-stack, at ~80 micron thickness each, was taken with a Zeiss LSM 510 AxioImager.M1 confocal microscope using an Achroplan 40x/0.8 W objective with an argon laser (488 nm) and a helium-neon laser (543 nm).

2.3.5 Morpholino design, resuspension and microinjection

A splice-modifying antisense morpholino oligonucleotide (MO) against *hmgcrb* pre-mRNA (*hmgcrb* MO), a translation blocking MO targeting the AUG initiation site of *hmgcrb* mRNA (AUG MO), a splice-modifying MO against *pggt1b* pre-mRNA (*pggt1b* MO), and a standard control MO against a splice targeting the human β-globin pre-mRNA (control MO), were obtained from GeneTools (Philomath, OR, USA). The sequences for the morpholinos used were:

(5'-AACTGCATTCATAAACTCACCCAGT-3') (*hmgcrb*-splice MO);

(5'-GCCTGAAGAGACGCGACAGCATCAT 3') (*hmgcrb*-ATG MO);

(5'-CACGCGGTGTGTGGACTCACGGTCA-3') (*pggt1b*-splice MO); and

(5'-CCTCTTACCTCAGTTACAATTTATA-3') (control MO).

All MO solutions were diluted in Danieau buffer (58 mM NaCl, 0.7 mM KCl, 0.4 mM $MgSO_4$, 0.6 mM $Ca(NO_3)_2$, 5.0 mM HEPES, pH 7.6) to a final concentration of 0.2 mM. The embryos were positioned in individual wells placed on a plate containing

1.0% agarose. The morpholino solution was then injected at quantities ranging from 0.5-10 ng into 1 to 2 cell-stage embryos through the cell-yolk boundary.

2.3.6 Microangiography

Briefly, 50-56 hpf embryos were anesthetised in tricaine mesylate and injected intra-vascularly with red fluorescent microspheres of 0.4 μm diameter (Thermo Scientific) through the sinus venosus and/or common cardinal vein. Fluorescence micrographs were acquired during a series of observations under the Nikon NBZ 1500 dissecting microscope, which was equipped with a standard dsRED filter set using a Nikon DXM 1200C digital camera.

2.3.7 DAF-2DA Staining

DAF-2DA (4-amino-5-methylamino-2′-7′-difluoro-fluorescein diacetate; Calbiochem) staining was performed as previously described (Lou et al., 2011), with reduced incubation time. In brief, live embryos were incubated in 10 μM DAF-2DA (in embryo medium, pH 7.0) and incubated for 5 h in the dark at 28.5°C, after which fluorescence micrographs were acquired under the Nikon NBZ 1500 dissecting microscope equipped with a standard GFP filter set, and photographed using a Nikon DXM 1200C digital camera.

2.3.8 RNA extraction, RT-PCR and sequencing

Total RNA was extracted from a pool of embryos using TRIzol reagent (Invitrogen). The RNA was DNase-treated using the Deoxyribonuclease kit (Invitrogen) to minimise genomic DNA contamination. cDNA was synthesised from equal concentrations of RNA using a 1st Strand cDNA Synthesis Kit and M-MLV RT

(Invitrogen) and used as a template in RT-PCR. PCR products were run on 1.75% agarose gels. Band intensities were quantified using ImageJ software. The primers used for PCR analysis were:

(5'-CAAACATGGGCTGGTTCAAG-3') (*Elf1a* forward) and

(5'-AGTGGTTACATTGGCAGGG-3') (*Elf1a* reverse).

The efficiency of the *hmgcrb* splice MO was assessed using primers flanking exon 3:

(5'-CCGTGACAATGTGCCTAATG-3') (*hmgcrb* forward) and

(5'-CAGATCAATCAGCAGCAGGA-3') *(hmgcrb* reverse).

The efficiency of the *pggt1b* splice MO was assessed using primers flanking exon 2:

(5'-TCTTCTGCCGGTCCATCC-3') (*pggt1b* forward) and

(5'-GCGGTAGTGAGCGGTGAT-3') *(pggt1b* reverse).

The PCR products were first separated by gel electrophoresis then excised from the gel and purified using the Qiagen gel purification kit (Qiagen), according to the manufacturer's instructions. Sequencing was performed to verify *hmgcrb* MO-induced splicing using the CEQ-8000 Genetic Analysis System and the aforementioned set of primers.

2.4 Results

2.4.1 Pharmacological inhibition of the HMGCR enzyme leads to cerebral-vascular defects in developing zebrafish

Sequence alignment of the partial catalytic sites of the HMGCR proteins revealed that the statin-binding residues (Istvan and Deisenhofer, 2001) are conserved in both zebrafish HMGCR paralogs, which might suggest functional conservation between mammals and fish. We first used the Tg(*fli1:EGFP;Gata-1:dsRED*) line for the simultaneous visualisation of the vascular network and circulating erythrocytes during development. Treatment of these embryos beginning at 1-2 hpf with 0.5 mg/L ATV in embryo medium, in a single-exposure manner, did not affect the vascular patterning or morphology at the 15-25 somite stage (19 hpf) (data not shown). However, by 28 hpf, ATV treatment resulted in grossly dilated and diffusely shaped primitive cerebral vessels in the forebrain and midbrain (**Fig**. **2.1A-E and Fig. 2.2A-D**), in addition to the abnormal confinement of stagnant dsRED-positive erythrocytes and an attenuated circulation in the cerebral region (**Fig. 2.1F and G**). These observations are indicative of impaired vessel wall function as the primary cause for the extravasation of erythrocytes at subsequent stages of development. At the doses used, ATV-exposure did not induce defects in angiogenesis, as the trunk vasculature and the formation of the segmental arteries were unaffected in these embryos, reflecting the cerebral-vascular-specific nature of these effects at the doses of statins used (**Fig. 2.3A-D**).

By 33 hpf, cerebral hemorrhage was evident in 46% of embryos (137/298). The locality and severity of the phenotype were variable in the brain, reflecting the multifocal nature of the hemorrhages (**Fig. 2.4A-D**). At 48 hpf, the extent of hematoma was

evaluated with o-Dianisidine (OD), a sensitive marker of hemoglobin, which revealed extensive hemorrhaging in the forebrain, midbrain and the ventricular zone, along with appreciable reductions in the abundance of circulating erythrocytes in the pericardium, the sinus venosus and the tail region (**Fig. 2.4E and F**). Cross sections of embryos stained with OD at 48 hpf revealed hematomas predominantly in the telencephalon and tectum (**Fig. 2.4G and H**). The incidence of hemorrhage increased in a dose-dependent manner with ATV treatment (**Fig. 2.4I**).

To confirm the vascular specificity of these defects, we performed confocal microscopy at 48-52 hpf on Tg(*fli1:EGFP*);(*gata-1:DsRed*) embryos. This analysis revealed progressive leakage of erythrocytes from the prosencephalic artery (PrA) in ATV-treated embryos, and when compared with the fully functional PrA observed in DMSO-treated embryos, the PrA in ATV-treated embryos supported only markedly attnuated circulation (**Fig. 2.5A-D**). Taken together, these data confirm that the blood-filled and vastly enlarged nascent cranial vessels observed at 26-28 hpf (**Fig. 2.1A-G**) are prone to leakiness and rupture at subsequent stages of development.

Loss of vascular integrity in the brain was further substantiated using fluorescence microangiography. This revealed that unlike the fully lumenised brain vasculature in DMSO-treated embryos (judged by the retention of the fluorescent microspheres in these vessels), ATV-treated embryos appeared to have less lumenisation and also exhibited a general tendency to extravasate the injected microspheres at the sites of hemorrhage (**Fig. 2.5E and F**), hence further attesting to the loss of vascular stability in the brain. We next sought to assess the smooth muscle cell coverage in these embryos using DAF-2 DA, a membrane-permeable compound that reacts with nitric oxide (NO) to

Figure 2.1: Pharmacological inhibition of the HMGCR pathway induces cerebral-vascular defects in developing zebrafish. (A) Representative **s**chematic diagram of a 28 hpf zebrafish embryo, with the blue boxed area denoting the forebrain and the pink boxed area showing the midbrain regions. Scale bar = 200 μm. (B-G) Representative photomicrographs of Tg(*fli1:EGFP*);(*gata-1:DsRed*) embryos incubated in DMSO or 0.5 mg/L ATV (Atorvastatin) and imaged at 28 hpf. Abbreviations: PMBC, primordial midbrain channel; MCeV, middle cerebral vein; PPrA, primitive prosencephalic artery. White *arrows* indicate the abnormally dilated vessels in the forebrain and midbrain, whereas the black *arrow* denotes area of stagnant erythrocyte accumulation in the head. Scale bar = 40 μm.

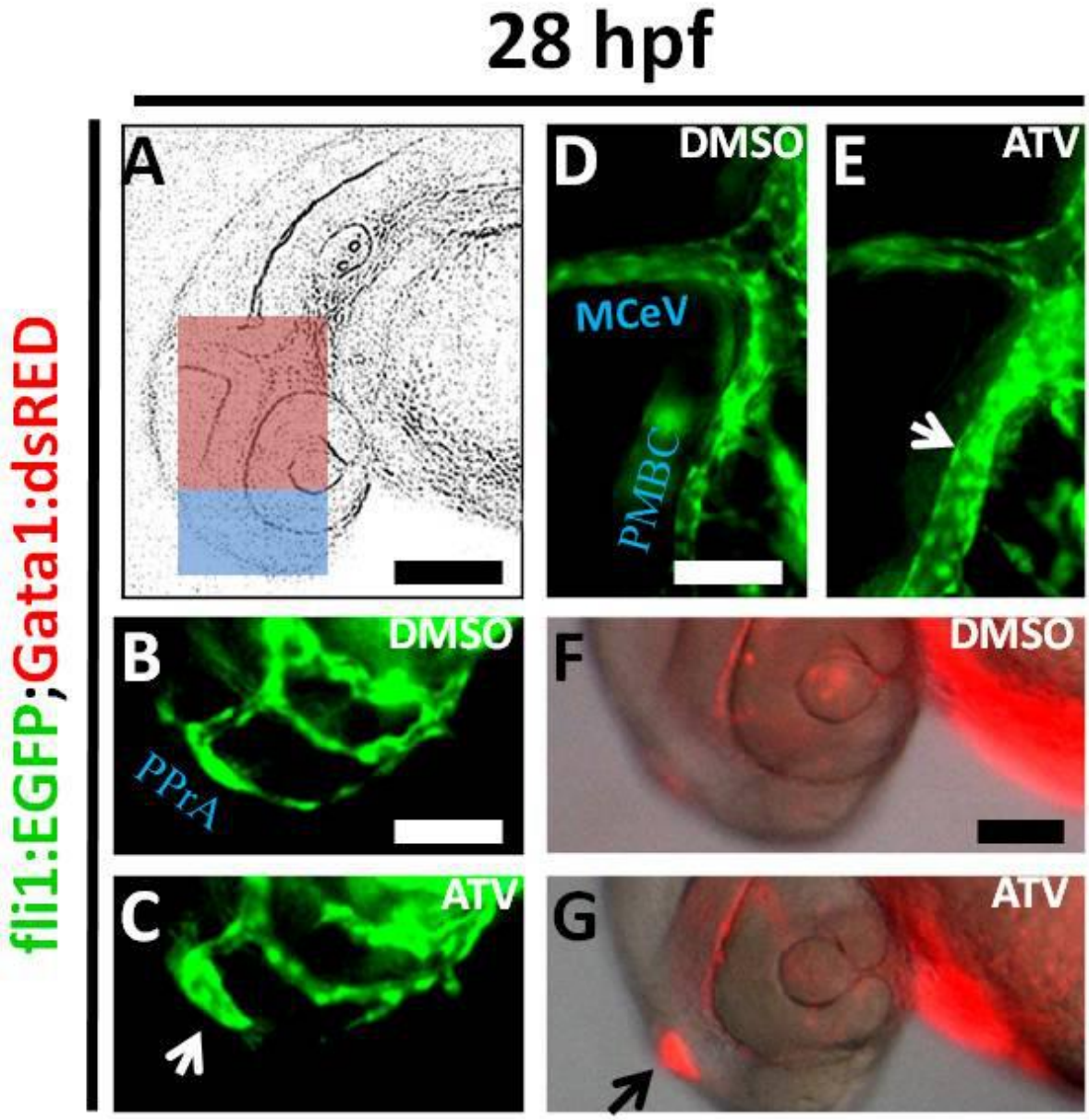
28 hpf
fli1:EGFP;Gata1:dsRED
A
D
DMSO
MCeV
PMBC
E
ATV
B
DMSO
PPrA
F
DMSO
C
ATV
G
ATV

Figure 2.2: Atorvastatin (ATV) exposure results in clusters of abnormally dilated cerebral vessels in the forebrain and hindbrain. (A, B) Representative photomicrographs of Tg(*fli1:EGFP*) embryos exposed to DMSO or 0.5 mg/L ATV and imaged at 28 hpf. White *asterisks* indicate abnormally dilated PPrA and PMBC (see Fig. 2.1 legend for abbreviaions). Anterior is to the left and dorsal to the top. Scale bar = 40 μm. (C, D) 2D quantification of 28 hpf zebrafish cerebral vessel diameters. Data are presented as the mean and standard error of the mean; N = 11, $p = 0.002$ (C) and N=11, $p < 0.001$ (D).

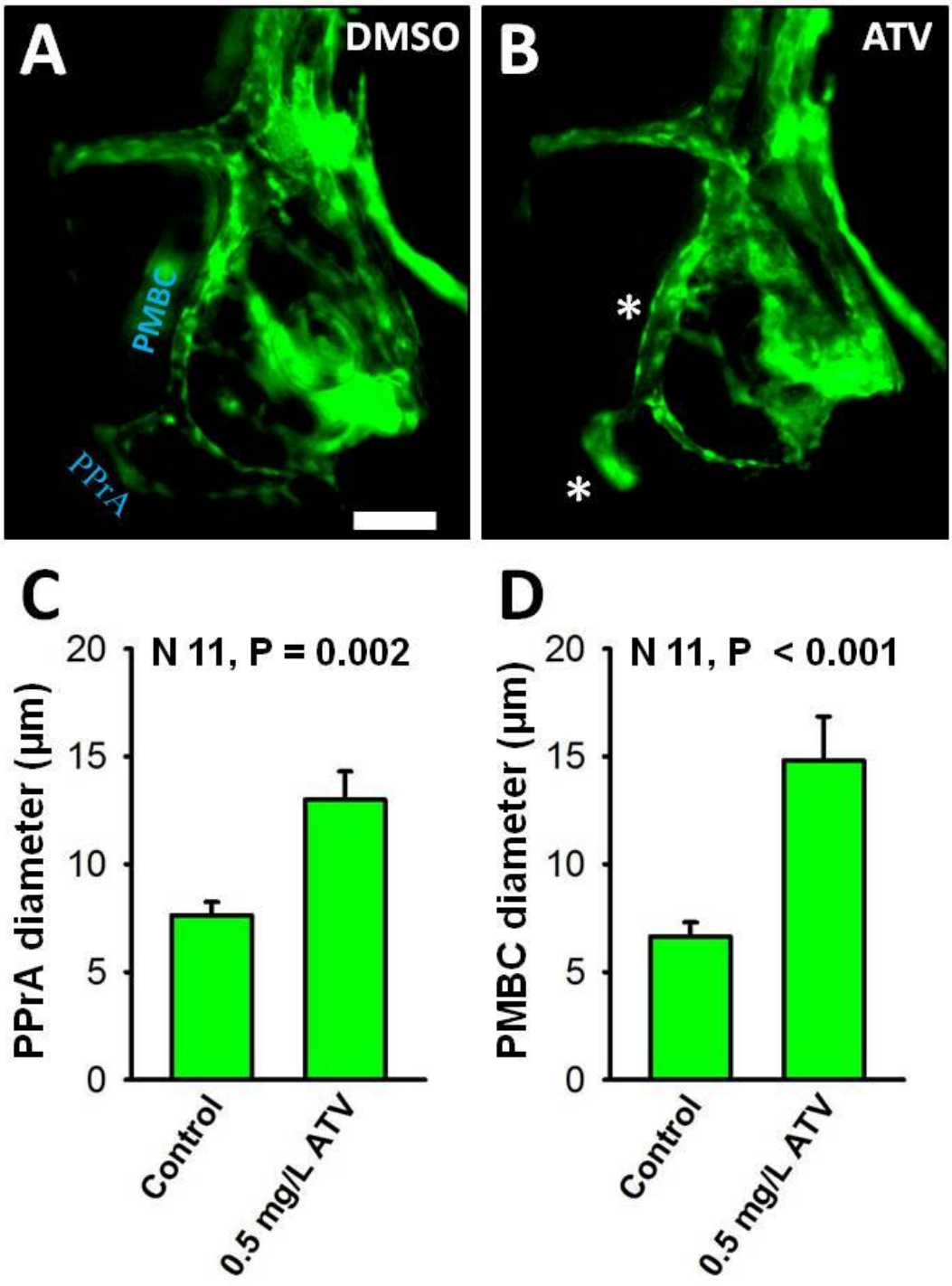
A
DMSO
PMBC
PPrA
B
ATV
*
*
C
N 11, P = 0.002
PPrA diameter (µm)
20
15
10
5
0
Control
0.5 mg/L ATV
D
N 11, P < 0.001
PMBC diameter (µm)
20
15
10
5
0
Control
0.5 mg/L ATV

Figure 2.3: Embryos with CNS hemorrhaging do not have defects in trunk angiogenesis and patterning. (A, B) Representative fluorescent photomicrographs of Tg(*fli1:EGFP*) embryos at 48 hpf, showing the trunk vasculature after exposure to DMSO or 0.5 mg/L ATV. Boxed area denotes the field of view in C and D. Scale bar = 100 μm. (C, D) Close-up of the trunk vasculature of embryos in panels A and B. Abbreviations: DLAV: dorsal-longitudinal anastomatic vessel, ISV: intersegmental vessel. Scale bar = 50 μm.

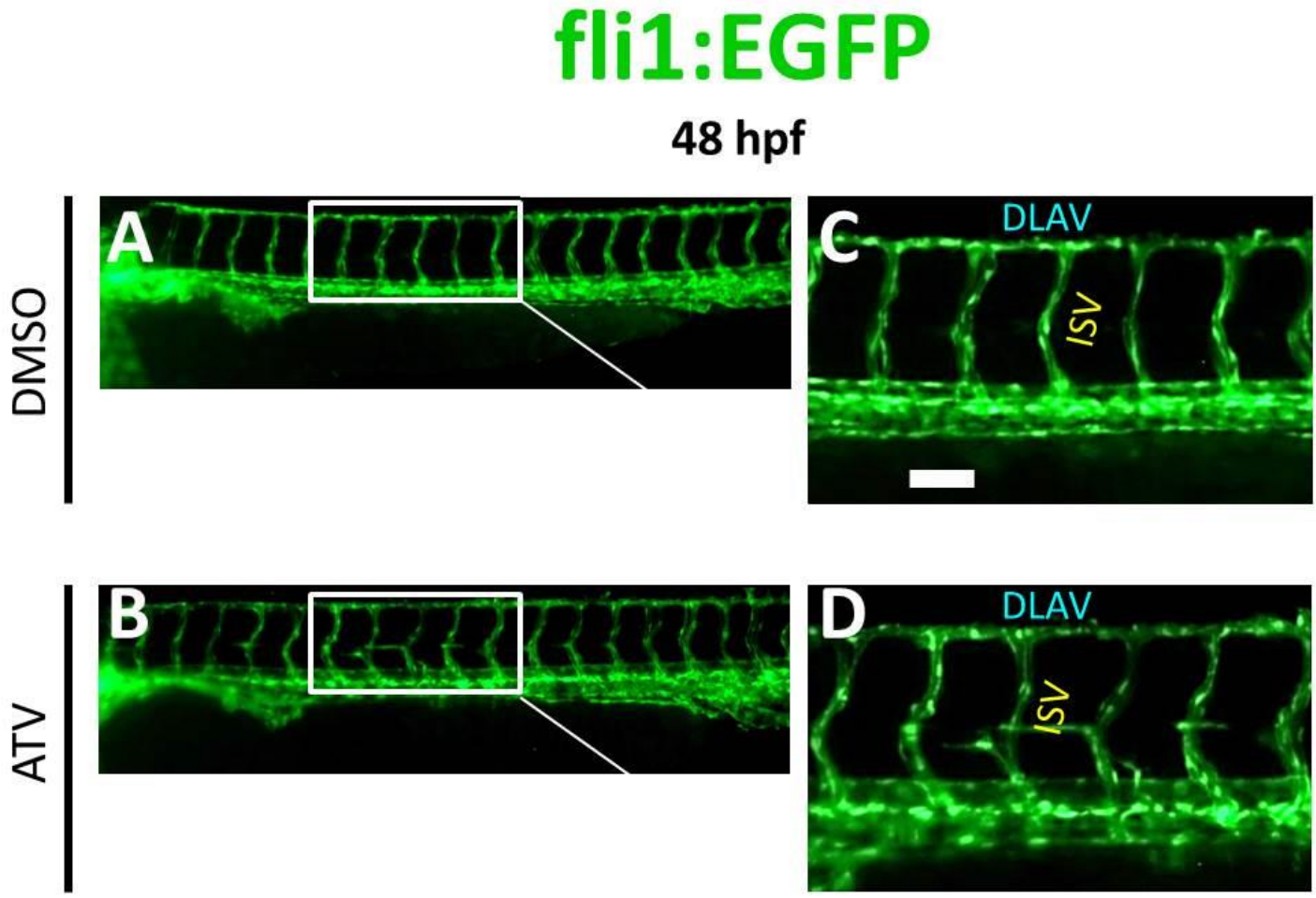
fli1:EGFP
48 hpf
DMSO
ATV
A
B
C
D
DLAV
ISV
DLAV
ISV

Figure 2.4: **Pharmacological inhibition of the HMGCR pathway induces cerebral hemorrhage in developing zebrafish.** (A-D) Photomicrographs of embryos incubated in 0.5 mg/L ATV and imaged at 33 hpf. Black *arrows* denote areas of hemorrhage. Scale bar = 200 μm. (E, F) Bright-field images of zebrafish embryos incubated in DMSO or 0.5 mg/L ATV, stained with o-Dianisidine (OD) and imaged at 48 hpf. Black *arrows* indicate sites where abnormal accumulation of hemoglobin-containing blood was detected in the brain. Blue *arrow* denotes OD-positive cells in the pericardium, green *arrow* shows the sinus venosus and red *arrow* designates the tail region. Scale bar = 200 μm. (G, H) Transverse sections through the embryo head at 48 hpf stained with OD. Abbreviations: te, tectum; tel, telencephalon. Scale bar = 200 μm. (I) Percentage of embryos treated with various doses of ATV and scored for the presence of cerebral hemorrhage at 48 hpf. Numbers above the bars represent the ratios used to calculate the percentages.

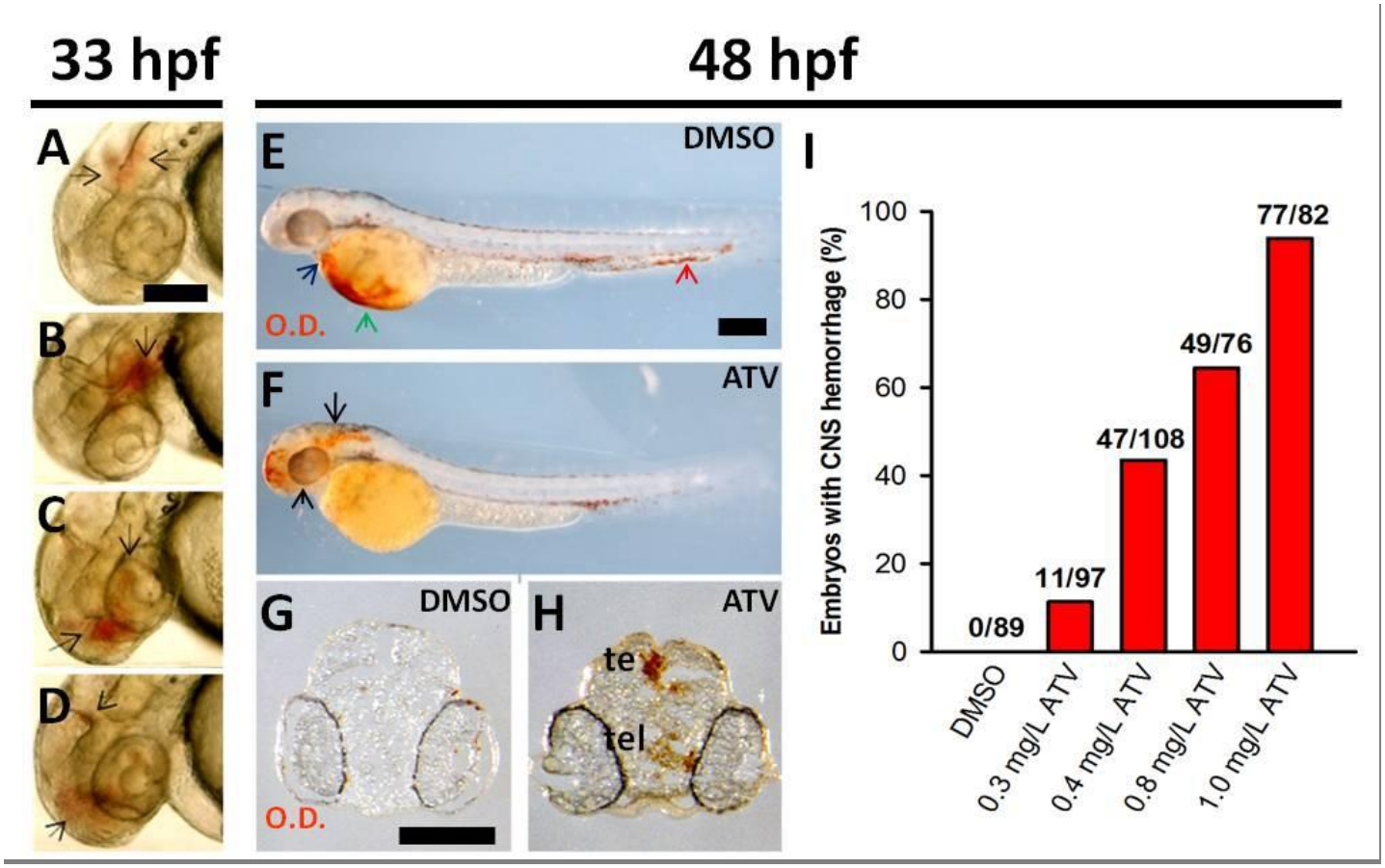
33 hpf
48 hpf
A
B
C
D
E
DMSO
O.D.
F
ATV
G
DMSO
O.D.
H
ATV
te
tel
I
Embryos with CNS hemorrhage (%)
100
80
60
40
20
0
0/89
11/97
47/108
49/76
77/82
DMSO
0.3 mg/L ATV
0.4 mg/L ATV
0.8 mg/L ATV
1.0 mg/L ATV

form the fluorescent DAF-2T which is a marker for functional smooth muscle cell coverage in zebrafish (Zeng et al., 2009; Lou et al., 2011).

However, no vascular smooth muscle cell coverage was detected in the brain or trunk during the early stages of normal zebrafish development (data not shown), which suggests that nascent vessels are more prone to statin-induced hemorrhage, at least partly by virtue of inadequate coverage with smooth muscle support. This observation is consistent with molecular and genetic evidence suggesting that the expression of early vascular smooth muscle cell markers in zebrafish are not detectable before the larval stage (before hpf) (Santoro et al., 2009; Seiler et al., 2010).

We also exposed embryos at 1-2 hpf to Cerivastatin (CVT), a structurally different statin molecule with a comparable affinity for the active site of HMGCR (Istvan and Deisenhofer, 2001). Incubation of 2 hpf embryos in CVT (0.15 mg/L), in a single exposure manner, resulted in 58% of embryos demonstrating cerebral hemorrhage by 33 hpf (108/174), which was a phenocopy of the ATV-treatment.

To further test the specific nature of the pharmacological treatments, a metabolite rescue experiment was conducted using mevalonate, the immediate product of the HMGCR-catalysed reaction and a precursor of both cholesterol and isoprenoids. Treatment of 1-cell stage embryos with ATV (0.5 mg/L) in the presence of mevalonate (3.2 μmol/L) was sufficient to rescue the hemorrhage phenotype, as none of these embryos exhibited apparent hemorrhages (0/121). In contrast, 53% of the embryos treated with ATV (0.5 mg/L) in the presence of DMSO showed cerebral hemorrhage by 48 hpf (59/112). Treatment with mevalonate alone did not induce any overt developmental defects. The ability of mevalonate to rescue the phenotype suggests that deficiencies in

Figure 2.5: **Pharmacological inhibition of the HMGCR results in loss of vascular stability and induces vessel rupture.** (A, B) Representative bright-field micrographs of 48-52 hpf Tg(*fli1:EGFP*);(*gata-1:DsRed*) embryos treated with DMSO or 0.5 mg/L ATV. The boxed region shows where hemorrhage is observed. Scale bar = 200 μm. (C, D) Representative composite confocal z-stack projections of the boxed regions in the same Tg(*fli1:EGFP*);(*gata-1:DsRed*) embryos. Abbreviations: PrA, prosencephalic artery. Scale bar = 40 μm. (E, F) Representative photomicrographs of 48-52 hpf embryos treated with DMSO or 0.5 mg/L ATV and subjected to fluorescent microangiography by intravascular injection of red-fluorescent microspheres. White *arrow* shows the site of microsphere extravasation. Scale bar = 200 μm.

48-52 hpf
A
DMSO
B
ATV
C
DMSO
PrA
fli1:EGFP
Gata1:dsRED
D
ATV
E
DMSO
Microangiography
F
ATV

one or more of the metabolites downstream of mevalonate within the HMGCR pathway may be implicated in the emergence of the hemorrhage phenotype.

2.4.2 Morpholino-mediated depletion of *hmgcrb* mRNA levels leads to cerebral-vascular defects in developing zebrafish

Zebrafish possess two paralogous genes encoding HMGCR proteins. It is speculated that teleosts, including zebrafish, underwent a complete genome duplication event 250 million years ago (Van de Peer et al., 2009), resulting in the retention of many genes in duplicate. Of the genes, The *hmgcrb* transcripts are maternally-enriched and exhibit a ubiquitous expression pattern throughout early embryogenesis, whereas *hmgcra* mRNA is only detected at 5 dpf and is confined to the liver and the anterior intestine (Thorpe et al., 2004). A similar temporal expression pattern for these genes was observed using RT-PCR on total RNA harvested from a pool of embryos at different developmental stages (data not shown).

To substantiate the phenotypic specificity of the statin-induced cranial vascular defects, we induced a transient loss of *hmgcrb* gene function with a morpholino oligonucleotide (MO) designed to hybridise with the third exon-intron boundary of the *hmgcrb* pre-mRNA (**Fig. 2.6A**). The injection of 2 ng of this *hmgcrb* MO resulted in approximately 45% (91/203) of the embryos displaying cerebral hemorrhage at 48 hpf, along with reduced abundance of erythrocytes in the pericardium and the sinus venosus as detected by whole-mount OD staining (**Fig. 2.6B and C**).

The morphants demonstrated no other overt developmental defects and eventually recovered from the initial hemorrhage, further indicating that the impaired

HMGCR function only affected cerebral-vascular development during a critical period when nascent vessels in the brain are more prone to rupture. This suggests that *hmgcrb* expression is dispensable in more mature vessels. Injection of higher quantities of the *hmgcrb* MO (>8 ng) resulted in developmental arrest, defective angiogenesis in the trunk, lack of circulation and occasional pericardial edema, and most of these embryos lacked the cranial hemorrhage phenotype (data not shown). The efficiency of the genetic ablation of *hmgcrb* expression was tested at 48 hpf by RT-PCR (**Fig. 2.6D**) and sequencing (**Fig. 2.6E and F**) using primers spanning the third exon-intron boundary.

As with the statin-treatment, the exogenous supplementation of these embryos with mevalonate nearly completely rescued the splice MO-induced vascular defects at 48 hpf, with only 2.2% of the MO-injected embryos (2 ng) incubated in mevalonate (4.4 μmol/L) showing cerebral vascular defects (7/318) at 48 hpf. A second MO directed against the AUG translation-start site also mirrored the statin-induced hemorrhage phenotype (data not shown). Overall, these observations further support an essential role for HMGCR-mediated lipid metabolism in cerebral-vascular morphogenesis.

Figure 2.6: **MO-mediated depletion of the HMGCR levels phenocopies ATV-treatment.** (A) Partial *hmgcrb* pre-mRNA structure (not to scale) showing the exons (*boxes*), introns (*black lines*), the target of *hmgcrb* MO (*red vertical arrow*) and the positions of forward and reverse primers (*black arrows*) used to test the efficiency of the *hmgcrb* MO. (B, C) Representative bright-field micrographs of 48 hpf embryos injected with *hmgcrb* MO and control MO, stained with OD. Black *arrow*s indicate sites of hemorrhage and blue *arrow* denotes the sinus venosus. Anterior is to the left and dorsal to the top. Scale bar = 200 μm. (D) RT-PCR analysis of *hmgcrb* mRNA in *hmgcrb* morphant and control MO-injected embryos at 48 hpf. MO injection results in the dose-dependent appearance of a band corresponding to a transcript lacking exon-3. Doses of ATV are indicated above each lane. (E-F) Sequence analysis of cDNA from *splice* MO-injected embryos confirms the deletion of Exon-3.

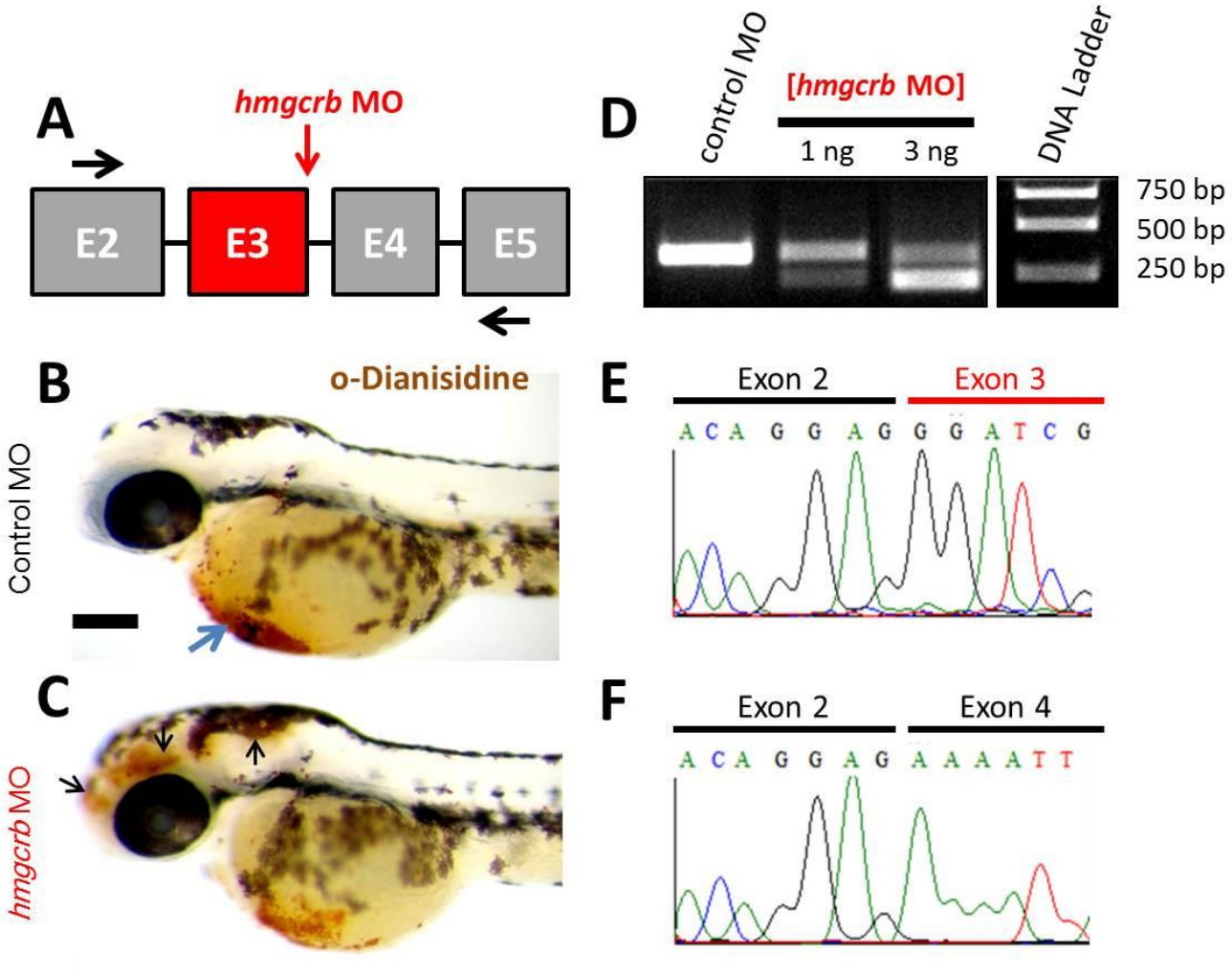
A
hmgcrb MO
E2
E3
E4
E5
B
o-Dianisidine
Control MO
C
hmgcrb MO
D
control MO
[hmgcrb MO]
1 ng
3 ng
DNA Ladder
750 bp
500 bp
250 bp
E
Exon 2
Exon 3
A C A G G A G G G A T C G
F
Exon 2
Exon 4
A C A G G A G A A A A T T

2.4.3 A deficiency in GGPP biosynthesis and impaired GGTase I-facilitated prenylation of Rho GTPases leads to cerebral-vascular defects in developing zebrafish

We next tested the hypothesis that statin-induced defects in vascular stability were attributable to perturbations in GGPP biosynthesis. To test this hypothesis, 1-cell stage embryos (1-2 hpf) were treated with ATV (0.5 mg/L) in the presence of geranylgeranyl-pyrophosphate (GGPP, 4 mg/L) or the vehicle (DMSO:methanol; 50:50, v/v). The addition of GGPP effectively rescued the hemorrhage phenotype, and by 48 hpf approximately 7% of the embryos co-administered with ATV and GGPP demonstrated cerebral hemorrhages (9/131), compared with 56% of control embryos receiving ATV and the vehicle (80/143). The near-complete rescue of the vascular phenotype with GGPP supplementation suggested a requirement for prenylation in the establishment of developmental cerebral-vascular stability. To further demonstrate that decreased GGPP bioavailability underlies these cerebral-vascular defects, we selectively targeted the prenylation pathway. Prenylation of small GTPases, such as Rac1, RhoA and cdc42, is catalyzed by the cytosolic isoprenyl transferase, geranylgeranyl pyrophosphate I (GGTase I) (Peterson et al., 2006; Roberts et al., 2008).

This enzyme, GGTase I, catalyzes the transfer and binding of the 20-carbon geranylgeranyl isoprenoid to the cysteine-residue of the CAAX motif at the C-terminus of target Rho GTPases (**Fig. 2.7A**). This coupling constitutes a critical step for the translocation of the Rho GTPases to the plasma membrane and interaction with other lipophilic proteins. To specifically impair this pathway, we injected a splice-blocking morpholino targeting the second exon-intron boundary of the *pggt1b* pre-mRNA, which

encodes the β-subunit of GGTase I (**Fig. 2.7B**). Injection of 2.5 ng of the *pggt1b* MO into 1-cell stage embryos resulted in 23% of the embryos showing cerebral hemorrhage by 48 hpf (49/213) (**Fig. 2.7C and D**), thus phenocopying, both spatially and temporally, the cerebral-vascular defect associated with the inhibition of HMGCR. Injection of higher doses of *pggt1b* MO (6 ng) only slightly increased the frequency of hemorrhages (28%, 51/180), but most of these embryos were developmentally delayed (data not shown). The efficacy of the *pggt1b* MO was tested by RT-PCR on total RNA harvested from 48 hpf embryos that were previously injected with 2.5 ng MO, and showed a near complete depletion of wild-type *pggt1b* transcripts (**Fig. 2.7E and F**). Based on sequence analysis, we predicted that MO-induced alternative splicing of exon-2 would result in a frame-shift, thereby introducing a premature termination codon (TAA) in exon-3, thus targeting this mRNA for nonsense-mediated decay.

These results support that MO- and statin-induced inhibition of the HMGCR pathway impairs cerebral-vascular stability due to reduced GGPP biosynthesis and the consequential decrease in the prenylation status and membrane targeting of CAAX proteins, which serve as substrates for GGTase I. The molecular nature of these statin-induced vascular defects were further characterised by the use of the Tg(*fli1:EGFP-cdc42wt*)^{y48} line in which the expression of EGFP-cdc42 fusion protein shows a perivacuolar co-localisation and is restricted to the endothelial cells (Kamei et al., 2005). The protein cdc42, a RhoA GTPase, is implicated in the regulation of vacuole formation, lumenisation and mediation of endothelial barrier function (Kouklis et al., 2003; Broman et al., 2006; Ramchandran et al., 2008; Spindler et al., 2010) and it requires

Figure 2.7: MO-mediated ablation of *pggt1b* mimics statin and *hmgcrb* MO-induced cerebral hemorrhages and effectively reduces the wild-type *pggt1b* mRNA. (A) Schematic representation of GGTase I-mediated transfer of a 20-carbon geranylgeranyl lipid to the cysteine residue of Rho GTPases. (B) Partial *pggt1b* pre-mRNA structure (not to scale) showing the exons (*boxes*), introns (*black lines*), the target of *pggt1b* MO (*red vertical arrow*) and the positions of forward and reverse primers (*black arrows*) used to test the efficiency of the *pggt1b* MO. (C and D) Representative bright-field photomicrographs of 48 hpf embryos. The blue *arrow* denotes the site of blood extravasation in the midbrain region of the embryo injected with *pggt1b* MO. Anterior is to the left and dorsal to the top. Scale bar = 200 μm. (E, F) RT-PCR on total RNA extracted from non-injected and MO-injected embryos at 48 hpf to assess *pggt1b* mRNA levels. MO injection results in the loss of wild-type *pggt1b* mRNA (see text for details).

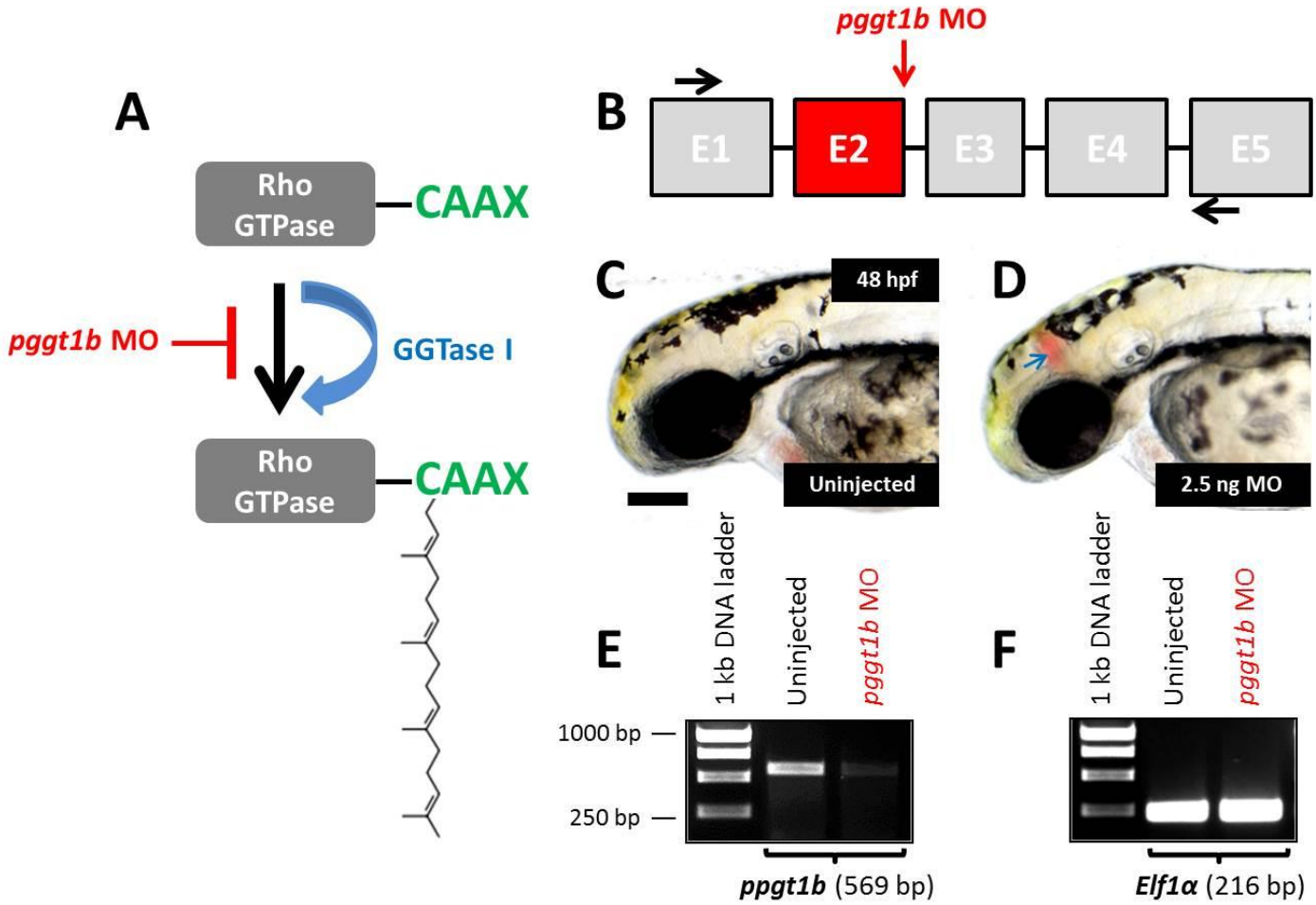
A
Rho GTPase
CAAX
pggt1b MO
GGTase I
Rho GTPase
CAAX
B
pggt1b MO
E1
E2
E3
E4
E5
C
48 hpf
Uninjected
D
2.5 ng MO
E
1 kb DNA ladder
Uninjected
pggt1b MO
1000 bp
250 bp
ppgt1b (569 bp)
F
1 kb DNA ladder
Uninjected
pggt1b MO
Elf1α (216 bp)

geranylgeranylation, downstream of HMGCR pathway, for its activation (Peterson et al., 2006; Roberts et al., 2008).

Treatment of Tg(*fli1:EGFFP-cdc42wt*)^{y48} embryos with ATV at the 1-cell stage led to a noticeable reduction in intra-endothelial expression of EGFP-cdc42 in the brain and the trunk as early as 24 hpf (data not shown). The decline in vascular-specific EGFP-cdc42 expression was also clearly evident in the head and trunk vasculature of these embryos at 48 hpf (**Fig. 2.8A and B**), the stage when cerebral hemorrhage was most preponderant in statin-treated embryos. The attenuated EGFP-cdc42 expression was further validated by measuring EGFP signal intensity using ImageJ software (**Fig. 2.8E and F**).

We further established that the reduction in fluorescence intensity was not attributable to global developmental defects, vascular regression or defective angiogenesis resulting from a down-regulation of the *fli* promoter in Tg(*fli1:EGFP-cdc42wt*)^{y48}, since the expression of fli1:EGFP was unaffected in response to statin treatment, and the brain and trunk vessel morphology and segmental artery formation was unaltered (**Fig. 2.8C and D**). Similarly, quantification of the EGFP signal intensity in these fish confirmed unaltered expression of the fli1:EGFP protein in the head or trunk vessels (**Fig. 2.8G and H**). Together, these data reflect a specific reduction in cdc42 levels as a consequence of statin treatment. To investigate the localisation of cdc42 in response to statin exposure, we performed confocal microscopy on 48-52 hpf Tg(*fli1:EGFP-cdc42wt*)^{y48} embryos. We focused our attention on intersegmental vessels (ISVs) due to the ease of imaging. Whereas the EGFP-cdc42 expression in DMSO-treated embryos exhibited perivacular localisation, outlining the boundaries of the

intercellular lumen in the ISVs, the ATV-treated embryos had reduced EGFP-cdc42 expression in the ISVs and any expression was concentrated primarily at the base of the ISVs (**Fig. 2.8I and J**). Taken together, our evidence suggests that the endothelial-specific expression of cdc42 is markedly reduced concomitant with the onset and expansion of hematoma in the brain.

2.5 DISCUSSION

Through a combination of pharmacological blockers, metabolite rescue and genetic approaches, this study demonstrates that a transient disruption in the HMGCR pathway induces intracranial hemorrhaging in zebrafish at a predictable embryonic stage, which highlights a metabolic contribution to developmental vessel stabilisation. This cerebral-vascular-specific phenotype was not associated with any other developmental abnormalities. Of particular clinical significance is that these embryos manifest certain pathophysiological features that closely resemble CCM pathologies in humans and mice, such as abnormally dilated and blood-filled cranial microvessels prior to the onset of extravasation, intracranial hemorrhage and expansion of hematoma, along with evidence of thrombosis in the vicinity of the lesions. It is likely that inhibition of the HMGCR pathway perturbs signalling processes that mitigate the assemblage of angioblasts into nascent vascular tubes, thus making them more prone to rupture and leakage.

Interestingly, the extravasation of blood components is only detected in the head, implying that the vessels in this region are more fragile at this developmental period, hence hence more easily ruptured.

Figure 2.8: Inhibition of the HMGCR pathway abolishes the intra-endothelial expression of cdc42. (A, B) Representative photomicrographs of Tg(*fli1:EGFP-cdc42wt)*^{y48} embryos treated with DMSO or 1.0 mg/L ATV and imaged at 48-52 hpf. (C, D) Representative photomicrographs of Tg(*fli1:EGFP*) embryos treated with DMSO or 1.0 mg/L ATV and imaged at 48-52 hpf. Anterior is to the left and dorsal to the top. Scale bar = 200 μm. (E-H) Graphs plotting relative EGFP signal intensities in the head and trunk vasculature (as denoted by the dotted white boxes in A-D) of (*fli1:EGFP-cdc42wt)*^{y48} and Tg(*fli1:EGFP*) embryos treated with DMSO or 0.5 mg/L ATV. Data are presented as the mean and standard error of the mean. N = 15 embryos, t-test, $p<0.001$ (for E and F). (I, J) Representative composite confocal z-stack projections of the trunk region of Tg(*fli1:EGFP-cdc42wt)*^{y48} embryos, showing the localisation of EGFP-cdc42 in a single intersegmental artery (ISV). Green *arrow* denotes perivacuolar expression of EGFP-cdc42. Scale bar = 40 μm. Anterior is to the left and dorsal to the top.

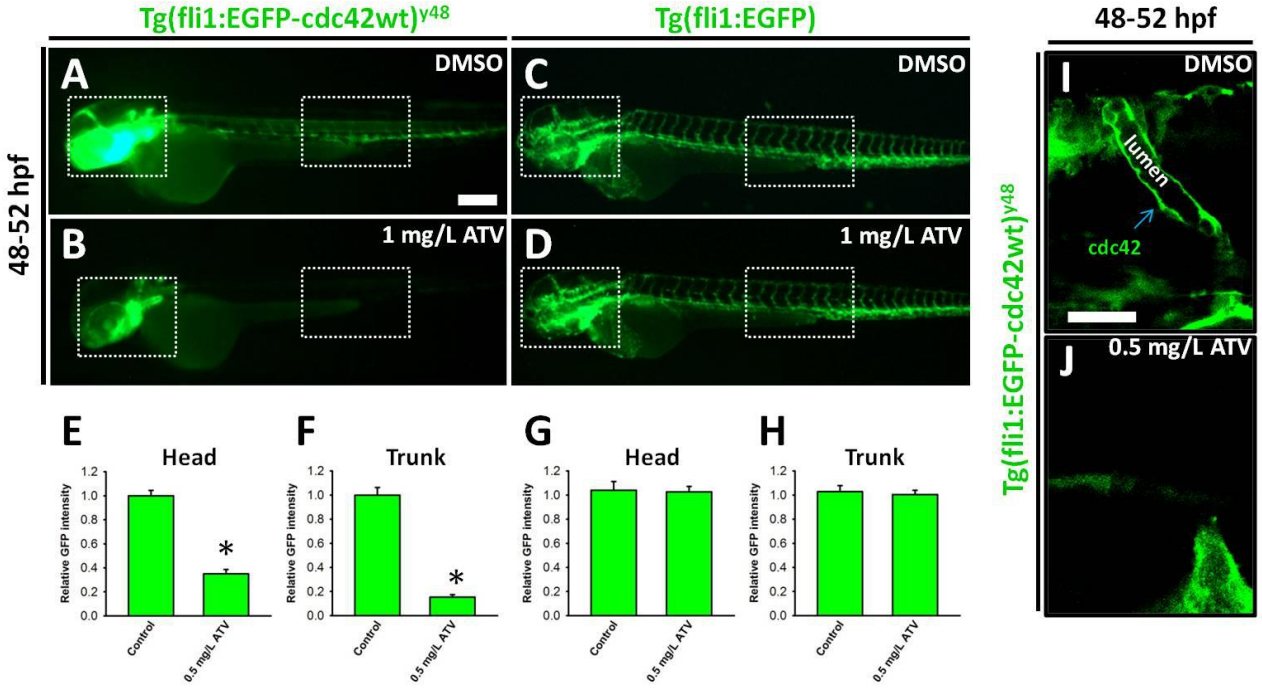
Tg(fli1:EGFP-cdc42wt)y48
Tg(fli1:EGFP)
48-52 hpf
A
DMSO
C
DMSO
B
1 mg/L ATV
D
1 mg/L ATV
48-52 hpf
I
DMSO
lumen
cdc42
J
0.5 mg/L ATV
Tg(fli1:EGFP-cdc42wt)y48
E
Head
F
Trunk
G
Head
H
Trunk
Relative GFP intensity
Control
0.5 mg/L ATV

Since the onset of hemorrhage and the expansion of hematoma correspond to a period of rapid angiogenesis during which numerous newly formed blood vessels invade the brain (Isogai et al., 2001), it is plausible that these nascent vessels that carry blood for the first time would lack adequate coverage with support cells, making them weak and prone to rupture. Consistent with this, DAF-2DA staining showed no positive signal for smooth muscle cells in the brain or trunk vasculature during early development, consistent with previous studies (Santoto et al., 2009), which suggests that inadequate endothelial contact with support cells can predispose these early vessels to statin-induced hemorrhage. We have shown by fluorescence microangiography that defects in the establishment of endothelial cell-to-cell associations contribute to the loss of vascular stability in these embryos. Consistent with this assertion, zebrafish deficient in VE-cadherin, an endothelial-specific adhesion protein located in cell-to-cell junctions and important for vessel stabilisation, exhibit cerebral-vascular fragility and hemorrhage at 48 hpf in zebrafish (Montero-Balaguer et al., 2009).

At higher doses (5-10 mg/L), we observed that statin treatment significantly inhibited angiogenic processes in the trunk (**Fig. 2.9A-C**), as evidenced by the incomplete or defective anterior to posterior sprouting of intersegmental vessels (ISV) emanating from the dorsal aorta (DA), thereby severely restricting circulation in the fish, and often resulting in pericardial edema, with almost no cerebral hemorrhages observed. This leads us to speculate that at higher doses, statin-treatment affects endothelial survival and migration, whereas at lower doses, vascular stability in the brain is compromised, to which the hemorrhage phenotype attests. This is also confirmed through

our reverse genetics approach, with high doses of *hmgcrb* MO inducing defective angiogenesis in the trunk.

It is intriguing that the temporal and spatial distribution of the vascular defects reported here are similar to those associated with the *bbh* (bubblehead) and *rhd* (redhead) mutations which were previously characterised in zebrafish (Buchner et al., 2007; Liu et al., 2007; see Chapter 1). These fish were reported to have hypomorphic mutations in the *pak2a* and *βpixA* genes that otherwise encode for proteins involved in regulating the activity and mediating the function of the Rho GTPases, Rac and cdc42 (Buchner et al., 2007; Liu et al., 2007). The disruption of vascular permeability in these embryos is consistent with the well-established roles of Rac and Cdc42 in the maintenance and stabilisation of endothelial barrier function (Spindler et al., 2010). The similar nature of the hemorrhages described in zebrafish that are deficient in pak2a and βPixA and those we have reported here suggests a molecular interaction between the HMGCR pathway and Rho GTPase signalling in the regulation of developmental vascular stability. This is further supported by the fact that both Rac and cdc42 are natural substrates for the β-subunit of GGTase I, which facilitates their post-translational modification by the addition of a mevalonate-derived geranylgeranyl lipid, a critical step required for the activation of these Rho GTPases (Peterson et al., 2006; Roberts et al., 2008). Interestingly, using the Tg(fli1:*EGFP-cdc42wt*)^{y48} line in which cdc42 protein is over-expressed in an endothelial-specific manner, we observed a decrease in the expression of EGFP-cdc42 in the cerebral and trunk vessels upon treatment with statins. This decrease was evident as early as 24 hpf and persisted to the onset of hemorrhage. We showed that the reduction in fluorescence intensity was not attributable to global developmental

Figure 2.9: At high dose (5-10 mg/L) ATV-exposure induces defective angiogenesis. (A-B) Representative fluorescent photomicrographs of the trunk region in embryos incubated in DMSO or 6 mg/L ATV and imaged at 28 hpf. Anterior is to left. Blue *arrows* show fully sprouted intersegmental vessels (ISV), red *arrows* show where endothelial cell migration is completely stalled and the white *asterisks* denote partially sprouted ISVs. (C) Percentage of embryos treated with various doses of ATV and scored for the presence of ISV sprouting defects at 28 hpf. Numbers above the bars represent the ratios used to calculate the percentages.

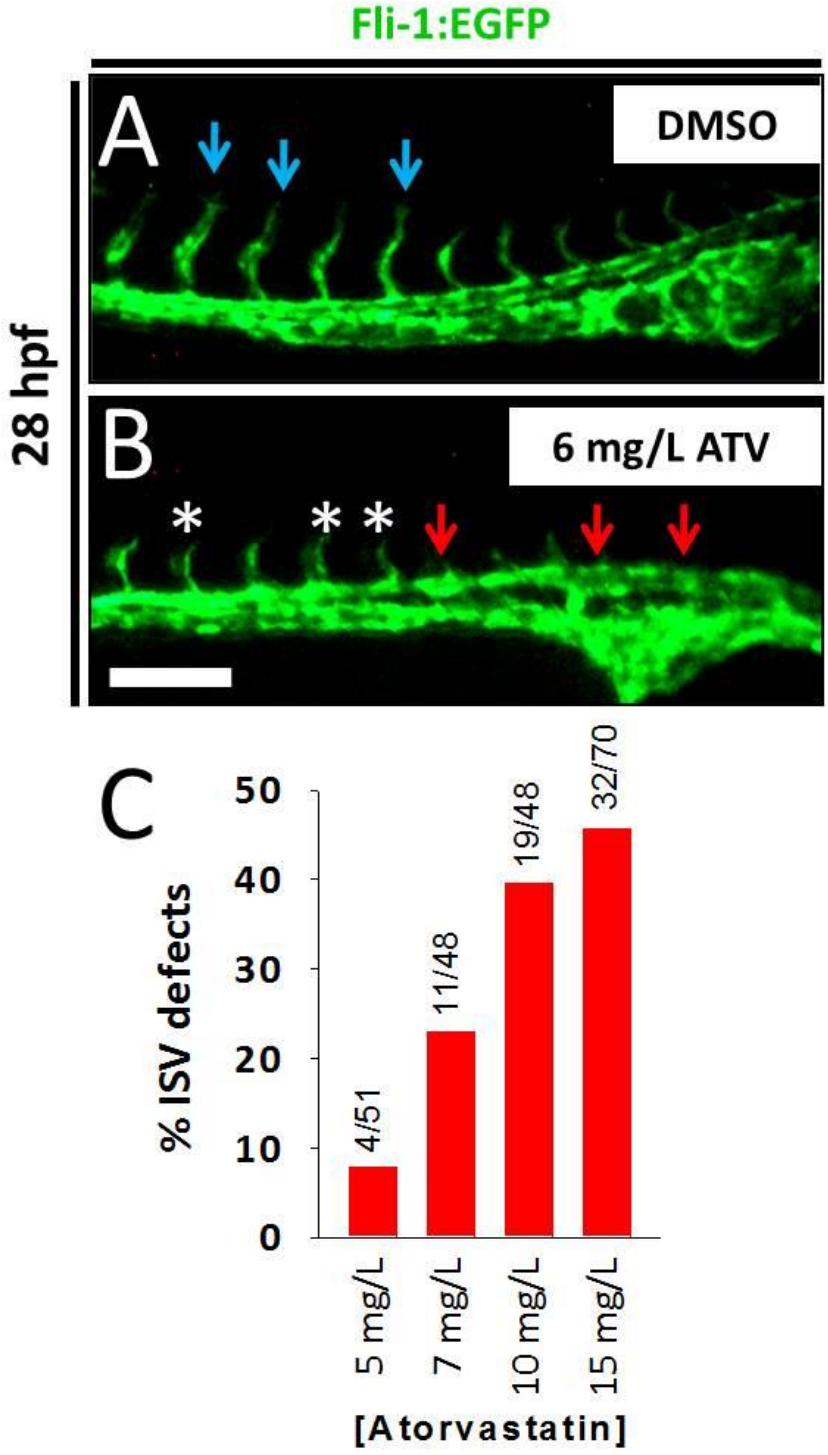
Fli-1:EGFP
28 hpf
A
DMSO
B
6 mg/L ATV
C
% ISV defects
0
10
20
30
40
50
4/51
11/48
19/48
32/70
5 mg/L
7 mg/L
10 mg/L
15 mg/L
[Atorvastatin]

defects or down-regulation of *fli1* promoter activity, since examination of Tg(fli1:eGFP) embryos showed no apparent alterations in fluorescence intensity nor signs of defects in cranial or segmental angiogenesis.

Collectively, this observation is suggestive of statin-induced degradation of cdc42 expression in the vasculature, and it further highlights *in vivo* how alterations of HMGCR activity can exert effects on the cellular dynamics of cdc42 expression. On the whole, the rescue of statin-induced hemorrhages by the addition of GGPP, along with the hemorrhage phenotype elicited by the disruption of GGTase I-mediated prenylation in zebrafish strongly supports a requirement for HMGCR activity for the stabilisation of nascent vessels during early angiogenesis. These data contrast, however with previous findings in mice. More specifically, in mice, the defective endothelial stability underlying CCM pathogenesis, thought to be mediated by RhoA hyperactivation, is greatly attenuated upon pharmacological ablation of the HMGCR pathway, possibly due to non-cholesterol dependent processes (Whitehead et al., 2009). This raises the possibility that modulation of HMGCR activity could be a therapeutic strategy to ameliorate CCM pathobiology (Li and Whitehead, 2010). More recently using a separate murine model of CCM, a more specific pharmacological inhibition of RhoA activity through direct targeting of the Rho kinase signalling pathway, was reported to be similarly effective in significantly reducing CCM genesis (McDonald et al., 2012). The hemorrhage phenotype described here does not induce lethality, as these embryos eventually resolve the brief disruption in vascular stability and resume normal development (**Fig. 2.10A-H**). This is in contrast with the embryonic lethality observed in mouse models of intracranial hemorrhage.

Recent studies in zebrafish have served to independently confirm a functional role for HMGCR pathway in the stabilisation of CNS vessels, thus lending further strength to the hypothesis we proposed (Hung et al., 2012; Shen et al., 2013). However, a shortcoming of this study is that we were unable to address the cell autonomy of HMGCR-function. More specifically, we could not clearly address whether HMGCR function is required in an endothelial-specific manner or whether it involves contribution from mural cells? Although, *hmgcrb* seems to be expressed in a ubiquitous manner during embryogenesis (Thorpe et al., 2004; Thisse and Thisse, 2004), it is important to establish the consequences of conditional endothelial-specific deletion or knockdown of *hmgcrb*.

Furthermore, the robust and spontaneous nature of the vascular phenotype described here, coupled with the optical transparency and accessibility of all of these processes, aided by the presence of tissue-specific transgenic lines and the possibility for high resolution imaging, make this model applicable for elucidating the pathophysiology of CCM-like lesions at various stages of progression.

On balance, I believe that this part of my Ph.D. dissertation has provided an additional level of insight into the critical pathways regulating vascular integrity by providing evidence for a metabolic contribution to this process. This raises the likelihood that reduced HMGCR activity could account for some of the unknown cases of CCM in individuals.

Figure 2.10: Embryos resolve cerebral-vascular defects and resume normal development. (A-H) Representative bright-field photomicrographs of zebrafish embryos incubated in DMSO or 0.5 mg/L ATV and stained with OD at various developmental stages. Black *arrows* indicate areas of hemorrhage and blue *arrows* indicate sinus venosus. Anterior is to the left and dorsal to the top. Scale bar = 200 μm.

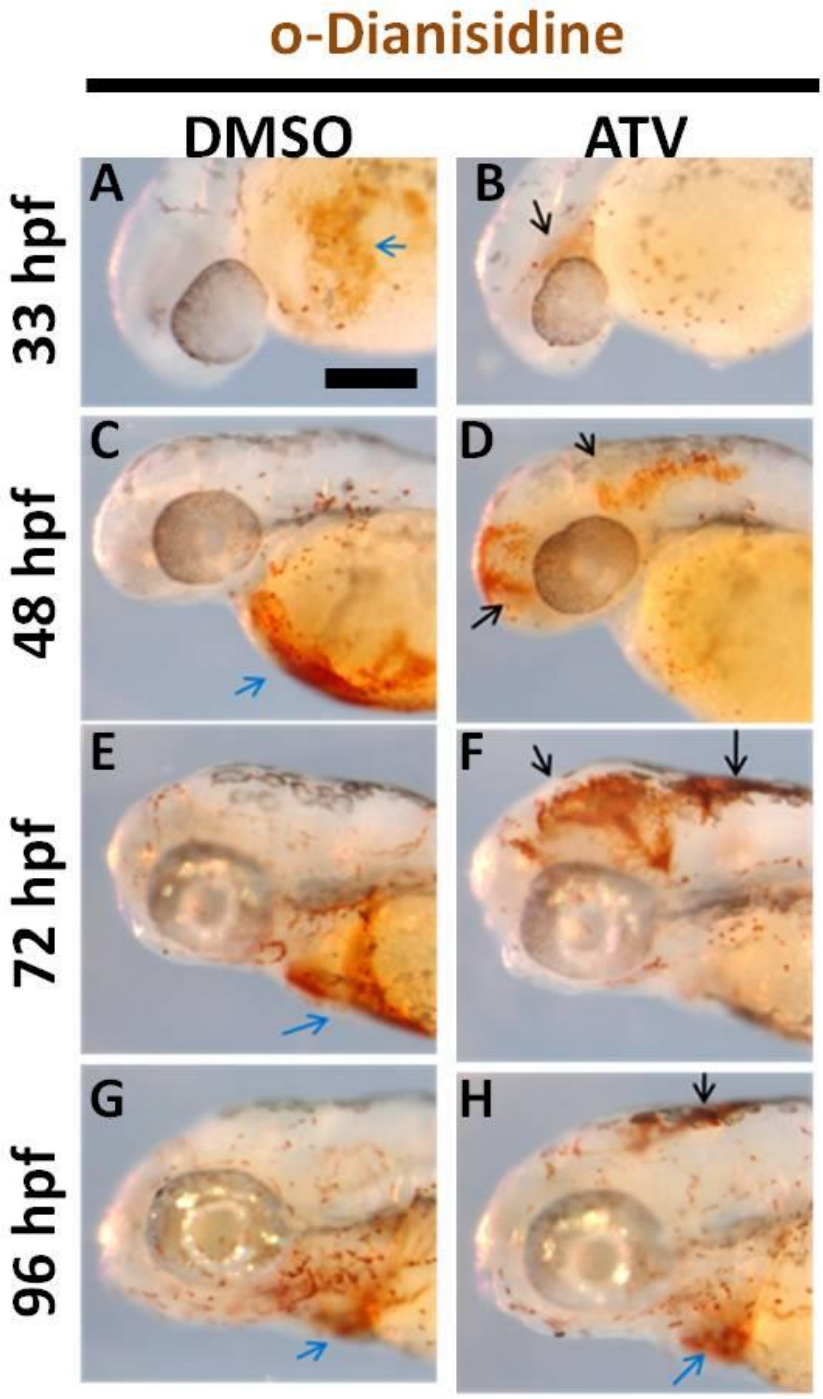
o-Dianisidine
DMSO
ATV
33 hpf
48 hpf
72 hpf
96 hpf
A
B
C
D
E
F
G
H

Chapter 3

Molecular and pathophysiological processes underlying intracerebral hemorrhage (ICH) in developing zebrafish

Author contributions:

Dr. Raymond W.M. Kwong helped with the RT-PCR analysis and assisted me with the western blot analysis. Ms. Sandra Noble and Mr. Rafael Godoy trained me for use of confocal microscopy and helped me in preparing and processing embryos for imaging. Dr. Steve F. Perry provided reagents for real-time RT-PCR and western blot analysis. Dr. Thomas W. Moon and Dr. Marc Ekker helped me design the experiments and assisted me in writing and revising this chapter to ensure that the content is scientifically sound and the style is in accordance with the FGPS requirements. I am profoundly grateful for the assistance of the aforementioned individuals, without whom this chapter would not have been completed.

Shahram Eisa-Beygi

May 1, 2013

3.1 Abstract

In spite of the high mortality and morbidity associated with ICH, treatment options remain ineffective. Several studies have used murine models as prognostic tools in elucidating the pathophysiological processes induced by ICH. However, these studies are limited by the heterogeneity, low expression and reproducibility of the desired phenotype, as well as the high mortality observed in these models. Zebrafish are an excellent vertebrate model to elucidate the etiology of cerebral-vascular disorders. We previously reported that exposure to the statin drug Atorvastatin (ATV) resulted in ICH in developing zebrafish. In this study, we expand upon these previous studies and draw upon the unique advantages of the zebrafish system to evaluate several pathophysiological processes associated with ICH and to use these variables to develop an outcome model during vertebrate development. The pharmacologically-induced model consistently replicates common underlying pathologies associated with ICH. We demonstrate that hemorrhage is associated with the disruption of the blood-brain barrier and cerebral vascular disintegration. Within hours of vascular rupture, rapid hematoma expansion, accompanied by edema formation, is observed in the adjacent brain regions. Enhanced TUNEL-positive staining is observed in and around the periphery of the hematoma, which was also associated with the activation of an inflammatory response, up-regulation of heme oxygenase 1 (HO-1) mRNA and protein levels, generation of reactive oxygen species (ROS), and was followed by localised thrombosis. All of these biomarkers serve as points of intervention for future studies geared towards large-scale screening of zebrafish for potential therapeutics to mitigate symptoms of ICH. Hence, we suggest a holistic approach towards modelling ICH pathophysiology, incorporating *in*

vitro studies using other vertebrate models including zebrafish, which can accelerate drug discovery.

3.2 Introduction

Intracerebral hemorrhage (ICH), the pathological accumulation of blood within the cranial vault, represents the second most common cause of stroke, as approximately 15% of all stroke subtypes are hemorrhagic in nature (Counsell et al., 1995; Qureshi et al., 2005). Furthermore, ICH is associated with the greatest mortality rate of all stroke subtypes, leaving most survivors with permanent neurological deficits and significant disabilities (Broderick et al., 1993; Qureshi et al., 1999). Spontaneous hemorrhage can arise as a result of cavernous malformations of the brain, typified by the accumulation of dilated blood vessels that lack adequate investment by mural cells, which as a result support only sluggish blood flow (Maeder et al., 1998; Eerola et al., 2003; Murakami et al., 2012).

At the ultra-structural level, the disruption of endothelial cell-to-cell junctions results in the detachment of endothelial cells from the vessel wall, making them fragile and prone to rupture (Louvi et al., 2011). The timing for the onset of these vascular malformations can be as early as the embryonic or postnatal stages of development (Boulday et al., 2011). However, ICH can also arise in the absence of primary vascular malformations and result from elevated blood pressure (Ebrahimi et al., 1999; Lang et al., 2001; Sutherland and Aurer, 2006), bacterial infection (Babamahmoodi and Babamahmoodi, 2011), trauma (Marion et al., 1997; Perel et al., 2009), or tumors (Lieu et al., 1999).

Despite the relevant incidence and the high mortality and morbidity associated with ICH, no surgical treatment or medical therapy has been effective in improving functional outcomes (Yu et al., 1992; Morgenstern et al., 1998; Broderick et al., 1999; Steiner et al., 2011). This is due in part to the variability in the timing of onset, the location and severity of this condition, as well as incomplete penetrance of genetic mutations pre-disposing the organism to the condition (Sahni and Weinberger, 2007).

Considerable progress has been made using murine models in dissecting the pathophysiology and progression of ICH using a number of interventions, including injection of bacterial collagenase into the basal ganglia (Rosenberg et al., 1990; Clark et al., 1998), infusion of autologous blood into the brain parenchyma (Belayev et al., 2003), and through genetic knockouts (Louvi et al., 2011). However, these studies are limited by the low expression and reproducibility of the desired phenotype, heterogeneity of the resulting hemorrhages, lack of feasibility for real-time/*in vivo* imaging of hematoma expansion and edema formation, lack of optical clarity, high cost, and the high mortality observed in the murine models utilised. Zebrafish continue to gain recognition as a reliable model to complement *in vitro* and clinical studies to address vascular malformations underlying human pathologies, such as ICH (Liu et al., 2007; Buchner et al., 2007; Gore et al., 2008; Kwon et al., 2012; Eisa-Beygi et al., 2013; Hegarty et al., 2013). However, to date no studies elaborating the pathophysiological features associated with cerebral hemorrhage have been reported in this species.

We had previously reported that, in contrast with mammalian models, zebrafish embryos and larvae with ICH exhibit functional recovery, as their development seems unimpaired (Eisa-Beygi et al., 2013; Chapter 2). In addition, zebrafish embryos provide a

relatively rapid screening system with the genomic and functional complexity of a vertebrate model organism (Lieschke and Currie, 2007). Hence, we reasoned that improved understanding of the pathophysiological cascade of events and molecular mechanisms ensuing ICH can have clinical relevance in terms of identifying potential targets for new prognosis and therapeutic interventions to ameliorate the progression of this disease *in vivo*. As a first step, we present here a highly reproducible and versatile model of pharmacologically-induced ICH in a developing vertebrate, exhibiting numerous primary and secondary pathological processes that closely mimic murine and human ICH pathologies. In addition, the amenability of this model to small-molecule screening makes it ideal for functional analysis of gene modulators or therapeutics that can ameliorate ICH-induced secondary injury, thereby increasing the preclinical utility of the model.

3.3 Materials and Methods

3.3.1 Zebrafish husbandry and transgenic lines

Adult zebrafish were maintained under a constant temperature of 28°C and a 14 h light: 10 h dark photoperiod in the University of Ottawa Aquatic Care Facility. Embryos were acquired by natural breeding of adult zebrafish and were kept at 28.5°C in E3 embryo medium (5 mmol/L NaCl, 0.17 mmol/L KCl, 0.33 mmol/L $CaCl_2$, 0.33 mmol/L $MgSO_4$). The Tg(*CD41:GFP*) line was a gift from Dr. Robert Handin (Harvard University, Massachusetts); the Tg(*mpx:GFP*) line was kindly provided by Dr. Steve Renshaw (University of Sheffield, UK); and, the Tg (*gata-1:DsRed*) line was provided by Dr. Beth Roman (University of Pittsburgh, Pennsylvania). All experiments were

performed in compliance with a protocol approved by the University of Ottawa Protocol Review Committee and conform to the published guidelines of the Canadian Council on Animal Care for the use of animals in research and teaching.

3.3.2 Drug treatment

For pharmacological inhibition of HMGCR, zebrafish embryos (1-2 hours post fertilisation; hpf) were incubated in Atorvastatin (ATV; Pfizer Inc., Connecticut USA) in embryo medium at a final concentration of 0.5 mg/L as previously noted (Eisa-Beygi et al., 2013; see Chapter 2).

3.3.3 Detection of apoptotic cells

Apoptotic cells were detected in 48 hpf embryos that were pre-treated with 1-phenyl 2-thiourea (PTU) and fixed in 4% PFA/1X Phosphate Buffered Saline Tween-20 (PBST) overnight, then dehydrated and stored in 100% methanol at -20°C overnight. After rehydration in PBST, embryos were permeabilised in acetone at -20°C for 10 min. Apoptotic cells were detected using whole-mount terminal deoxynucleotidyltransferase-mediated dUTP nick end labeling (TUNEL), according to the manufacturer's instructions (ApopTag *In situ* Apoptosis Detection Kit Plus-Millipore). TUNEL-positive cells were visualised using diaminobenzidine (DAB) and the DAB-stained cells in the ventral head region were quantified by manual counting. Treated embryos were visualised using a Nikon NBZ 1500 dissecting microscope with a Nikon DXM 1200 C digital camera and stored in 50% glycerol at 4°C. For acridine orange (AO) staining, embryos were treated with a 5 µg/mL solution of AO (Sigma-Aldrich) for 1 h at room temperature, followed by several rinses in embryo medium. The embryos were then anesthetised in 0.017% tricaine, after which fluorescence micrographs of embryos were acquired under the Nikon

NBZ 1500 dissecting microscope, equipped with a standard GFP filter set, using a Nikon DXM 1200C digital camera.

3.3.4 Neutral-red staining of macrophages

Macrophages in live embryos were visualised by incubating 48 hpf embryos in a 2.5 μg/mL neutral-red (Sigma-Aldrich) solution in E3 embryo medium at 25–30°C for 8 h, as previously described (Gray et al., 2007). These embryos were then visualised using a Nikon NBZ 1500 dissecting microscope equipped with a Nikon DXM 1200 C digital camera as above.

3.3.5 Sudan-black staining of neutrophils

Neutrophils in embryos were visualised by whole-mount Sudan black staining, as previously described (Yoo and Huttenlocher, 2011). In brief, 48 hpf embryos were fixed in 4% PFA/PBST for 2 h at RT, followed by incubation in 0.18% Sudan Black solution (Sigma-Aldrich), followed by extensive washes in 70% ethanol. Treated embryos were visualised using a Nikon NBZ 1500 dissecting microscope with a Nikon DXM 1200 C digital camera as above and stored in 50% glycerol at 4°C.

3.3.6 Whole-mount o-Dianisidine (OD) staining of erythrocytes

Zebrafish embryos at 48 hpf were fixed in 4% PFA/PBST overnight, followed by several washes in PBST. Erythrocytes were stained using o-Dianisidine, a sensitive marker for hemoglobin, as previously described (Eisa-Beygi et al., 2013; Chapter 2). In brief, embryos were incubated in OD (0.6 mg/mL) (Sigma-Aldrich), containing 0.01 M sodium acetate (pH 4.5), 0.65% hydrogen peroxide, and 40% (v/v) ethanol in the dark for

15 min. Stained embryos were washed in PBST and visualised using Nikon DXM 1200 C digital camera as above and stored in 50% glycerol at 4°C.

3.3.7 CM-H_2DCFDA staining

Embryos at 48 hpf with or without cerebral hemorrhage were incubated in 5-(and-6)-chloromethyl-2′,7′-dihydrodichlorofluorescein diacetate (CM-H_2DCFDA; 1000 ng/mL; Molecular Probes) for 1 h at 25–30°C and imaged under the Nikon NBZ 1500 dissecting microscope, which was equipped with a standard GFP filter set, using a Nikon DXM 1200C digital camera.

3.3.8 RNA extraction, cDNA synthesis and real-time RT-PCR

Total RNA was extracted from a pool of 20-30 embryos using TRIzol reagent (Invitrogen). The RNA was DNase-treated using the Deoxyribonuclease kit (Invitrogen) to minimise genomic DNA contamination. cDNA was synthesised from equal concentrations of RNA using a 1st Strand cDNA Synthesis Kit and Super Script II RT (Invitrogen) and used as a template in real-time RT-PCR (qPCR). The qPCR assays were performed using a Bio-Rad CFX96 qPCR system with Brilliant III SYBR Green Master Mix (Agilent Technologies, USA). All qPCR reactions were performed using the following conditions: 95°C for 3 min, 40 cycles of 95°C for 20 s and 58°C for 20 s, with a final extension for 5 min at 72°C. The data were normalised to the expression of *18S* rRNA gene, and were presented relative to the control group. Values are reported with standard errors. The primers used for qPCR analysis were:

(5'-CTGTCTGAACAGATAAAAGCAGTC-3') (*HO-1* forward) and
(5'-TGTGTTTGTGTGATCTGTCCTT-3') (*HO-1* reverse).
(5'-CAAACATGGGCTGGTTCAAG-3') (*18S* forward) and

(5'-GGTGGTGCCCTTCCGTCAATTC-3') (*18S* reverse).

3.3.9 Confocal microscopy

For confocal microscopy, 48-52 hpf Tg(*flk1:EGFP;gata1:dsRED*) or Tg(*mpx:EGFP;gata1:dsRED*) embryos that were previously treated with ATV or DMSO were embedded in 1% low melting agarose in E3 embryo medium and tricaine mesylate (Sigma-Aldrich). A rendered Z-stack, at ~80 μm thickness, was taken with a Zeiss LSM 510 AxioImager.M1 confocal microscope using an Achroplan 40x/0.8 W objective with an argon laser (488 nm) and a helium-neon laser (543 nm).

3.3.10 Western blot analysis

Fifteen larvae were pooled as one sample and homogenised in RIPA lysis buffer (150 mM NaCl, 1% Triton X-100, 0.5% sodium deoxycholate, 0.1% SDS, 50 mM Tris-HCl, 1 mM EDTA, 1 mM phenylmethanesulfonyl fluoride) containing a general protease inhibitor cocktail (Roche, USA). Extracted protein samples was heated for 10 min at 70°C, loaded onto a 10% SDS-PAGE and transferred to a PVDF membrane (Bio-Rad, USA). The membrane was blocked for 1 h with 5% skimmed milk, probed with anti-HO-1 antibody at a 1:1000 dilution in 2% skimmed milk, and subsequently incubated at 4°C overnight. Subsequently, the membrane was probed with 1:15,000 dilution of goat anti-rabbit secondary antibody (Pierce, USA) for 2 h at room temperature, and immune-reactive bands were detected using Luminata Western HRP Substrates (Millipore, USA). To control for equal protein loading, the membrane was re-probed with β-actin antibodies (1:4000; A2066, Sigma-Aldrich) for 2 h at room temperature after stripping with Re-Blot Plus solution (Millipore, USA). Ban intensities were quantified using ImageJ software.

3.4 Results and Discussion

3.4.1 Vessel disintegration, hematoma expansion and cerebral edema mark the early phases of ICH

We previously reported that pharmacological and genetic ablation of HMGCR function perturbs vascular development in zebrafish as early as 28 hpf (Eisa-Beygi et al., 2013; Chapter 2). This is characterised by prevalence of abnormally dilated, diffusely shaped and blood-filled nascent vessels in the forebrain and midbrain which support noticeably attenuated or sluggish blood circulation. This phenotype closely mimics the cerebral cavernous malformation (CCM)-like lesions observed in humans and murine models. Furthermore, these vascular-specific effects are heterogeneous in severity and distribution (**Fig. 3.1A-D**), as observed using the Tg(*fli1:EGFP*) embryos in which cranial blood vessels are marked by GFP expression (Lawson and Weinstein, 2002). This reflects a requirement for products of the mevalonate pathway in the stabilisation of nascent cranial vessels, particularly during development.

Using confocal microscopy of Tg(*fli1:EGFP*);(*gata-1:DsRed*) embryos, these bulged vessels in statin-treated embryos (marked by GFP expression) are leaky and prone to rupture at later stages of development. This is evidenced by extravasation of *DsRed*-positive erythrocytes from a specific site into adjacent brain regions at 48 hpf, resulting in the fragmentation and complete disintegration of the underlying vascular architecture (**Fig. 3.1E-J**). In more than 70% of humans experiencing ICH, hematoma growth is observed, from single or multiple vessels, which is an independent determinant of mortality and functional outcome of this disease (Davis et al., 2006).

Consistently within hours after the onset of hemorrhage in the zebrafish brain, rapid hematoma expansion is observed into the adjacent brain regions, along with significant hydrocephalus or edema formation between 36-48 hpf in the forebrain and the ventricular zones, due predictably to the resulting intracranial pressure exerted by the accumulation of blood (**Fig. 3.2A-C**). Approximately 81% of the embryos treated with 0.5 mg/L ATV showed a significant degree of hematoma expansion between 36-48 hpf (53/65). Hematoma expansion could exacerbate brain injury, resulting in the herniation of adjacent brain structures; as such pharmacological cessation of hematoma growth has been shown to lead to improved clinical outcomes (Davis et al., 2006).

3.4.2 Apoptosis is enhanced in response to ICH

Evidence from murine models of ICH suggests that part of the cell-death in the hematoma and surrounding tissues may involve apoptosis (Matsuchita et al., 2000; Karwacki et al., 2005; Huang et al., 2012). We further reasoned that the rapid expansion of the hematoma and the resulting mass effect, along with the activity of cytotoxic blood components in the brain parenchyma shortly after the onset of hemorrhage, could trigger apoptosis within the hematoma region and the surrounding tissues. Furthermore, this could underlie the basis for effects such as degeneration of the vasculature and, possibly neuronal injury and dysfunction (please refer to Chapter 4 for more on this aspect).

To test if statin-induced ICH would provoke apoptosis, we used a whole-mount TUNEL assay to detect cells with DNA fragmentation *in situ* (Espín et al., 2013). In

Figure 3.1: Exposure to Atorvastatin (ATV) induces vascular dilation, followed by hemorrhage and vascular disintegration. (A-D) Representative photomicrographs of Tg(*fli1:EGFP*) embryos incubated in DMSO or 0.5 mg/L ATV from 1-2 hpf and imaged at 33 hpf. Abbreviation: PMBC, primordial midbrain channel. White *arrows* indicate the abnormally dilated vessels. Scale bar: 50 μm. (D-E) Representative bright-field photomicrographs of Tg(*fli1:EGFP*);(*gata-1:DsRed*) embryos incubated as above and imaged at 48 hpf. The *asterisk* denotes the hemorrhage and the black dotted area shows the field of interest. Anterior is to the left and dorsal to the top. (E-J) Representative composite confocal Z-stack projections of the black dotted area in the same Tg(*fli1:EGFP*);(*gata-1:DsRed*) embryos. The white *asterisk* denotes DsRed-positive erythrocytes and the white *arrows* show regions where vascular fragmentation is observed. Anterior is to the top and scale bar: 200 μm.

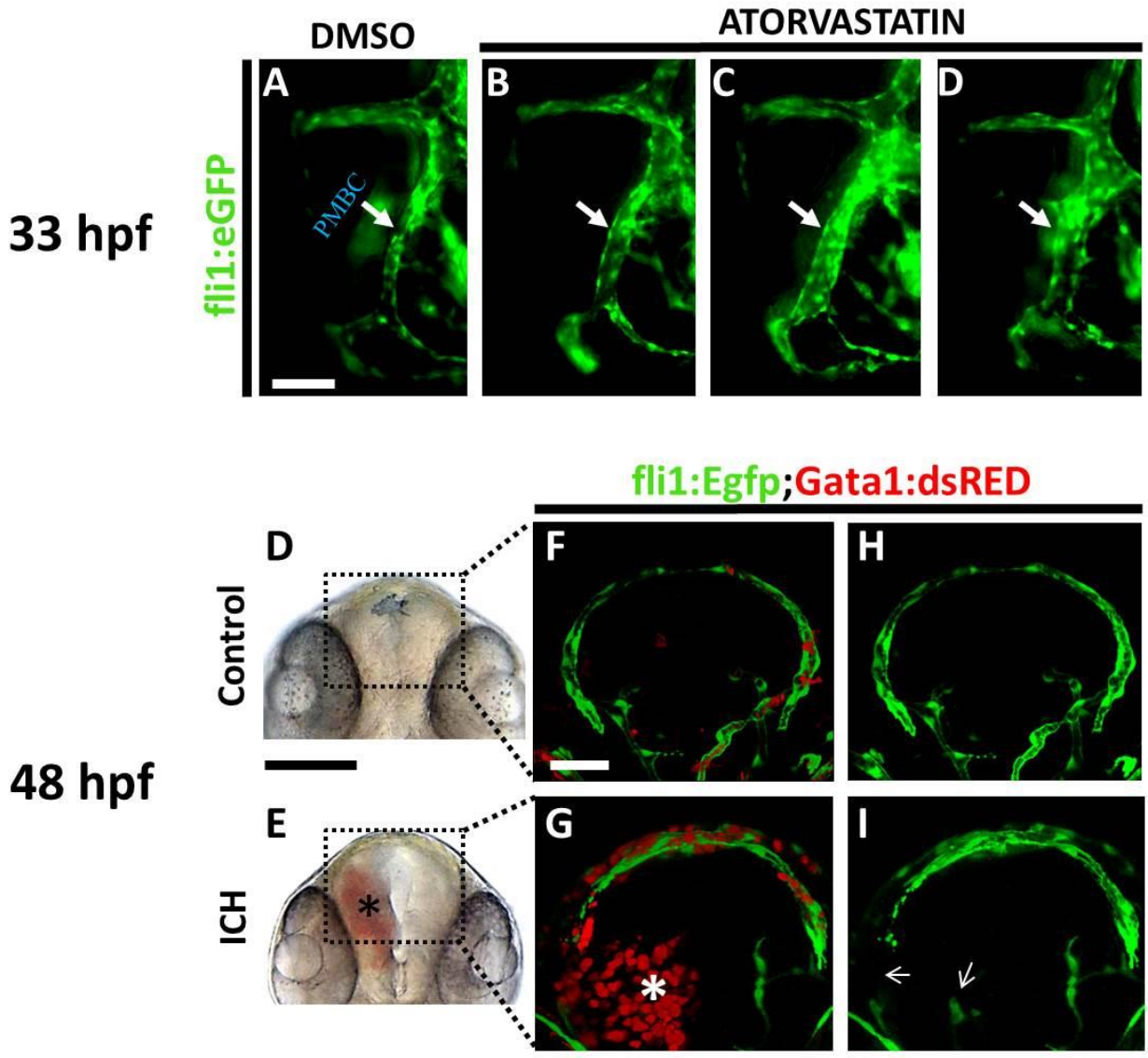
DMSO
ATORVASTATIN
A
B
C
D
PMBC
fli1:eGFP
33 hpf
fli1:Egfp;Gata1:dsRED
D
F
H
Control
48 hpf
E
G
I
ICH
*
*

contrast with intact embryos, those with ICH showed enhanced apoptosis in the hematoma area and the regions surrounding the hemorrhagic mass, particularly at 48 hpf when the spatial extent of hemorrhage was maximal (**Fig. 3.3A-D**) (*t*-test, $p<0.001$, N=14). Although the control group displayed some TUNEL-positive staining albeit to a lesser degree than the ICH group, we speculate that this trend reflects programmed cell death related to developmental and homeostatic mechanisms. Even though the triggers responsible for initiating apoptosis in the ICH group are yet to be explored, we observed a positive correlation between the number of apoptotic cells and the severity of hemorrhage or the extent of hematoma expansion (data not shown). These observations were also confirmed *in vivo* using acridine orange (AO), a cell-permeable nucleic acid marker (**Fig. 3.3E and F**). It is plausible that some of these apoptotic cells include neuronal populations, as dopaminergic (DA) neurons have been shown to be co-localised in the pretectum and telencephalon regions at this stage (please refer to Chapter 4).

3.4.3 ICH triggers an immune response

In human patients and murine models of ICH, an acute inflammatory response constitutes part of the normal physiological cascade of events triggered by the entry of cytotoxic blood components into the brain parenchyma (Zhao et al., 2007; Loftspring et al., 2009). Furthermore, this response is generally characterised by the infiltration of activated leukocytes (neutrophils and macrophages) to the sites of injury for the removal and neutralisation of the blood components and other cellular debris (Power et al., 2003; Zhao et al., 2007; Lotfspring et al., 2009).

Figure 3.2: Exposure to Atorvastatin (ATV) induces hematoma expansion and edema formation in the brain. (A-C) Representative bright-field photomicrographs of a wild-type embryo treated with 0.5 mg/L ATV and imaged at 36 hpf, 42 hpf, 48 hpf. Black *arrows* indicate ventricle. Anterior is to top. Scale bar: 150 μm.

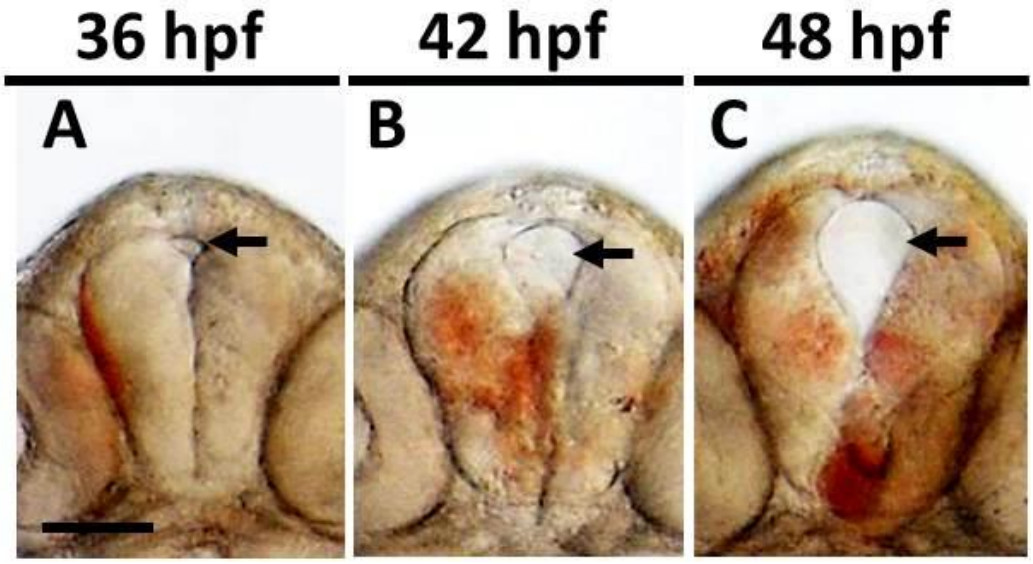

To test whether statin-induced hemorrhage in the zebrafish brain would trigger a similar inflammatory response during early phases of development, we used neutral red, a histological dye that is readily taken up by early granulocytes, to localise active macrophages in the brain (Gray et al., 2007). Compared with intact embryos in which a small population of resident macrophages were noted, in embryos with ICH, there were clearly more macrophages which also appeared enlarged in diameter, concentrated in and around the periphery of hemorrhage in the head by 48-52 hpf (**Fig. 3.3G and H**), supporting the recruitment and activation of these cells. In contrast, neutrophils distribution and abundance as assessed by whole-mount sudan-black staining remained unaltered when compared with untreated embryos (**Fig. 3.3I and J**).

To further verify that the neutrophil abundance in the brain is unaffected by ICH, the Tg(*mpx:eGFP*) line was outcrossed with the erythrocyte marker Tg(*gata-1:DsRed*) line. The resulting double-transgenic Tg(mpx:EGFP);(gata-1:DsRed) line allowed for the simultaneous visualisation of neutrophils (marked by EGFP expression) and the area occupied by the hematoma (marked by DsRED expression) in live embryos. This transgenic model further confirmed that there was no recruitment or localised proliferation of neutrophils (**Fig. 3.3K and L**), suggesting that the neutrophils observed belong to a non-circulating, resident population of neutrophils. These analyses further confirmed macrophage involvement in ICH pathogenesis, but there was, as expected, no significant difference in the number of neutrophils (data not shown).

Overall, our data provides evidence that macrophage activation constitutes part of the robust inflammatory response coincident with maximal hematoma size (48-52 hpf). By contrast, the number of neutrophils in the vicinity of hemorrhage was unchanged,

suggesting that the primary immune response is characterised by the phagocytosis of blood components through the activation macrophages.

3.4.4 Increased heme oxygenase (HO-1) expression and ROS generation following ICH

Heme oxygenase-1 (HO-1) is the rate limiting enzyme facilitating the metabolism of pro-oxidant heme into ferrous iron, carbon monoxide and biliverdin, which is further oxidised to bilirubin (Prawan et al., 2005) (**Fig. 3.4A**). Since blood-derived heme cannot be recycled, its timely metabolism is critical to alleviate the symptoms of ICH and for the resolution of hemorrhage (Koeppen et al., 2004). Ferrous iron, derived from the catabolism of heme, could potentiate the generation of reactive oxygen species (ROS), which could induce secondary brain injury including endothelial cell apoptosis or cerebral edema, as well as neuro-degeneration (Wagner et al., 2003; Goldstein et al., 2003; Hua et al., 2007). *HO-1* mRNA transcript levels in embryos at 48-52 hpf were assessed using qPCR on total RNA harvested from a pool of embryos. In embryos with ICH, the HO-1 transcript levels were significantly enriched (3.5-fold, n=4; 20 embryos per sample) (**Fig. 3.4B**).

Concomitant with the elevated *HO-1* mRNA levels, the protein expression of HO-1, assessed by western blot analysis in embryos experiencing ICH, also showed a marked increased (n=3; 20 embryos per sample) (**Fig. 3.4C**). Using an intercellular fluorescent ROS marker in live embryos (CM-H2DCFDA) (Anichtchik et al., 2008), we noted that ICH induced significant ROS generation in the brain and ventricles of 48-52 hpf embryos (**Fig. 3.4D and E**). Taken together, these data highlight the functional

applicability of zebrafish embryos in replicating some of the pathophysiological details associated with the degradation/lysis of blood components following ICH as early as 48 hpf.

3.4.5 Evidence for thrombosis after ICH

Hemostatis, the adhesion and aggregation of platelets to the sub-endothelium of ruptured vessels, is a pivotal process to stop excessive bleeding (English et al., 2000). In patients with ICH, hematoma expansion can elicit local activation of hemostatic mechanisms (Fujii et al., 2001). In fact, pharmacological enhancement of hemostatis is suggested to reduce hematoma growth, resulting in improved clinical outcomes (Mayer, 2005). In zebrafish, thrombocytes are the functional equivalent of mammalian platelets and are implicated in hemostasis in embryos and adults (Lin et al., 2005; Kim et al., 2010). To test whether ICH in zebrafish initiate hemostasis and to analyze the temporal and spatial distribution of thrombocytes in response to ICH *in vivo*, we used the Tg(*CD41:GFP*) line in which nascent thrombocytes are tagged with a green fluorescent reporter protein (GFP) (Lin et al., 2005). At earlier stages (24-48 hpf) and during the onset of vascular leakage, GFP-positive cells were confined strictly to the cardiac sinus/yolk sac, along with localisation in the caudal region (data not shown). This distribution pattern closely mimicked that of wild-type embryos at the same developmental stages (data not shown). However, by 3 dpf a large number of non-circulating GFP-positive cells had infiltrated the sites of hemorrhage, which was visualised by o-Dianisidine (OD) staining (**Fig. 3.5A-D**).

Figure 3.3: ICH-induced pathophysiological processes observed at 48 hpf. (A-B) Representative bright-field photomicrographs of control and ICH embryos, imaged at 48 hpf. Two-headed *arrows* mark the inter-eye distance. The blue dotted area shows the field of interest. Anterior is to the top. (C-D) Representative bright-field images of control and ICH-positive embryos, subjected to whole-mount TUNEL assay, showing apoptotic cells (brown). (E-F) Representative merged bright-field and fluorescent images of control and ICH-positive embryos subjected to AO staining showing apoptotic cells (green fluorescent cells). (I-J) Representative bright-field images of control and ICH-positive embryos stained with neutral red, a marker of macrophages (red). (G-H) Representative bright-field images of control and ICH-positive embryos stained with neutral red to visualise macrophages (red). (I-J) Representative bright-field images of control and ICH-positive embryos stained with sudan black to visualise neutrophils (purple). (K-L) Representative merged bright-field and fluorescent images of control and ICH-positive Tg(*mpx:eGFP*);(*gata-1:DsRed*) embryos showing neutrophils (GFP-positive cells) and erythrocytes (DsRed-positive cells). Scale bars: 100 μm, except for A-B: 200 μm.

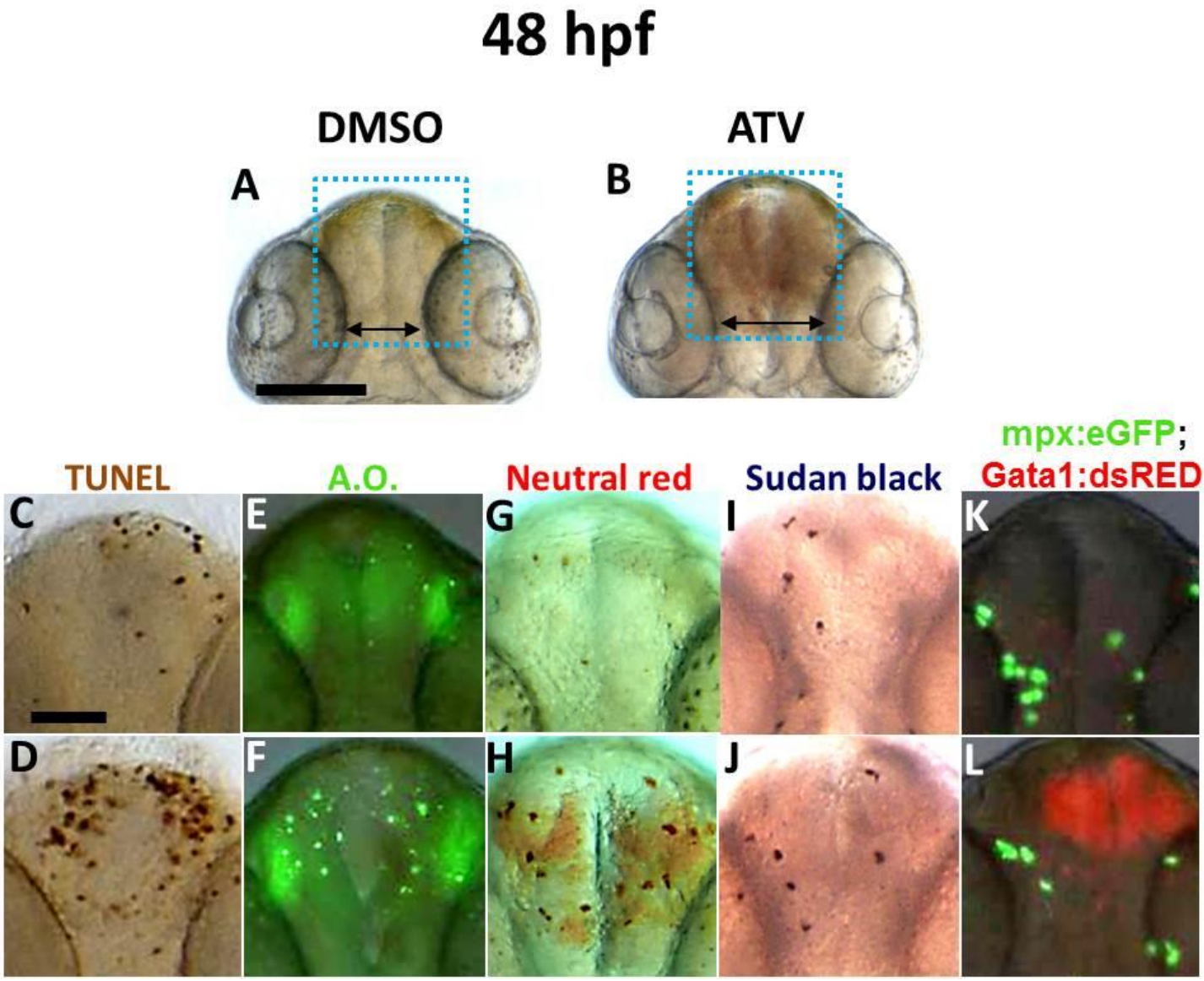
48 hpf
DMSO
ATV
A
B
mpx:eGFP;
Gata1:dsRED
TUNEL
A.O.
Neutral red
Sudan black
C
D
E
F
G
H
I
J
K
L

Figure 3.4: Increased heme oxygenase HO-1 expression and ROS generation following ICH at 48 hpf. (A) Simplified schematic diagram of the heme oxygenase-1 (HO-1)-catalysed metabolism of heme, resulting in the generation of Iron (Fe), carbon monoxide (CO) and biliverdin; NADPH and O_2 are required for this reaction. (B) Real-time RT-PCR (qPCR) analysis for the *HO-1* mRNA transcript levels at 48 hpf in DMSO-treated embryos (grey bar) and embryos with ICH (green bar). Relative gene expression is presented as fold-change (±standard error mean) based on a four embryo pools each containing 30 embryos; * indicates significant difference (*t*-test, $p<0.05$, N= 4). The data were normalised to the transcript levels of the *18S* rRNA gene, and were presented relative to the control group. (C) Representative western blots of three different experiments of embryonic lysates from control and ICH embryos at 48 hpf, probed with an anti-HO-1 antibody at a 1:1000 dilution. To control for equal protein loading, the membrane was re-probed with β-actin antibodies. (D-E) Representative merged bright-field and fluorescent photomicrographs of control and ICH embryos at 48 hpf, stained with CM-H_2DCFDA, an *in vivo* ROS indicator. Anterior is to left. Scale bar: 200 μm.

48 hpf

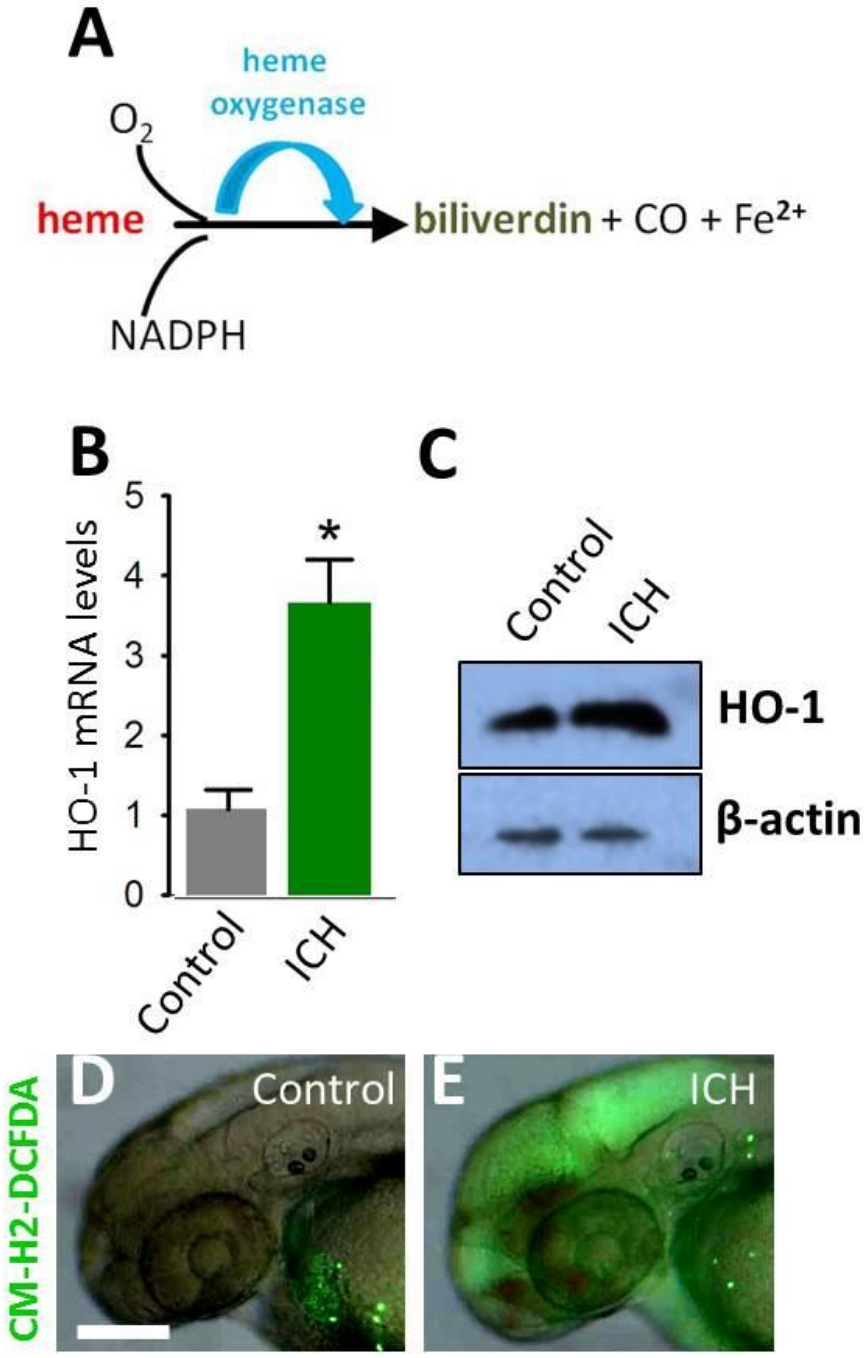
A
heme
oxygenase
O_2
heme
biliverdin + CO + Fe^{2+}
NADPH
B
HO-1 mRNA levels
0
1
2
3
4
5
*
Control
ICH
C
Control
ICH
HO-1
β-actin
CM-H2-DCFDA
D
Control
E
ICH

This result suggests that hemostatic mechanisms are not impaired and that enhanced hemostasis at the sites of vascular lesion constitutes part of the pathophysiological cascade of events associated with ICH. We propose that hemostasis at the sites of vascular lesion prevent excessive expansion of the hematoma, thereby contributing to the resolution of hemorrhages in these embryos by 96 hpf.

3.5 Conclusions

ICH is the most debilitating type of all stroke subtypes, with the highest mortality rate of all strokes (Broderick et al., 1993; Qureshi et al., 1999). Therapies geared towards management of the disease have been ineffective; hence presently no consistently effective surgical or pharmacological methods exist to reduce the mortality and morbidity of ICH (Yu et al., 1992; Morgenstern et al., 1998; Broderick et al., 1999; Steiner et al., 2011). This shortcoming is further compounded by the fact that there exists no high-throughput chemical screening system for rapid assessment of pharmaceuticals that may ameliorate the progression of ICH-associated pathological events. In addition, pathophysiological studies using mammalian vertebrates tend to involve laborious histological analysis that is often subject to bias. Here, we propose that zebrafish is a reproducible model for the systematic assessment of the pathophysiological processes resulting in ICH.

We have previously shown that embryonic and larval exposure to statin drugs results in ICH in zebrafish (Eisa-Beygi et al., 2013; Chapter 2) which is consistent with recent clinical evidence from human studies, suggesting a link between high dose statin use and the risk of ICH (Amarenco et al., 2006; Westover et al., 2011). Of particular

Figure 3.5: Evidence for thrombosis after ICH. (A-B) Representative bright-field photomicrographs of control and ICH whole-mount embryos at 72 hpf stained with o-Dianisidine (OD) to visualise the expression of hemoglobin (orange) in the brain. (C-D) Merged bright-field and fluorescent photomicrographs of the same embryos showing individual cells expressing *CD41-GFP* in the brain. Anterior is to the top. Scale bar: 200 μm. (E) Quantification of *CD41:GFP*-positive cells in the head region (dorsal view) in control and ICH embryos at 72 hpf (N=14 embryos; $p<0.05$, *t*-test).

72 hpf

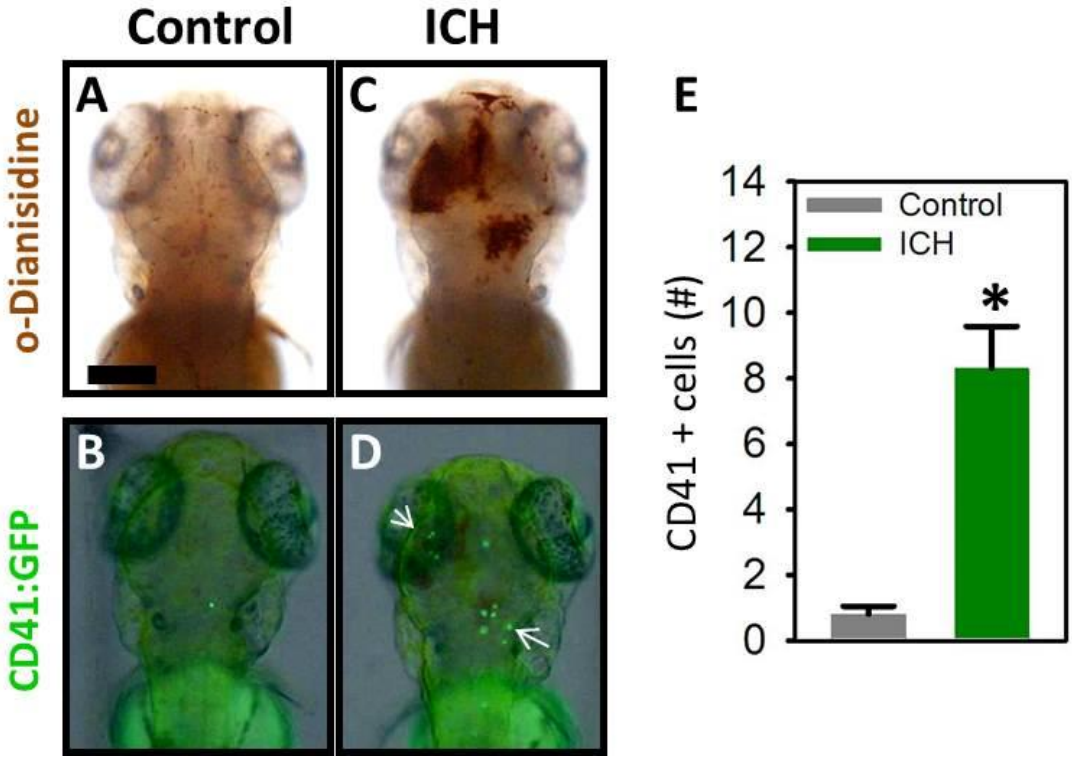
Control
ICH
A
C
o-Dianisidine
B
D
CD41:GFP
E
CD41 + cells (#)
14
12
10
8
6
4
2
0
Control
ICH
*

\

interest is that our model exhibits several of the clinical manifestations associated with ICH pathophysiology, namely disruption of the blood-brain barrier and vascular degeneration, hematoma expansion, apoptosis, inflammation, cerebral edema and thrombosis. The optical transparency of the model, enhanced by the presence of tissue-specific transgenic lines, and the reproducibility of the desired phenotypes make the model applicable for high-throughput assessment of the efficacy and possible side-effects of a broad range of small molecules that could promote hematoma resolution, mediate inflammation, prevent apoptosis and neuro-degeneration and trigger vascular stabilisation. Furthermore, the complete dissection of the entire suite of mechanisms aiding recovery from ICH can yield important therapeutic potential.

Chapter 4

Disruption of catecholaminergic neuron development and impaired locomotor function in zebrafish with intracerebral hemorrhage

Author contributions:

Ms. Sandra Noble and Mr. Rafael Godoy trained me for the use of confocal microscopy and helped me in preparing and processing embryos for imaging. Dr. Thomas W. Moon and Dr. Marc Ekker helped me design the following experiments and assisted me in writing and revising this chapter to ensure that the content is scientifically sound and the style is in accordance with the FGPS requirements. I am profoundly grateful for the assistance of the aforementioned individuals, without whom this chapter would not have been completed.

Shahram Eisa-Beygi

May 14, 2013

4.1 Abstract

Hematoma expansion and perihematomal edema formation account for the major causes of neurological deterioration following ICH. The extent of neurological deterioration is generally exacerbated depending on the location and volume of hematoma and the extent of edema. A recurrent problem with murine models is that the degree of neuronal damage in tissues surrounding the hematoma is generally quantified by means of laborious histological methods which can also be subject to bias. I have previously shown that embryonic and larval exposure to statin drugs results in ICH in zebrafish (Eisa-Beygi et al., 2013; Chapter 2). I have also documented some of the conserved pathophysiological processes underlying ICH formation (Chapter 3), which can potentiate neuronal damage or displacement.

The purpose of this aspect of my research is to evaluate some of the basic neurological parameters in a zebrafish (*Danio rerio*) model of a pharmacologically-induced ICH during development. To this end, the patterning and distribution of dopaminergic (DA) neurons, response to sensory stimuli, and swimming speed were assessed. Confocal microscopy using Tg(*dat:EGFP*);(*Gata-1:DsRed*) embryos revealed that following ICH, blood components rapidly extravasate into the brain parenchyma where DA-positive cells normally exhibit a spatially restricted distribution at 48 hpf. Expansion of the hematoma is associated with loss and disorganisation of these DA neurons, evidenced by marked reduction in dat:EGFP expression. Immunohistochemical staining for tyrosine hydroxylase (TH), a marker for catecholaminergic neurons, showed disruption of TH-positive cells in embryos demonstrating ICH. In addition, we observed impaired swimming performance and response to tactile stimulation in these embryos, in

the absence of any apparent developmental defects. These analysis, will pave the way for the modeling of ICH-induced neurodegeneration and, more importantly, establish the basis for further studies into the possible mechanisms aiding functional recovery in zebrafish and screening for putative neuroprotectants against ICH-induced neurotoxicity.

4.2 Introduction

There are presently no medical interventions or therapeutics to effectively benefit in improving patient outcome after intracerebral hemorrhage or ICH (Broderick et al., 2007). The rupture of cerebral vessels leads to the development of a space-occupying hematoma in the brain parenchyma. Although ICH accounts for 10-15% of all stroke cases (Counsell et al., 1995; Qureshi et al., 2005), it has a poorer prognosis than any other form of stroke. The neurological deterioration in ICH patients is generally irreversible and disabling (Hua et al., 2002). Several animal studies have been utilised to establish prognostic tools in elucidating the neurological deficits induced by ICH and to test the efficacy of drugs. Thanks to work on model organisms, there has been an upsurge, over the last decade or so, in our understanding of the mechanisms underlying brain injury induced by ICH.

The pathophysiological processes accompanying ICH (some of which are reported in Chapter 3) can affect the viability of adjacent neurons. Several lines of evidence have shown that the mechanical force exerted by the expanding hematoma and edema can expand and displace neurons in the brain parenchyma (Hua et al., 2002; Chang et al., 2011). In fact, the progressive deterioration of neurological condition in patients with ICH is most often due to continuous bleeding and enlargement of the

hematoma (Kazui et al., 1996; Fujii et al., 1998). Similarly, as reported in Chapter 3, zebrafish embryos demonstrating ICH display rapid hematoma expansion into the adjacent brain regions and significant hydrocephalus in the forebrain and the ventricular zones. These dynamic processes can account for the major causes for neuronal disorganisation and neurotoxicity in the surrounding regions (Fujii et al., 1998). Other secondary insults including macrophage activation, enhanced HO-1 expression and ROS generation, could also potentiate further neurotoxicity in the form of loss and disintegration of neurons. Each of these was also demonstrated in the zebrafish model reported in Chapter 3.

In vitro studies have shown that activated macrophages can induce neuronal toxicity through ROS generation and production of cytokines (Fordyce et al., 2005; Kaushal et al., 2007). The extent of neuronal loss following ICH correlates, both spatially and temporally, with the build-up of activated macrophages (Wasserman and Schlichter, 2007a). Furthermore, iron overload due to break-up of blood components and the lysis of the blood clot can induce neuronal apoptosis (Wagner et al., 2004; Hua et al., 2006; Gu et al., 2009). In addition, the neurons in a developing brain are particularly fragile (Anderson et al., 2000).

Following from Chapter 3 this study hypotheses that hemorrhages in the brain can provoke neuronal damage. Therefore, as a first step in establishing a preclinical transitional model for small molecule screening of neuroprotective agents, this study will evaluate some of the basic and well-established neurological parameters in zebrafish coinciding with ICH.

The general organisation of the central nervous system (CNS) between the zebrafish and mammalian vertebrates share similar features, despite the apparent differences in structural complexity and scale (Xi et al., 2011). Furthermore, the utility of the zebrafish model for imaging and transgenesis has enabled the generation of lines expressing fluorescent proteins in specific populations of neurons (Xi et al., 2011). For example, ample information regarding the spatio-temporal expression and the function of the dopaminergic (DA) neuron system has recently been reported in zebrafish thanks to the generation of the dat:EGFP line where green fluorescent protein (GFP) is expressed under the control of *cis*-regulatory elements of the *dopamine transporter* (*dat*) (Xi et al., 2011). Analysis of these embryos has revealed that DA neurons can be detected as early as 18 hpf as a collection of cells expressing GFP in the ventral diencephalon region (Xi et al., 2011), thus making them ideal candidates to assess the possible neurotoxicity associated with ICH.

DA neurons participate in various physiological functions including neuroendocrine secretion, cognitive function, control of voluntary movement and behavioural responses (Bjorklund and Lindvall, 1984). In addition, DA neurons are shown to display similar function and expression patterns across vertebrates, including zebrafish (Xi et al., 2011). The DA system was characterised in zebrafish development on the basis of the expression patterns of tyrosine hydroxylase (TH) and the dopamine transporter (DAT), both of which are specific markers of DA neurons (Holzschuh et al., 2001; Rink and Wullimann, 2002; Zhao et al., 2012).

Furthermore, progressive degeneration of DA neurons is implicated in the pathogenesis of Parkinson's disease, which is characterised by reduced levels of

dopamine in the striatum and the accompanying movement and speech disorders (Bjorklund et al., 2002). Similarly, selective ablation of DA neurons in developing zebrafish results in locomotor defects, thus phenocopying some of the pathological and behavioural aspects of the mammalian Parkinson's disease (Zhao et al., 2012).

There is presently a need for development of an appropriate animal model that can both facilitate the study of ICH and would be beneficial for evaluating novel approaches to restore neurological function. Although several experimental models of ICH have been developed (Kobari et al., 1988; Rosenberg et al., 1992; Wagner et al., 1996; Del Bigio et al., 1996; Foerch et al., 2013), a major limitation of these models is the fact that hematoma development, brain edema and neurological deterioration are either evaluated by tedious histological analysis of different specimens or through expensive magnetic resonance imaging (MRI). To bypass these challenges, there is a need to use a model in which these pathophysiological and neurological consequences of ICH can be evaluated *in vivo*, without sacrificing the animals. Such a model would allow for the evaluation of the onset and progression of neurotoxicity following ICH, thus allowing for the testing of the efficacy of potential therapeutics on these parameters. This chapter will provide some preliminary evidence that zebrafish can provide a critical first step in identifying novel and effective therapies for ICH-induced neurotoxicity. The results outlined here can further strengthen the utility of zebrafish as an ideal model for the study of ICH, at the level of etiology and pathophysiology.

4.3 Materials and Methods

4.3.1 Zebrafish husbandry and transgenic lines

Adult wild-type and transgenic zebrafish were maintained under a constant temperature of 28°C and a 14 h light:10 h dark photoperiod in the University of Ottawa Aquatic Care Facility. Embryos were obtained through natural breeding of adult zebrafish and were kept at 28.5°C in E3 embryo medium (5 mmol/L NaCl, 0.17 mmol/L KCl, 0.33 mmol/L $CaCl_2$, 0.33 mmol/L $MgSO_4$). The double transgenic Tg(*dat:EGFP*);(*gata-1:DsRed*) zebrafish line was obtained by crossing Tg(*dat:EGFP*) fish (Xi et al., 2011) with Tg (*gata-1:DsRed*) fish (Traver et al., 2003). Pigmentation was inhibited by incubating the embryos in 1-pheny1-2-thiourea (PTU) (Elsalini and Rohr, 2003). All experiments were carried out in accordance with a protocol approved by the University of Ottawa Protocol Review Committee and conform to the published guidelines of the Canadian Council on Animal Care for the use of animals in research and teaching.

4.3.2 Drug treatment

For pharmacological inhibition of HMGCR, zebrafish embryos (1-2 hours post fertilisation; hpf) were treated with Atorvastatin (ATV; Pfizer Inc., Connecticut USA) in a single-exposure manner in embryo medium. ATV was dissolved in DMSO.Drug solutions were aliquoted and stored at -20°C until used. Embryos were either incubated in 0.5 mg/L ATV in embryo medium or DMSO as vehicle control.

4.3.3 Confocal microscopy

For confocal microscopy, 48 hpf Tg(*dat:EGFP*);(*gata-1:DsRed*) embryos previously treated with DMSO or 0.5 mg/L ATV were embedded in 1% low melting

agarose in E3-embryo medium and tricaine mesylate (Sigma-Aldrich). A rendered Z-stack, at ~80 micron thickness each, from the ventral head position, was taken with a Zeiss LSM 510 AxioImager.M1 confocal microscope using an Achroplan 40x/0.8 W objective with an argon laser (488 nm) and a helium-neon laser (543 nm).

4.3.4 Whole-mount anti-tyrosine hydroxylase (TH) immunohistochemistry

Zebrafish embryos at 48 hpf were fixed in 4% paraformaldehyde (PFA)/1X Phosphate Buffered Saline Tween-20 (PBST) overnight, rinsed and stored at -20°C in 100% EtOH. Upon re-hydration, the embryos were then permeabilised by incubation in acetone at -20°C or 1% Triton/1X PBST for 30 min at room temperature, followed by blocking in 10% calf-serum/1X PBST, 0.1% BSA for 1 h at room temperature. Embryos were then incubated in a mouse monoclonal anti-tyrosine hydroxylase primary antibody (EMD Millipore, AB152) (1:200 diluted in 10% calf-serum blocking solution) overnight at 4°C. The next day, samples were washed with repeated washes in 1X PBST for 1 h. This was followed by incubation with secondary antibody conjugated with horseradish peroxidase (HRP). The signal was detected using DAB Peroxidase Subtrate Kit. After staining, zebrafish were mounted with 3.5% methylcellulose and imaged, with the ventral head region facing the field of view.

4.3.5 Testing for locomotor activity

The response of embryos to tactile stimulation at 48 hpf was evaluated using a method previously described by Xi et al. (2010). In brief, the embryos were first individually placed in a petri dish containing E3 medium and allowed to habituate for 10 min, after which a gentle tactile stimulus using forceps was applied to the tail of the

embryo and the response was recorded using a high-speed digital video camera (DXM 1200C). For each treatment condition, 25 embryos were used. The numbers of embryos with an immediate or delayed response were manually counted. Embryos exhibiting no tail movement or an absence of any movement were also noted. For statistical analysis, a student's *t*-test was conducted and average values ± standard errors of the mean was plotted. All data analysis was performed using SigmaPlot 11.0 software Systat Software Inc, Chicago, IL).

For the assessment of swimming speed, we used a high-speed digital video camera (FASTCAM) to measure the time it took for an embryo to disappear from the microscopic field of view immediately following the application of the tactile stimulus.

4.4 Results and Discussion

4.4.1 Pharmacologically induced ICH disrupts catecholaminergic neuron development and swimming behaviour in zebrafish

There are a plethora of animal studies highlighting the ICH-induced neurotoxicity and behavioural defects. However, these studies are generally limited by the labour-intensive histological analysis, unfeasibility of *in vivo* imaging, high cost, external injection of collagenase or autologous blood into the brain parenchyma, and the inability to control the heterogeneity in lesion size or neurological outcome. Nonetheless, I have provided several lines of evidence in previous chapters that these aforementioned limitations do not apply to zebrafish. In fact, zebrafish is gaining recognition as an alternative model for ICH research (Gore et al., 2012; Butler et al., 2011). As mentioned

in these earlier chapters, an ICH phenotype can consistently be induced by incubating embryos in a solution containing 0.5 mg/L ATV.

In order to simultaneously establish the progression of the hematoma and the distribution of DA neuron networks in embryos with ICH, I out-crossed the Tg(*dat:EGFP*) line (Xi et al., 2011) with the Tg(*gata-1:DsRed*) line (Traver et al., 2003) and obtained a line expressing both transgenes. Using confocal microscopy on Tg(*dat:EGFP*);(*gata-1:DsRed*) embryos, I observed at the onset of hemorrhage, the aggregation of DsRed-positive erythrocytes into the pretectum and telencephalon regions of the brain, where distinct populations of GFP-expressing DA neurons exhibit a spatially-restricted distribution (**Fig. 4.1B, D**). By contrast, in embryos treated with DMSO, the blood-brain barrier remains intact, and the DA neurons do not come into contact with potentially cytotoxic blood components or are they subjected to the mechanical stress of the hematoma (**Fig. 4.1A, C**). This non-invasive approach, which takes advantage of the relatively translucent nature of the embryos and the prolific nature of the zebrafish, enables us to assess the patterning and distribution of DA neurons in response to hematoma expansion at various stages of development *in vivo*. As a further measure of the neurological status in response to hemorrhage, individual neurons can also be quantified, at higher magnification. Furthermore, it has been shown that DA neurons can be partially replaced through proliferation of new DA neurons as a consequence of selective ablation (Xi et al., 2011). Hence, the potential processes of neuroplasticity and proliferation can also be evaluated *in vivo* without resorting to laborious histological analysis.

Figure 4.1: The Tg(*dat:EGFP*);(*gata-1:DsRed*) facilitates real-time analysis of ICH-induced DA-neuron neurotoxicity. (A-B) Representative bright-field photomicrographs of the head in control and ICH embryos, imaged at 48 hpf. The blue *arrow* marks the maximum aggregation of extravasated blood and the blue dotted area shows the field of interest. Scale bar: 200 μm. (C-D) Representative composite confocal Z-stack projections of the blue dotted area in the same Tg(*dat:EGFP*);(*gata-1:DsRed*) embryos. The white *asterisk* denotes DsRed-positive erythrocytes and the white *arrows* indicate the position of DA-neurons in the peritectum and telencephalon. Anterior is to the top and scale bar: 40 μm.

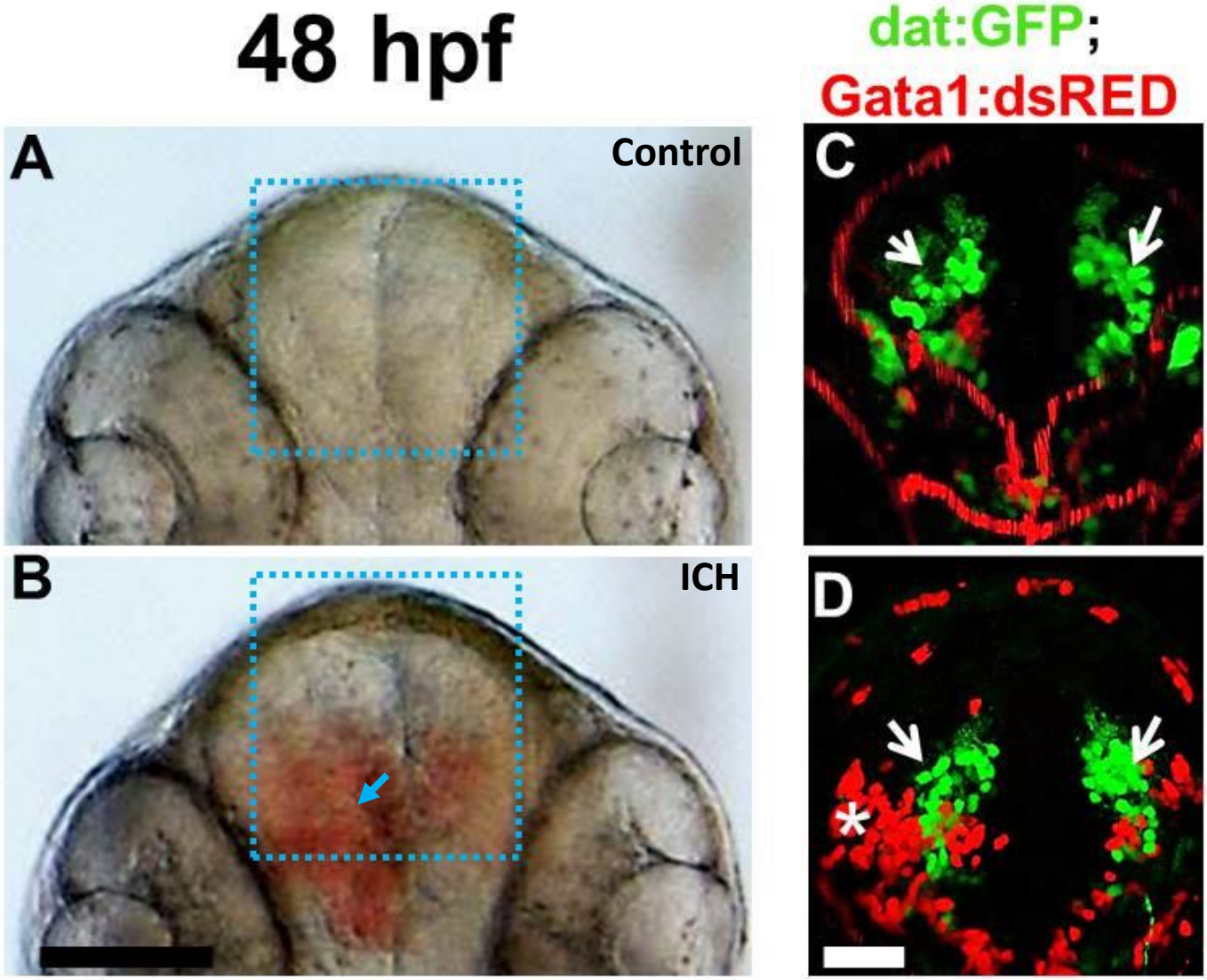
48 hpf
dat:GFP;
Gata1:dsRED
A
Control
B
ICH
C
D
*

It is apparent that the infiltration of blood components farther into the brain parenchyma results in complete ablation of DA neurons, evidenced by the marked reduction of dat:eGFP expression in embryos with ICH (**Fig. 4.2A-D**). Hence, there seems to be a positive correlation between blood volume and the severity of neuronal loss. The Tg(*dat:EGFP*);(*gata-1:DsRed*) line offers the potential of testing the effects of various compounds on modifying the neurological defects induced by ICH.

Whole-mount immunohistochemistry was also performed at 48 hpf to detect the spatial distribution of tyrosine hydroxylase (TH), a marker of neurons expressing catecholamines (including dopamine and its derivatives) in the CNS. TH is the rate-limiting enzyme in the first committed step of the synthesis of cateholamines, hence an ideal marker for dopaminergic and noradrenergic neurons in the CNS (Chen et al., 2009). The TH polyclonal antibody was purified from rabbit and it was kept in a buffer containing liquid in 10 mM HEPES (pH 7.5), 150 mM NaCl (pH 7.5), 100 ug/mL BSA and 50% glycerol.(EMD Millipore, AB152) (1:200 diluted in 10% calf-serum blocking solution). My preliminary experiments suggest that ICH can affect the distribution and abundance of TH-positive neurons. In the control group, TH was strongly expressed in the diencephalon (**Fig. 4.2E**). However, in embryos with ICH, edema formation and the enlarged inter-eye distance resulted in the TH-positive cell populations to move farther apart and exhibit reduced intensity of staining, suggesting displacement and reduced levels of catecholimenergic neurons (**Fig. 4.2F**). Surprisingly, TH-staining did not co-localise with the dat:GFP expression observed in the pretectum and telencephalon regions, but it co-localised with the dat:GFP expression in the diencephalon. This could

be due to reduced TH expression in those cells at this stage or the low sensitivity of colourimetric immunohistochemistry.

As a further measure of neurological outcome following ICH, I assessed locomotor function (swimming speed, the acuteness of response to tactile stimulation in these embryos). Zebrafish embryos have been shown to respond to tactile stimulation as early as 24 hpf (Saint-Amant and Drapeau, 2000) and these behavioural responses have been well-characterised at various stages of development (McLean and Fetcho, 2008). A behavioural response is simply elicited by applying a tactile stimulation at the tail or head regions. This response is typically expressed as a twitch at 1 dpf to a rapid escape by 2 dpf. Assessment of locomotor function is another method by which I can further document ICH-induced neurological defects.

To accomplish this, embryos with or without ICH were individually subjected to a gentle tactile stimulus (see Materials and Methods) at 48 hpf 10 min after individual transfer to a petri dish. Individual responses were characterised as "immediate" (requiring one touch), "delayed" (requiring at most three touches) or as "no-response". Whereas more than 80% of DMSO-treated embryos (n=25 embryos) displayed an immediate response, of the embryos demonstrating ICH, only approximately 23% of this group (n=25) showed rapid escape behaviour. In most embryos with ICH (more than 40%), several repeated tactile stimuli were applied in order to provoke an escape response. In addition, approximately 30% of embryos with ICH showed no response, even after three repetitive tactile stimuli were applied. Differences in the mean proportion of responses to tactile stimulation in the control and ICH groups were measured using a Student's *t*-test

(N=25 embryos per treatment by only comparing the mean values for each of the three response categories (**Fig. 3A**).

In addition, preliminary evidence regarding swimming speed was obtained upon administration of a gentle tactile stimulus. Using a high-speed digital video camera and ImageJ software, it took approximately 0.09 sec for control embryos to escape out of the field of view, accompanied with high frequency tail-beat frequency. By contrast, embryos with ICH showed lower frequency undulation of the tail, and, traveled at a much slower speed, as judged by the slower time it takes them to disappear from the field of view (**Fig. 3B**).

Although it has been shown that reduced locomotion and weakened response to sensory stimulus constitute part of the pathophysiology of DA neuron loss in zebrafish (Xi et al., 2011), the observed phenotype could just as well be attributed to musculoskeletal defects or loss of mechanosensory neurons. Further studies are warranted to elaborately dissect the spatio-temporal fate of different subtypes of neurons, before and after the induction of hemorrhage and to expand on the functional consequences of neuronal loss as well as establish precisely the molecular basis for the observed locomotor defects. In light of the detrimental neurological outcome of ICH in murine models and patients, it is worth underscoring that zebrafish exhibit a tendency for full functional recovery. Hence, there is merit in exploring how neurological function is regained after stroke, which can yield potential benefits in the treatment of ICH.

Figure 4.2: Disruption of catecholaminergic-neuron development in zebrafish with ICH. (A-B) Representative bright-field photomicrographs of the head in control and ICH embryos, imaged at 48 hpf. The *asterisk* marks the aggregation of extravasated blood and the black dotted area shows the field of interest. Anterior is to the top and scale bar: 200 μm. (C-D) Representative fluorescent photomicrographs of the black dotted area in Tg(dat:EGFP) embryos. White *arrows* indicate the position of DA-neurons (E-F). Representative bright-field photomicrographs of the black dotted area in wild-type embryos immunostained for TH. Black arrows indicate the position of TH-positive neurons.

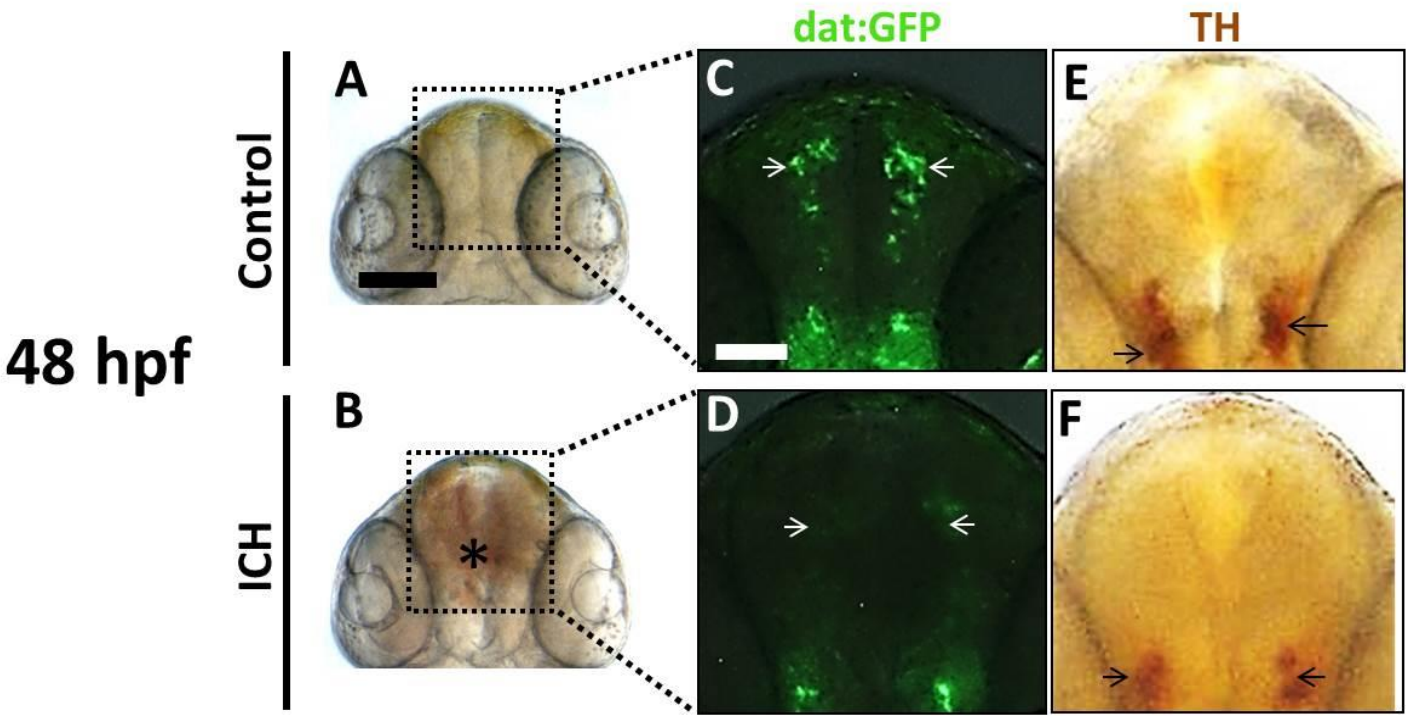
48 hpf
Control
ICH
A
B
C
D
E
F
dat:GFP
TH
*

Figure 4.3: Impaired locomotor function in zebrafish with ICH. (A) Quantification of the percentage of embryos showing immediate, delayed or no response in the wake of gentle tactile stimulation. Differences in the mean proportion of responses to tactile stimulation in the control and ICH groups were measured using Student's t-test (25 embryos were used per each treatment. N=3 separate experiments) by only comparing the mean values for immediate ($p<0.001$), delayed ($p<0.05$) and no-response categories. (B) Representative photomicrographs of 3 separate experiments showing stimulus-evoked escape response over different time frames, measured using a high-speed digital video camera (FASTCAM).

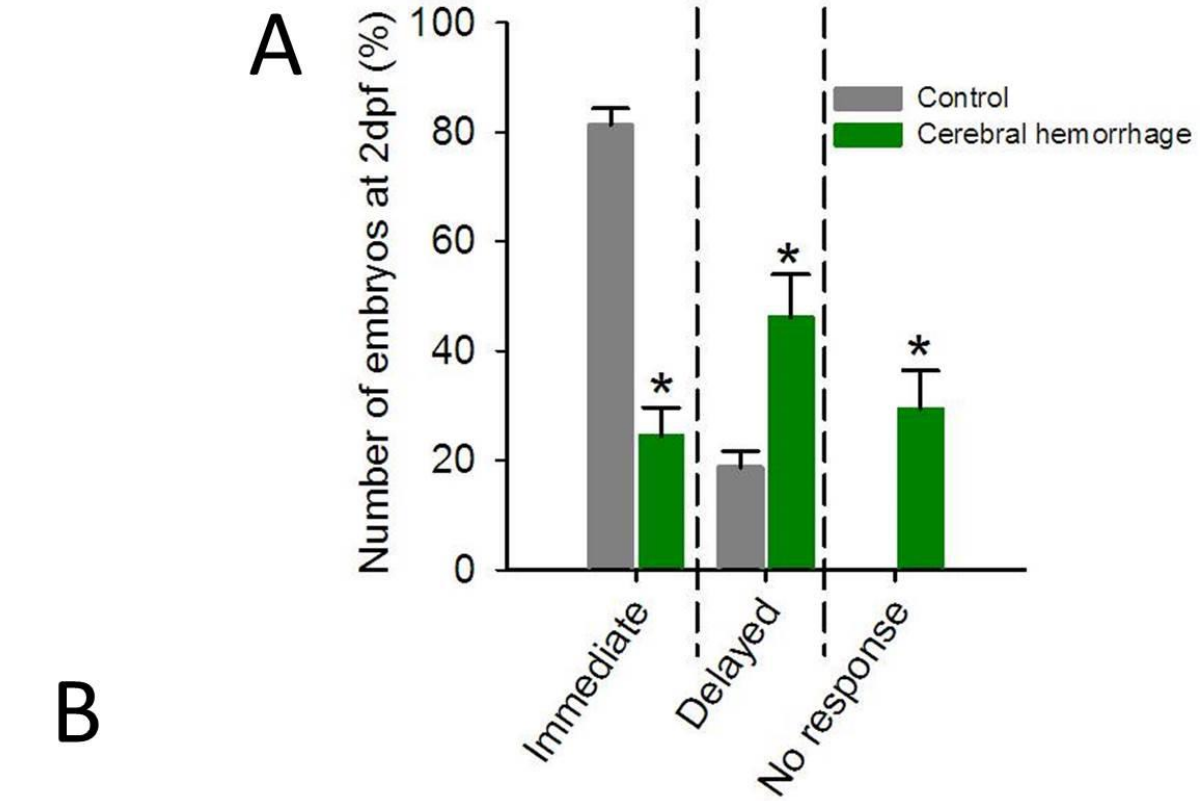
A
Number of embryos at 2dpf (%)
100
80
60
40
20
0
Control
Cerebral hemorrhage
*
*
*
Immediate
Delayed
No response

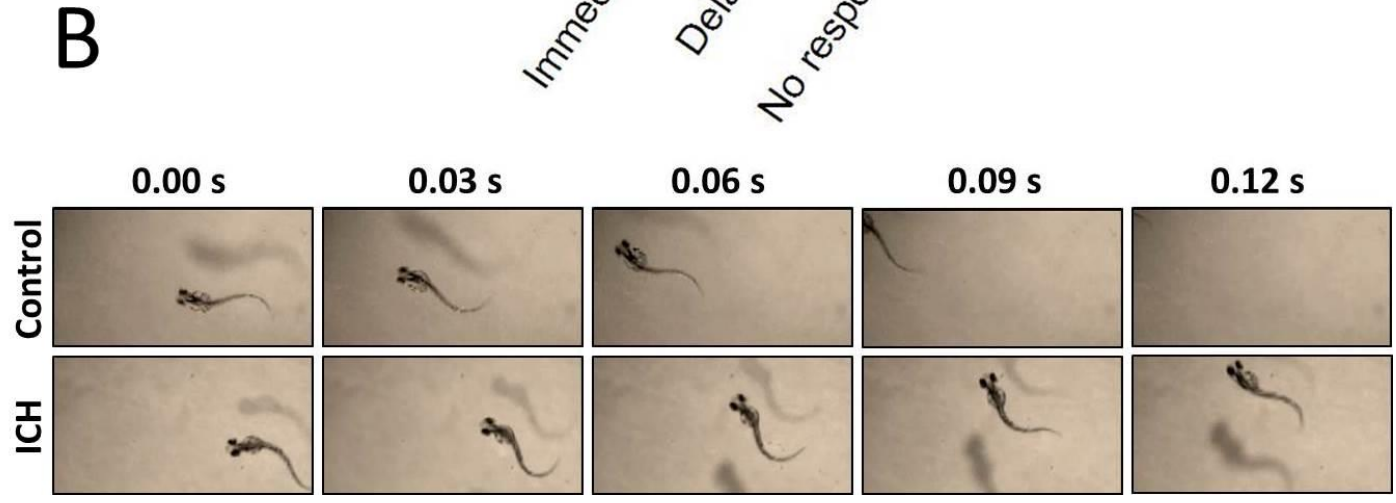
B
0.00 s
0.03 s
0.06 s
0.09 s
0.12 s
Control
ICH

Chapter 5

General Discussion & Future Directions

Intracerebral hemorrhage (ICH) accounts for 10-15% of all stroke subtypes. Furthermore, it has the highest mortality and morbidity rates of stroke cases (Counsell et al., 1995; Qureshi et al., 2005). The hemorrhages in the CNS are triggered by various factors and these also include cerebral cavernous malformations (CCMs), which can arise sporadically or through a familial autosomal pattern of inheritance (Maeder et al., 1998; Boulday et al., 2011, Eerola et al., 2003). Neither surgical evacuation nor pharmacological interventions have been shown to confer clear post-stroke benefits to individuals with ICH (Broderick et al., 1999; Badjatia and Rosand, 2005; Steiner et al., 2011). This bleak outcome is due predominantly to rapid hematoma expansion, activation of inflammatory mediators, disintegration of cranial vasculature, and focal neurological deterioration (Davis et al., 2006; Zhao et al., 2007; Lotfspring et al., 2009; Huang et al., 2012).

As a consequence, in addition to optimising and investigating novel treatment options, more research needs to be directed towards gaining insights into the development and maintenance of cerebral-vascular stabilisation. For this reason, it is imperative to develop novel approaches in order to characterise the etiological and pathophysiological processes underlying ICH genesis and progression, since treatment options remain limited and ineffectual. This kind of an approach would pave the way for:

A) *In vivo* assessment of small molecules and pharmaceuticals to identify modifiers of cerebral-vascular stabilisation;

B) Identification of additional genes and signalling pathways mediating cerebral-vascular stabilisation; and,

C) Sequencing for mutations in these newly identified candidate genes in human vascular disorders for early screening.

This can be accomplished through comparative analysis of different model organisms, including zebrafish, along with functional work and pathway analysis. Zebrafish, *Danio rerio*, continues to gain recognition as an ideal model for the study of ICH given that the genes and molecular mechanisms contributing to vascular morphogenesis are highly conserved across vertebrates (Gore et al., 2012) and that this species is highly amenable to functional/expression analyses and imaging assays.

For my Ph.D. project I was primarily interested in defining the precise mechanisms through which the HMGCR pathway contributes to cerebral-vascular stabilisation in the context of a developing vertebrate. In its final format, this dissertation further contributes to our understanding of the etiology of ICH and the ensuing pathophsyiology. It is worth noting that this study was also motivated by the emerging clinical evidence, which suggested that statin drug use confers an increased risk for ICH in humans (Amarenco et al., 2006; Arboix et al., 2010; Westover et al., 2011) and that no follow-up animal studies have, hitherto, been conducted to further explore and test this clinical association. Could inhibition of HMGCR weaken CNS blood vessels and make them prone to hemorrhage? There is already abundant evidence from *in vitro* studies that statin drug use can induce apoptosis in endothelial cells (ECs) and smooth muscle cells (Weiss et al., 2002; Hippenstiel et al., 2002; Acquevella et al., 2010; Guijarro et al., 1999). Are the results strictly confined to zebrafish embryos and larvae? Does these findings harbour any clinical relevance and, if so, what are the possible mechanistic explanations?

To address these questions, it was important to first look at the processes that regulate vascular stabilisation. Abnormal endothelial barrier function can be caused by inadequate investment by mural cells and/or due to disruption of endothelial cell-cell contacts. This is associated with aneurysms in micro-vascular channels, loss of vascular stability and frequent hemorrhaging in the CNS (Maeder et al., 1998). Although these defects in vascular stabilisation are equally likely to arise in vascular beds throughout the body, the vessels in the CNS region seem to be particularly prone to hemorrhaging. The severity of these vascular lesions can vary greatly and the onset can be as early as embryonic or postnatal stages of development (Boulday et al., 2011). Mice and rats have generally been utilised as models for elucidating the genetic basis and the signalling pathways necessary for vascular stabilisation. As a result of these studies and based upon sequencing of patients with familial cavernous malformations, several loss-of-function mutations affecting endothelial barrier function have been identified. These mutations result in the disruption of vascular stability and have been implicated in the pathogenesis of ICH in both murine models and humans (Sahoo et al., 1999; Verlaan et al., 2004).

Studies in animal models have greatly contributed to our current knowledge regarding the etiology, pathophysiology and neuro-pathology associated with ICH. However, there is a need to identify novel genes and additional interacting signalling molecules that contribute to the disease given that the prevalence of cerebral cavernous malformations (CCMs) in the general population is relatively high (estimated to be 1 in 200) and the genes implicated in the pathogenesis of CCM (*KRIT1*, *CCM2*, and *PDCD10*) account for only part of the disease phenotype (Cunningham et al., 2011). However, despite the characterisation of these genes, relatively little is known about their

mode of function. In addition, almost nothing is known about the mechanisms leading to the vascular lesions and hemorrhage in individuals harbouring these mutations. To further complicate this issue, not all of the individuals exhibiting a CCM phenotype carry mutations in any of three CCM genes, suggesting additional genetic modifiers that can increase the susceptibility of individuals to the CCM pathology (Lucas et al., 2003).

The three genes implicated in CCM have similar expression patterns. Their transcripts are particularly enriched in endothelial cell-cell junctions (Fischer et al., 2013). The CCM proteins, all of which are non-homologous and lack catalytic domains, interact to establish a protein complex (Serebriiskii et al., 1997; Glading et al., 2007; Voss et al., 2007). These proteins have also been shown to interact with Rho GTPases to maintain the functional integrity of ECs. However, models explaining this mechanism are only speculative. Expression analyses show that loss-of-function mutations in CCM genes are associated with hyper-activation and over-expression (protein and mRNA) of Rho GTPases (Li and Whitehead, 2010). However, the precise nature of the signalling cascades under the control of CCM genes remains to be explored. It is reasonable to assert that blocking HMGCR function would invariably reduce Rho GTPase signalling and, hence, can disrupt vascular stabilisation.

In sharp contrast with this assertion, a recent study in mice harbouring a genetic predisposition for cerebral-vascular permeability defect resulting from heterozygous mutation of *CCM2*, statin-treatment restores the endothelial barrier function by inhibiting Rho GTPase activation (Whitehead et al., 2009). This result is conflicting and warrants further studies.

As such, the identification and characterisation of genes and signalling pathways contributing to cerebral-vascular stabilisation was one of the chief aims of my PhD project. In this project I obtained numerous lines of evidence to support the hypothesis that down-regulation of HMGCR activity can exert an effect on signalling pathways under the control of CCM-interacting proteins, such as Rho GTPases.

More specifically, I demonstrated that geranylgeranylation of Rho GTPases is a requirement for cerebral-vascular stabilisation in developing zebrafish, particularly at a time when blood vessels lack adequate investment by smooth muscle cells. In these embryos, inhibition of the HMGCR/mevalonate pathway results in bulged CNS blood vessels, loss of vascular stability, vessel fragmentation and frequent cerebral hemorrhages. Similar results were obtained when geranlygeranylation was blocked by inhibition of GGTase I. These observations made in embryonic zebrafish resemble the CCM lesions observed in murine models and human patients. Additionally, an identical vascular-specific phenotype was reported in zebrafish in which components of Rho GTPase signalling were down-regulated due to point-mutations in those genes (Buchner et al., 2007; Liu et al., 2007). Lending further support to my findings is that at least two recent studies independently confirmed a functional role for HMGCR in cerebral-vascular stabilisation in zebrafish (Hung et al., 2012, Shen et al., 2013). An issue which I could not address was the cell autonomy of HMGCR-function. Is HMGCR function required in an endothelial-specific manner or does it also involve contribution from mural cells?

On the basis of the data accumulated thus far, and based on the fact that vascular stabilisation pathways in humans and zebrafish share common features (Gore et

al., 2012), it is reasonable to propose that sequencing of humans for mutations in the *HMGCR* and *GGTase I* genes could be a valid diagnostic approach. Not only are these gene sequences highly conserved across species, they also seem to functionally perform identical enzyme functions.

In zebrafish embryos demonstrating ICH, the disruption of the blood-brain barrier and the initiation of hemorrhage is coincident with vascular degeneration, hematoma expansion, apoptosis, inflammation, cerebral edema and thrombosis. Furthermore, I have shown that the extravasation of blood components into the brain parenchyma can induce progressive loss of DA neurons, along with displacement of TH-positive (catecholaminergic) neuronal populations. Concomitant with the apparent neurotoxicity, I presented preliminary evidence for impaired locomotor function and diminished response to tactile stimulus in these ICH embryos.

This is the first zebrafish study assessing the parameters that are hallmarks of ICH pathophysiology and are points of intervention for future studies geared towards large-scale screening of zebrafish for therapeutics to mitigate symptoms of ICH. The optical transparency of the model, enhanced by the presence of tissue-specific transgenic lines, as well as the reproducibility of the desired phenotypes make the model applicable for high-throughput assessment of the efficacy and possible side-effects of a broad range of small-molecules that could promote hematoma resolution, mediate inflammation and minimise neuronal damage. Such a phenotype-based screening, facilitated by the presence of stable transgenic lines marking unique clusters of neurons, also enables assessment of neuroprotective agents.

References

Abramsson, A., Berlin, O., Papayan, H., Paulin, D., Shani, M. and Betsholtz, C. (2002). Analysis of mural cell recruitment to tumor vessels. *Circulation*. 105, 112–117.

Acquavella, N., Quiroga, M.F., Wittig, O. and Cardier, J.E., (2009). Effect of simvastatin on endothelial cell apoptosis mediated by Fas and TNF-alpha. *Cytokine*. 49, 45-50.

Adams, R.H. and Alitalo, K. (2007). Molecular regulation of angiogenesis and lymphangiogenesis. *Nat. Rev. Mol. Cell Biol*. 8, 464–478.

Alejandre, M.J., Ramirez, H., Suarez, M.D. and Garcia-Peregrin, E. (1981). Different developmental patterns of 3-hydroxy-3-methylglutaryl-CoA reductase in chick tissues according to their role in cholesterogenesis. *Biol. Neonate*. 40, 232-236.

Amarenco, P., Bogousslavsky, J., Callahan, A., 3rd, Goldstein, L.B., Hennerici, M., Rudolph, A.E. *et al.* (2006). High-dose atorvastatin after stroke or transient ischemic attack. *N. Engl. J. Med.* 355, 549–559.

Anderson, V., Catroppa, C., Morse, S., Haritou, F. and Rosenfeld, J. (2000). Recovery of intellectual ability following traumatic brain injury in childhood: impact of injury severity and age at injury. *Pediatr. Neurosurg*. 32, 282-290.

Anichtchik, O., Diekmann, H., Fleming, A., Roach, A., Goldsmith ,P., and Rubinsztein, DC. (2008). Loss of PINK1 function affects development and results in neurodegeneration in zebrafish. *J. Neurosci.* 28, 8199-8207.

Arboix, A., García-Eroles, L., Oliveres, M., Targa, C., Balcells, M. and Massons, J. (2010). Pretreatment with statins improves early outcome in patients with first-ever ischaemic stroke: a pleiotropic effect of statins or a beneficial effect of hypercholesterolemia? *BMC Neurol*. 10, 47.

Babamahmoodi, F. and Babamahmoodi, A. (2011). Brucellosis, Presenting with Guillain-Barré Syndrome. *J. Glob. Infect. Dis.* 3, 390-392.

Badjatia, N., and Rosand, J. (2005). Intracerebral hemorrhage. *Neurologist*. 11, 311-324.

Bagrodia, S., Taylor, S. J., Jordon, K. A., van Aelst, L. and Cerione, R. A. (1998). A novel regulator of p21-activated kinases. *J. Biol. Chem*. 273, 23633-23636.

Ballabh, P. Intraventricular hemorrhage in premature infants: mechanism of disease. *Pediatr Res*. 67, 1-8.

Bayliss, P.E., Bellavance, K.L., Whitehead, G.G., Abrams, J.M., Aegerter, S., Robbins, H.S., Cowan, D.B., Keating, M.T., O'Reilly, T., Wood, J.M., Roberts,

T.M. and Chan, J. (2006). Chemical modulation of receptor signaling inhibits regenerative angiogenesis in adult zebrafish. *Nat. Chem. Biol*. 2, 265-273.

Belayev, L., Saul, I., Curbelo, K., Busto, R., Belayev, A., Zhang, Y., Riyamongkol, P., Zhao, W. and Ginsberg, M.D. (2003). Experimental intracerebral hemorrhage in the mouse: histological, behavioral, and hemodynamic characterization of a double-injection model. *Stroke*. 34, 2221-2227.

Benjamin, L.E., D. Golijanin, A. Itin, D. Pode, and E. Keshet. (1999). Selective ablation of immature blood vessels in established human tumors follows vascular endothelial growth factor withdrawal. *J. Clin. Invest*. 103, 159–165.

Bergametti, F., Denier, C., Labauge, P., Arnoult, M., Boetto, S., Clanet, M., Coubes, P., Echenne, B., Ibrahim, R., Irthum, B. *et al.* (2005). Mutations within the programmed cell death 10 gene cause cerebral cavernous malformations. *Am. J. Hum. Genet*. 76, 42–51.

Berzat, A.C., Brady, D.C., Fiordalisi, J.J. and Cox, A.D. (2006). Using inhibitors of prenylation to block localization and transforming activity. *Methods Enzymol*. 407:575-597.

Bishop, A.L. and Hall, A. (2000). Rho GTPases and their effector proteins. *Biochem. J*. 348, 241–255.

Bjorklund, L.M., Sánchez-Pernaute, R., Chung, S., Andersson, T., Chen, I.Y., McNaught, K.S., Brownell, A.L., Jenkins, B.G., Wahlestedt, C., Kim, K.S. and Isacson, O. (2002). Embryonic stem cells develop into functional dopaminergic neurons after transplantation in a Parkinson rat model. *Proc. Natl. Acad. Sci. U S A*. 99, 2344-2349.

Bjorklund, A. and Lindvall, O. Dopamine-containing systmes in the CNS. *In: Handbook of Chemical Neuroanatomy: Classical Transmitter in the Rat, edited by Bjorklund A, Hokfelt T. Amsterdam: Elsevier*. 55–122.

Borghi, C, Prandin, M.G., Costa, F.V., Bacchelli, S., Degli Esposti, D. and Ambrosioni, E. (2000). Use of statins and blood pressure control in treated hypertensive patients with hypercholesterolemia. *J. Cardiovasc. Pharmacol*. 35, 549–555.

Boulday, G., Rudini, N., Maddaluno, L., Blécon, A., Arnould, M., Gaudric, A., Chapon, F., Adams, R.H., Dejana, E and Tournier-Lasserve, E. J. (2011). Developmental timing of CCM2 loss influences cerebral cavernous malformations in mice. *Exp. Med*. 208, 1835-1847.

Breier, G., Albrecht, U., Sterrer, S. and Risau, W. (1992). Expression ofvascular endothelial growth factor during embryonic angiogenesis andendothelial cell differentiation. *Development*. 114, 521-532.

Broderick, J.P., Brott, T., Tomsick. T., Miller, R. and Huster, G. (1993). Intracerebral hemorrhage more than twice as common as subarachnoid hemorrhage. *J. Neurosurg*. 78, 188–191.

Broderick, J.P., Adams, H.P.Jr., Barsan, W., Feinberg, W., Feldmann, E., Grotta, J., Kase, C., Krieger, D., Mayberg, M., Tilley, B., Zabramski, J.M. and Zuccarello, M. (1999). Guidelines for the management of spontaneous intracerebral hemorrhage: a statement for healthcare professionals from a special writing group of the Stroke Council, American Heart Association. *Stroke.* 30, 905–915.

Broman, M.T., Kouklis, P., Gao, X., Ramchandran, R., Neamu, R.F., Minshall, R.D. and Malik A.B.(2006). Cdc42 regulates adherens junction stability and endothelial permeability by inducing alpha-catenin interaction with the vascular endothelial cadherin complex. *Circ. Res*. 98, 73–80.

Brown, M.S. and Goldstein, J.L. (1997). The SREBP pathway: regulation of cholesterol metabolism by proteolysis of a membrane-bound transcription factor. *Cell*. 89, 331-340.

Brown, M.S. and Goldstein, J.L. (1999). A proteolytic pathway that controls the cholesterol content of membranes, cells, and blood. *Proc. Natl. Acad. Sci. U S A*. 96, 11041-11048.

Buchner, D.A., Su, F., Yamaoka, J.S., Kamei, M., Shavit, J.A., Barthel, L.K., McGee, B., Amigo, J.D., Kim, S., Hanosh, A.W., Jagadeeswaran, P., Goldman, D., Lawson, N.D., Raymond, P.A., Weinstein, B.M., Ginsburg, D. and Lyons, S.E. (2007). pak2a mutations cause cerebral hemorrhage in redhead zebrafish. . *Proc. Natl. Acad. Sci. USA.* 104, 13996–14001.

Butler, M.G., Gore, A.V. and Weinstein, B.M. (2011). Zebrafish as a model for hemorrhagic stroke. *Methods Cell Biol*. 105:137-161

Cao, J., Wang, J., Qi, W., Miao, H.H., Wang, J., Ge, L., DeBose-Boyd, R.A., Tang, J.J., Li, B.L. and Song, B.L. (2007). Ufd1 is a cofactor of gp78 and plays a key role in cholesterol metabolism by regulating the stability of HMG-CoA reductase. *Cell Metab*. 6, 115-128.

Cattelino, A., Liebner, S., Gallini, R., Zanetti, A., Balconi, G., Corsi, A., Bianco, P., Wolburg, H., Moore, R., Oreda, B., Kemler, R. and Dejana, E. (2003). The conditional inactivation of the beta-catenin gene in endothelial cells causes a defective vascular pattern and increased vascular fragility. *J. Cell Biol*. 2003. 162, 1111-1122.

Caveda, L., Martin-Padura, I., Navarro, P., Breviario, F., Corada, M.,Gulino, D., Lampugnani, M. G. and Dejana, E. (1996). Inhibition ofcultured cell growth by vascular endothelial cadherin (cadherin-5/VE-cadherin). *J. Clin. Invest*. 98, 886-893.

Chang, C.F., Chen, S.F., Lee, T.S., Lee, H.F., Chen, S.F. and Shyue, S.K. (2011). Caveolin-1 deletion reduces early brain injury after experimental intracerebral hemorrhage. *Am. J. Pathol*. 178, 1749-1761.

Chen, Y.C., Priyadarshini, M. and Panula, P. (2009). Complementary developmental expression of the two tyrosine hydroxylase transcripts in zebrafish. *Histochem. Cell Biol*. 132, 375-381.

Choi, J., Mouillesseaux, K., Wang, Z., Fiji, H.D., Kinderman, S.S., Otto, G.W., Geisler, R., Kwon, O. and Chen, J.N. (2011). Aplexone targets the HMG-CoA reductase pathway and differentially regulates arteriovenous angiogenesis. *Development*. 138, 1173-1181.

Clark, W., Gunion-Rinker, L., Lessov, N. and Hazel, K. (1998). Citicoline treatment for experimental intracerebral hemorrhage in mice. *Stroke*. 29, 2136-2140.

Clarke, P.R. and Hardie, D.G. (1990). Regulation of HMG-CoA reductase: identification of the site phosphorylated by the AMP-activated protein kinase in vitro and in intact rat liver. *EMBO J*. 9, 2439–2446.

Costa, C., Incio, J. and Soares, R. (2007). Angiogenesis and chronic inflammation: cause or consequence? *Angiogenesis* 10, 149–166.

Counsell, C., Boonyakarnkul, S., Dennis, M., Sandercock, P., Bamford, J., Burn, J. and Warlow, C. (1995). Primary intracerebral hemorrhage in the Oxfordshire Community Stroke Project. *Cerebrovasc Dis*. 5, 26–34.

Crawford, T.N., Alfaro, D.V., Kerrison, J.B. and Jablon, E.P. (2009). Diabetic retinopathy and angiogenesis. *Curr. Diabetes Rev*. 5, 8–13.

Cunningham, K., Uchida, Y., O'Donnell, E., Claudio, E., Li, W., Soneji, K., Wang, H., Mukouyama, Y.S. and Siebenlist, U. (2011). Conditional deletion of Ccm2 causes hemorrhage in the adult brain: a mouse model of human cerebral cavernous malformations. *Hum. Mol. Genet*. 20, 3198-3206.

D'amico, L., Scott, I.C., Jungblut, B. and Stainier, D.Y. (2007). A mutation in zebrafish hmgcr1b reveals a role for isoprenoids in vertebrate heart-tube formation. *Curr. Biol*. 17, 252–259.

Das, M., Ithychanda, S.S., Qin, J. and Plow, E.F. (2011). Migfilin and filamin as regulators of integrin activation in endothelial cells and neutrophils. *PLoS One*. 6, e26355.

Davis, S.M., Broderick, J., Hennerici, M., Brun, N.C., Diringer, M.N., Mayer, S.A., *et al.* (2006). Hematoma growth is a determinant of mortality and poor outcome after intracerebral hemorrhage. *Neurology*. 66, 1175-1181.

DeBose-Boyd, R.A. (2008). Feedback regulation of cholesterol synthesis: sterol-accelerated ubiquitination and degradation of HMG CoA reductase. *Cell Res*. 18, 609-621.

Dejana, E. and Del Maschio, A. (1995). Molecular organization andfunctional regulation of cell to cell junctions in the endothelium. *Thromb. Haemost*. 74, 309-312.

Del Bigio, M., Yan, H., Buist, R. and Peeling, J. (1996). Experimental intracerebral hemorrhage in rats. Magnetic resonance imaging and histopathological correlates. *Stroke*. 27, 2312–2319.

Denier, C., Goutagny, S., Labauge, P., Krivosic, V., Arnoult, M., Cousin, A., Benabid, A. L., Comoy, J., Frerebeau, P., Gilbert, B., *et al.* (2004). Mutations within the MGC4607 gene cause cerebral cavernous malformations. *Am. J. Hum. Genet*. 74, 326–337**.**

Deshpande, G. and Schedl, P. (2005). HMGCoA reductase potentiates hedgehog signaling in Drosophila melanogaster. *Dev. Cell*. 9, 629-38.

Dostal, L.A., Schardein, J.L. and Anderson, J.A. (1994). Developmental toxicity of the HMG-CoA reductase inhibitor, atorvastatin, in rats and rabbits. *Teratology*. 50, 387–394.

Dubuc, G., Chamberland, A., Wassef, H., Davignon, J., Seidah, N.G., Bernier, L. and Prat, A. (2004). Statins upregulate PCSK9, the gene encoding the proprotein convertase neural apoptosis-regulated convertase-1 implicated in familial hypercholesterolemia. *Arterioscler. Thromb. Vasc. Biol*. 24, 1454–1459.

Ebrahimi, H.A., Shafa, M.A. and Saha, M.D. (1999). Non-traumatic brain hemorrhage in Kerman, Iran. *Kerman University of medical sciences*. 10, 78.

Eerola, I., Boon, L.M., Mulliken, J.B., Burrows, P.E., Dompmartin, A., Watanabe, S., Vanwijck, R. and Vikkula, M. (2003). Capillary malformation-arteriovenous malformation, a new clinical and genetic disorder caused by RASA1 mutations. *Am. J Hum. Genet*.73, 1240-1249.

Eisa-Beygi, S., Hatch, G., Noble, S., Ekker, M. and Moon, T.W. (2013). The 3-hydroxy-3-methylglutaryl-CoA reductase (HMGCR) pathway regulates developmental cerebral-vascular stability via prenylation-dependent signalling pathway. *Dev. Bio*. 373, 258-366.

Eitzen, G., Thorngren, N. and Wickner, W. (2001). Rho1p and Cdc42p act after Ypt7p to regulate vacuole docking. *EMBO J*. 20, 5650-5656.

Elahi, M.M., Cagampang, F.R., Anthony, F.W., Curzen, N., Ohri, S.K. and Hanson, M.A. (2008). Statin treatment in hypercholesterolemic pregnant mice reduces cardiovascular risk factors in their offspring. *Hypertension*. 51, 939-944.

Elsalini, O.A. and Rohr, K.B. (2003). Phenylthiourea disrupts thyroid function in developing zebrafish. *Dev. Genes Evol*. 212, 593-598.

English, D., Welch, Z., Kovala, A.T., Harvey, K., Volpert, O.V., Brindley, D.N. and Garcia, J.G. (2000). Sphingosine 1-phosphate released from platelets during

clotting accounts for the potent endothelial cell chemotactic activity of blood serum and provides a novel link between hemostasis and angiogenesis. FASEB J. 14, 2255-2265.

Epting, D., Wendig, B., Bennewitz, K., Dietz, C.T., Driever, W. and Kroll, J. (2010). The Rac1 Regulator ELMO1 Controls Vascular Morphogenesis in Zebrafish. *Circ. Res*. 107, 45-55.

Espín, R., Roca, F.J., Candel, S., Sepulcre, M.P., González-Rosa, J.M., Alcaraz-Pérez, F., Meseguer, J., Cayuela, M.L., Mercader, N. and Mulero, V. (2013). TNF receptors regulate vascular homeostasis in zebrafish through a caspase-8, caspase-2 and P53 apoptotic program that bypasses caspase-3. *Dis. Model. Mech*. *6*, 383-396.

Etienne-Manneville, S. and Hall, A. (2002). Rho GTPases in cell biology. *Nature*. 420, 629-635.

Feng, Y., Chen, M. H., Moskowitz, I. P., Mendonza, A. M., Vidali, L., Nakamura, F., Kwiatkowski, D. J. and Walsh, C. A. (2006). Filamin A (FLNA) is required for cell-cell contact in vascular development and cardiac morphogenesis. *Proc. Natl. Acad. Sci. USA*. 103,19836–19841.

Fischer, A., Zalvide, J., Faurobert, E., Albiges-Rizo, C. and Tournier-Lasserve, E. (2013). Cerebral cavernous malformations: from CCM genes to endothelial cell homeostasis. *Trends Mol. Med*. 19, 302-308.

Foerch, C., Rosidi, N.L., Schlunk, F., Lauer, A., Cianchetti, F.A., Mandeville, E., Arai, K. Yigitkanli, K., Fan, X., Wang, X., van Leyen, K., Steinmetz, H., Schaffer, C.B. and Lo, E.H. (2013). Intravenous tPA Therapy does not worsen acute intracerebral hemorrhage in mice. *PLoS ONE*. 8, e54203.

Fordyce, C.B., Jagasia, R., Zhu, X. and Schlichter, L.C. (2005). Microglia Kv1.3channels contribute to their ability to kill neurons. *J. Neurosci*. 25, 7139–7149.

Freitas, R.N., Khaw, K.T., Wu, K., Bowman, R., Jeffery, H., Luben, R., Wareham, N.J. and Rodwell, S. (2010). HMGCR gene polymorphism is associated with stroke risk in the EPIC-Norfolk study. *Eur. J. Cardiovasc. Prev. Rehabil*. 17, 89-93.

Fujii, Y., Takeuchi, S., Sasaki, O., Minakawa, T. and Tanaka, R. (1998). Multivariate analysis of predictors of hematoma enlargement in spontaneous intracerebral hemorrhage. *Stroke*. 29, 1160-1166.

Fujii, Y., Takeuchi, S., Harada, A., Abe, H., Sasaki, O. and Tanaka, R. (2001). Hemostatic activation in spontaneous intracerebral hemorrhage. *Stroke*. 32, 883-890.

Futrakul, N., Butthep, P., Laohareungpanya, N., Chaisuriya, P. and Ratanabanangkoon, K. (2008). A defective angiogenesis in chronic kidney disease. *Ren. Fail*. 2008, 30, 215-217.

Gavard, J. and Gutkind, J.S. (2008). E-cadherin and claudin-5: it takes two to tango. *Nat. Cell Biol*. 10, 883-885.

Gerhardt, H., Golding, M., Fruttiger, M., Ruhrberg, C., Lundkvist, A., Abramsson, A., Jeltsch, M., Mitchell, C., Alitalo, K., Shima, D., *et al.* (2003). VEGF guides angiogenic sprouting utilizing endothelial tip cell filopodia. *J. Cell Biol*. 16, 1163–1177.

Gertler, F.B., Chiu, C.Y., Richter-Mann, L. and Chin, D.J. (1988). Developmental and metabolic regulation of the Drosophila melanogaster 3-hydroxy-3-methylglutaryl coenzyme A reductase. *Mol. Cell. Biol*. 8, 2713-2721.

Gil, G., Faust, J.R., Chin, D.J., Goldstein, J.L. and Brown, M.S. (1985). Membrane-bound domain of HMG CoA reductase is required for sterol-enhanced degradation of the enzyme. *Cell*. 41, 249-258.

Glading, A., Han, J., Stockton, R.A. and Ginsberg, M.H. (2007). KRIT-1/CCM1 is a Rap1 effector that regulates endothelial cell–cell junctions. *J. Cell Biol*. 179,247–254.

Glading, A.J. and Ginsberg, M.H. (2010). Rap1 and its effector KRIT1/CCM1 regulate beta-catenin signaling. *Dis. Model Mech*. 3, 73-83.

Goldstein, J. L., Dana, S. E., Brunschede, G. Y. and Brown, M. S. (1975). Genetic heterogeneity in familial hypercholesterolemia: evidence for two different mutations affecting functions of low-density lipoprotein receptor. *Proc. Nat. Acad. Sci*. U S A.72, 1092-1096.

Goldstein, J.L. and Brown, M.S. (1990). Regulation of the mevalonate pathway. *Nature*. 343, 425-430.

Goldstein, L., Teng, Z.P., Zeserson, E., Patel, M. and Regan, R.F. (2003). Hemin induces an iron-dependent, oxidative injury to human neuron-like cells. *J. Neurosci.* Res. 73, 113-121

Gore, A.V., Lampugnani, M.G., Dye, L., Dejana, E. and Weinstein, B.M. (2008). Combinatorial interaction between CCM pathway genes precipitates hemorrhagic stroke. *Dis. Model. Mech*. 1, 275-281.

Gore, A.V., Monzo, K., Cha, Y.R., Pan, W. and Weinstein, B.M. (2012). Vascular development in the zebrafish. *Cold Spring Harb. Perspect. Med*. 2, a006684.

Gray, C., Packham, I.M., Wurmser, F., Eastley, N.C., Hellewell, P.G., Ingham, P.W., Crossman,D.C. and Chico, T.J. (2007). Ischemia is not required for arteriogenesis in zebrafish embryos. *Arterioscler. Thromb. Vasc . Biol.* 27, 2135-2141.

Gu, Y., Hua, Y., Keep, R.F., Morgenstern, L.B. and Xi, G. (2009). Deferoxamine reduces intracerebral hematoma-induced iron accumulation and neuronal death in piglets. *Stroke*. 40, 2241–2243.

Guijarro, C., Blanco-Colio, L.M., Massy, Z.A., O'Donnell, M.P., Kasiske, B.L., Keane, W.F. and Egido, J. (1999). Lipophilic statins induce apoptosisof human vascular smooth muscle cells. *Kidney Int. Suppl*. 71, 88–91.

Gumbiner, B. M. (2000). Regulation of cadherin adhesive activity. *J. Cell Biol*. 148, 399-404.

Habeck, H., Odenthal, J., Walderich, B., Maischein, H., Schulte-Merker, S. and Tübingen 2000 screen consortium. (2002). *Curr. Biol*. 12, 1405-1412.

Hackam, D.G., Austin, P.C., Huang, A., Juurlink, D.N., Mamdani, M.M., Paterson, J.M., Hachinski, V., Li, P. and Kapral, M.K. (2012). Statins and intracerebral hemorrhage: a retrospective cohort study. *Arch. Neurol*. 69, 39-45.

Hardie, D.G. (1992). Regulation of fatty acid and cholesterol metabolism by the AMP-activated protein kinase. *Biochim. Biophys. Acta*. 12, 231–238.

Hegarty, J.M., Yang, H. and Chi, N.C. (2013). UBIAD1-mediated vitamin K2 synthesis is required for vascular endothelial cell survival and development. *Development.* 140, 1713-1719.

Hindler, K., Cleeland, C.S., Rivera, E. and Collard, C.D. (2006). The role of statins in cancer therapy. *Oncologist*. 11, 306-315.

Hippenstiel, S., Schmeck, B., N'Guessan, P. D., Seybold, J., Krüll, M., Preissner, K., Von Eichel-Streiber, C. and Suttorp, N. (2002). Rho protein inactivation induced apoptosis of cultured human endothelial cells. *Am. J. Physiol. Lung Cell Mol. Physiol*. 283, L830–L838.

Hirai, A., Nakamura, S., Noguchi, Y., Yasuda, T., Kitagawa, M., Tatsuno, I., Oeda, T., Tahara, K., Terano, T., Narumiya, S., Kohn, L.D. and Saito, Y. (1997). Geranylgeranylated rho small GTPase(s) are essential for the degradation of p27Kip1 and facilitate the progression from G1 to S phase in growth-stimulated rat FRTL-5 cells. *J. Biol. Chem*. 272, 13–16.

Hofmann, C., Shepelev, M. and Chernoff, J. (2004). The genetics of Pak. *J. Cell Sci*. 117, 4343–4354.

Hogan, B.M., Bussmann, J., Wolburg, H. and Schulte-Merker, S. (2008). ccm1 cell autonomously regulates endothelial cellular morphogenesis and vascular tubulogenesis in zebrafish. *Hum. Mol. Genet*. 17, 2424–2432.

Holzschuh, J., Ryu, S., Aberger, F. and Driever, W. (2001). Dopamine transporter expression distinguishes dopaminergic neurons from other catecholaminergic neurons in the developing zebrafish embryo. *Mech. Dev*. 101, 237-243.

Hua, Y., Nakamura, T., Keep, R.F., Wu, J., Schallert, T., Hoff, J.T. and Xi, G. (2006). Long-term effects of experimental intracerebral hemorrhage: the role of iron. *J. Neurosurg*. 104, 305–312.

Hua, Y., Keep, R.F., Hoff, J.T. and Xi, G. (2007). Brain injury after intracerebral hemorrhage: the role of thrombin and iron. *Stroke*. 38, 759-762.

Huang, M., Hu, Y.Y., Dong, X.Q., Xu, Q.P., Yu, W.H. and Zhang ZY. (2012). The protective role of oxymatrine on neuronal cell apoptosis in the hemorrhagic rat brain. *J. Ethnopharmacol*. 143, 228-235.

Hung, M.W., Zhang, Z.J., Li, S., Lei, B., Yuan, S., Cui, G.Z., Man, Hoi, P., Chan, K. and Lee, S.M. (2012). From omics to drug metabolism and high content screen of natural product in zebrafish: a new model for discovery of neuroactive compound. *Evid. Based Complement. Alternat. Med*. 2012, 605303.

Hutter, C.M., Austin, M.A. and Humphries, S.E. (2004). Familial hypercholesterolemia, peripheral arterial disease, and stroke: a HuGE minireview. *Am. J. Epidemiol*. 160, 430-435.

Hwa, J.J., Zollman, S., Warden, C.H., Taylor, B.A., Edwards, P.A., Fogelman, A.M. and Lusis, A.J. (1992). Genetic and dietary interactions in the regulation of HMG-CoA reductase gene expression. *J. Lipid Res*. 33, 711-725.

Igel, M., Sudhop, T. and von Bergmann, K. (2001). Metabolism and drug interactions of 3-hydroxy-3-methylglutaryl coenzyme A-reductase inhibitors (statins). *Eur. J. Clin. Pharmacol*. 57, 357-364.

Isgandarova, S., Jones, L., Forsberg, D., Loncar, A., Dawson, J., Tedrick, K. and Eitzen, G. (2007). Stimulation of actin polymerization by vacuoles via Cdc42p-dependent signalling. *J. Biol. Chem*. 282, 30466-30475.

Isogai, S., Horiguchi, M. and Weinstein, B.M. (2001). The vascular anatomy of the developing zebrafish: an atlas of embryonic and early larval development. *Dev. Biol*. 230, 278-301.

Istvan, E.S. and Deisenhofer, J. (2001). Structural mechanism for statin inhibition of HMG-CoA reductase. *Science*. 292, 1160-1164.

Jain, R.K. (2003). Molecular regulation of vessel maturation. *Nat. Med*. 9, 685-693.

Johnston, T.P., Nguyen, L.B., Chu, W.A. and Shefer, S. (2001). Potency of select statin drugs in a new mouse model of hyperlipidemia and atherosclerosis. *Int. J. Pharm*. 229, 75-86.

Joshi, H.N., Fakes, M.G. and Serajuddin, A.T.M. (1999). Differentiation of 3-hydroxy-3 methylglutaryl-coenzyme A (HMG-CoA) reductase inhibitors by their relative lipophilicity. *Pharm. Pharmacol. Commun*. 5, 269-271.

Kamei, M., Saunders, W.B., Bayless, K.J., Dye, L., Davis, G.E. and Weinstein, B.M. (2006). Endothelial tubes assemble from intracellular vacuoles in vivo. *Nature*. 442, 453–456.

Kaneta S., Satoh K., Kano S., Kanda M. and Ichihara K. (2003). All hydrophobic HMG-CoA reductase inhibitors induce apoptotic death in rat pulmonary vein endothelial cells. *Atherosclerosis*. 170, 237–243.

Karwacki, Z., Kowiański, P., Dziewiatkowski, J., Domaradzka-Pytel, B., Ludkiewicz, B., Wójcik, S., Narkiewicz, O. and Moryś, J. (2005). The influence of sevoflurane on the reactivity of astrocytes in the course of the experimental intracerebral haemorrhage in rat. *J. Physiol. Pharmacol.* 56, 455-469.

Kaushal, V., Koeberle, P.D., Wang, Y. and Schlichter, L.C. (2007). The Ca^{2+}-activated K^{+}channel KCNN4/KCa3.1 contributes to microglia activation and nitric oxide-dependent neurodegeneration. *J. Neurosci*. 27, 234–244.

Kazui, S., Naritomi, H., Yamamoto, H., Sawada, T. and Yamaguchi, T. (1996). Enlargement of spontaneous intracerebral hemorrhage. Incidence and time course. *Stroke*. 27, 1783–1787.

Khaidakov, M., Wang, W., Khan, J.A., J.A. Kang, B.Y., Hermonat, P.L. and Mehta, J.L. (2009). Statins and angiogenesis: Is it about connections? *Biochem. Biophys. Res. Commun*. 387, 543–547.

Kim, J., Wu, Q., Zhang, Y., Wiens, K.M., Huang, Y., Rubin, N., Shimada, H., Handin, R.I., Chao, M.Y., Tuan, T.L., Starnes, V.A. and Lien, C.L. (2010). PDGF signaling is required for epicardial function and blood vessel formation in regenerating zebrafish hearts. *Proc. Natl. Acad. Sci. U S A.* 107, 17206-17210.

Kleaveland, B., Zheng, X., Liu, J.J., Blum, Y., Tung, J.J., Zou, Z., Chen, M., Guo, L., Zhou, D., Kitajewski, J., Affolter, M., Ginsberg, M.H. and Kahn, M.L. (2009). Regulation of cardiovascular development and integrity by the heart of glass-cerebral cavernous malformation protein pathway. *Nat. Med*. 15, 169–176.

Kobari, M., Gotoh, F., Tomita, M., Tanahashi, N., Shinohara, T., Terayama, Y. and Mihara, B. (1988). Bilateral hemisphericreduction of cerebral blood volume and blood flowimmediately after experimental cerebral hemorrhage in cats. *Stroke*. 19, 991–996.

Kouklis, P., Konstantoulaki, M. and Malik, A. B. (2003). VE-cadherin-induced Cdc42 signalling regulates formation of membrane protrusions in endothelial cells. *J. Biol. Chem*. 278, 16230-16236.

Krycer, J.R., Kristiana, I. and Brown, A.J. (2009). Cholesterol homeostasis in two commonly used human prostate cancer cell-lines, LNCaP and PC-3. *PLoS ONE* . 4, e8496.

Kumar, M.S. and Owens, G.K. (2003). Combinatorial control of smooth muscle-specific gene expression. *Arterioscler. Thromb. Vasc. Biol*. 23, 737-747.

Kwon, H.B., Choi, Y.K., Lim, J.J., Kwon, S.H., Her, S., Kim, H.J., Lim, K.J., Ahn, J.C., Kim, Y.M., Bae, M.K., Park, J.A., Jeong, C.H., Mochizuki, N. and Kim ,K.W. (2012). AKAP12 regulates vascular integrity in zebrafish. *Exp. Mol. Med.* 44, 225-235.

Lang, E.W., Ren Ya, Z., Preul, C., Hugo, H.H., Hempelmann, R.G., Buhl, R., Barth, H., Klinge, H. and Mehdorn, H.M. (2001). Stroke pattern interpretation: the variability of hypertensive versus amyloid angiopathy hemorrhage. *Cerebrovasc. Dis.* 12, 121-130.

Larsson, J., Goumans, M. J., Sjostrand, L. J., van Rooijen, M. A., Ward, D.,Leveen, P., Xu, X., ten Dijke, P., Mummery, C. L. and Karlsson, S. (2001). Abnormal angiogenesis but intact hematopoietic potential in TGF-beta type Ireceptor-deficient mice. *EMBO J*. 20, 1663-1673.

Laufs, U., Kilter, H., Konkol, C., Wassmann, S., Bohm, M. and Nickenig, G. (2002). Impact of HMG CoA reductase inhibition on small GTPases in the heart. *Cardiovasc. Res*. 53, 911-920.

Lawson, N.D. and Weinstein, B.M. (2002). In vivo imaging of embryonic vascular development using transgenic zebrafish. *Dev. Biol*. 248, 307-318.

Lee, J.N., Song, B., DeBose-Boyd, R.A. and Ye, J. (2006). Sterol-regulated degradation of Insig-1 mediated by the membrane-bound ubiquitin ligase gp78. *J. Biol. Chem*. 281, 39308-39315.

Lennernas, H. and Fager, G. (1997). Pharmacodynamics and pharmacokinetics of the HMG-CoA reductase inhibitors. Similarities and differences. Clin. Pharmacokinet. 32, 403-425.

Li, D.Y. and Whitehead, K.J. (2010). Evaluating strategies for the treatment of cerebral cavernous malformations. *Stroke*. 41(suppl), S92-S94.

Li, X., Liu, L., Tupper, J.C., Bannerman, D.D., Winn, R.K., Sebti, S.M., Hamilton, A.D. and Harlan, J.M. (2002). Inhibition of protein geranylgeranylation and RhoA/RhoA kinase pathway induces apoptosis in human endothelial cells. *J. Biol. Chem*. 277, 15309–15316.

Li, L., Yan, B., Shi, Y.Q., Zhang, W.Q. and Wen, Z.L. (2012). Live imaging reveals differing roles of macrophages and neutrophils during zebrafish tail fin regeneration. *J. Biol. Chem*. 287, 25353-25360.

Liao, J.K. and Laufs, U. (2005). Pleiotropic effects of statins. *Annu. Rev. Pharmacol. Toxicol*. 45, 89-118.

Liao, J.K. (2002). Isoprenoids as mediators of the biological effect of statins. *J. Clin Invest*. 110, 285–288.

Lien, C. L., Schebesta, M., Makino, S., Weber, G. J., and Keating, M. T. (2006). Gene expression analysis of zebrafish heart regeneration. *PLoS Biol.* 4, e260.

Lieschke, G.J. and Currie, P.D. (2007). Animal models of human disease: zebrafish swim into view. *Nat. Rev. Genet.* 8, 353-367.

Lieu, A.S., Hwang, S.L., Howng, S.L. and Chai, C.Y. (1999). Brain tumors with hemorrhage. *J. Formos. Med. Assoc.* 98, 365-367.

Lin, H,F,, Traver, D,, Zhu, H., Dooley, K., Paw, B.H., Zon, L.I. and Handin, R.I. (2005). Analysis of thrombocyte development in CD41-GFP transgenic zebrafish. *Blood*. 106, 3803-3810.

Liu, J., Fraser, S.D., Faloon, P.W., Rollins, E.L., Vom Berg, J., Starovic-Subota, O., Laliberte, A.L., Chen, J.N., Serluca, F.C. and Childs, S.J. (2007). A betaPix Pak2a signaling pathway regulates cerebral vascular stability in zebrafish. *Proc. Natl. Acad. Sci. USA.* 104, 13990-13995.

Loeys, B. L., Chen, J., Neptune, E. R., Judge, D. P., Podowski, M., Holm, T., Meyers,J., Leitch, C. C., Katsanis, N., Sharifi, N., *et al.* (2005). A syndrome of alteredcardiovascular, craniofacial, neurocognitive and skeletal development caused bymutations in TGFBR1 or TGFBR2. *Nat. Genet*. 37, 275-281.

Loftspring, M.C., McDole, J., Lu, A., Clark, J.F. and Johnson, A.J. (2009). Intracerebral hemorrhage leads to infiltration of several leukocyte populations with concomitant pathophysiological changes. *J. Cereb. Blood Flow Metab*. 29, 137-143.

Lou X., Deshwar A. R., Crump J. G. and Scott I. C., 2011. Smarcd3b and Gata5 promote a cardiac progenitor fate in the zebrafish embryo. *Development.* 138, 3113–3123.

Louvi, A., Chen, L., Two, A. M., Zhang, H., Min, W. and Gunel, M. (2011). Loss of cerebral cavernous malformation 3 (Ccm3) in neuroglia leads to CCM and vascular pathology. *Proc. Natl. Acad. Sci. USA. 108, 3737-3742.*

Lu, D., Goussev, A., Chen, J., Pannu, P., Li, Y., Mahmood, A. and Chopp, M., 2004. Atorvastatin reduces neurological deficit and increases synaptogenesis, angiogenesis, and neuronal survival in rats subjected to traumatic brain injury. *J. Neurotrauma*. 21, 21–32.

Lucas, M., Costa, A. F., Garcia-Moreno, J. M., Solano, F., Gamero, M. A. and Izquierdo, G. (2003). Variable expression of cerebral cavernous malformations in carriers of a premature termination codon in exon 17 of the Krit1 gene. *BMC Neurol*. 3, 5.

Maeder, P., Gudinchet, F., Meuli, R. and de Tribolet, N. (1998). Development of a cavernous malformation of the brain. *AJNR Am. J. Neuroradiol*.19, 1141-1143.

Mammen, A.L., Chung, T., Christopher-Stine, L., Rosen, P., Rosen, A., Doering, K.R. and Casciola-Rosen, L.A. (2011). Autoantibodies against 3-hydroxy-3-methylglutaryl-coenzyme A reductase in patients with statin-associated autoimmune myopathy. *Arthritis Rheum*. 63, 713-721.

Manser, E., Loo, T.H., Koh, C.G., Zhao, Z.S., Chen, X.Q., Tan, L., Tan, I., Leung, T. and Lim, L. (1998). PAK kinases are directly coupled to the PIX family of nucleotide exchange factors. *Mol. Cell*. 1, 183-192.

Marion, D.W., Penrod, L.E., Kelsey, S.F., Obrist, W.D., Kochanek, P.M., Palmer, A.M., Wisniewski, S.R. and DeKosky, S.T. (1997). Treatment of traumatic brain injury with moderate hypothermia. *N. Engl. J. Med.* 336, 540–546.

Matsushita, K., Meng, W., Wang, X., Asahi, M., Asahi, K., Moskowitz, M.A. and Lo, E.H. (2000). Evidence for apoptosis after intercerebral hemorrhage in rat striatum. *J. Cereb. Blood Flow Metab*. 20, 396–404.

Mayer, S,A. (2005). Ultra-early Hemoastatic therapy for primary intracerebral hemmorhage: a review. *Can. J. Neurol. Sci.* S2, S31–37.

McCarty, J. H., Monahan-Earley, R. A., Brown, L. F., Keller, M.,Gerhardt, H., Rubin, K., Shani, M., Dvorak, H. F., Wolburg, H., Bader,B. L., *et al.* (2002). Defective associations between blood vessels and brainparenchyma lead to cerebral hemorrhage in mice lacking alphav integrins. *Mol. Cell. Biol*. 22, 7667-7677.

McDonald, D.A., Shi, C., Shenkar, R., Stockton, R.A., Liu, F., Ginsberg, M.H., Marchuk, D.A. and Awad, I.A., 2012. Fasudil decreases lesion burden in a murine model of cerebral cavernous malformation disease. *Stroke*. 43, 571–574.

McLean, D. L. and Fetcho, J. R. (2008). Using imaging and genetics in zebrafish to study developing spinal circuits in vivo. *Dev. Neurobiol*. 68, 817–834.

McKinney, J.S. and Kostis, W.J. (2012). Statin therapy and the risk of intracerebral hemorrhage: a meta-analysis of 31 randomized controlled trials. *Stroke*. 43, 2149-2156.

Medina, M.W., Gao, F., Ruan, W., Rotter, J.I. and Krauss, R.M. (2008). Alternative splicing of 3-hydroxy-3-methylglutaryl coenzyme A reductase is associated with plasma low-density lipoprotein cholesterol response to simvastatin. *Circulation*. 118, 355-362.

Medina, M.W. and Krauss, R.M. (2009). The role of HMGCR alternative splicing in statin efficacy. *Trends Cardiovasc Med*. 19, 173-177.

Medina, M.W. (2010). The relationship between HMGCR genetic variation, alternative splicing, and statin efficacy. *Discov. Med*. 9, 495-499.

Michalak, S. and Wender, M. (1996). Cholesterol synthesis in the rat brain in course of late development as determined by 3-hydroxy-3-methylglutaryl CoA reductase activity. *Folia Neuropathol*. *34*, 7-10.

Minsker, D.H., McDonald, J.S., Robertson, R.T. and Bokelman, D.L. (1983). Mevalonate supplementation in pregnant rats suppresses the teratogenity of mevalonic acid, an inhibitor of 3-hydroxy-3-methylglutaryl coenzyme A reductase. *Teratology*. 28,449–456.

Mizuguchi, T., Collod-Beroud, G., Akiyama, T., Abifadel, M., Harada, N., Morisaki,T., Allard, D., Varret, M., Claustres, M., Morisaki, H., *et al.* (2004). Heterozygous TGFBR2 mutation in Marfan syndrome. *Nat. Genet*. 36, 855-860.

Montero-Balaguer, M., Swirsding, K., Orsenigo, F., Cotelli, F., Mione, M. and Dejana, E. (2009). Stable vascular connections and remodeling require full expression of VE-cadherin in zebrafish embryos. *PLoS One*. 4, e5772.

Morgenstern, L.B., Frankowski, R.F., Shedden, P., Pasteur, W. and Grotta, J.C. (1998). Surgical treatment for intracerebral hemorrhage (STICH): a single-center, randomized clinical trial. *Neurology*. 51, 1359–1363.

Murakami, K., Endo, T. and Tominaga, T. (2012). An analysis of flow dynamics in cerebral cavernous malformation and orbital cavernous angioma using indocyanine green videoangiography. *Acta. Neurochir.* (Wien). 154, 1169-1175.

Nakanishi, M., Goldstein, J.L. and Brown, M.S. (1988). Multivalent control of 3-hydroxy-3-methylglutaryl coenzyme A reductase. Mevalonate-derived product inhibits translation of mRNA and accelerates degradation of enzyme. *J. Biol. Chem*. 263, 8929-8937.

Ohashi, K., Osuga, J., Tozawa, R., Kitamine, T., Yagyu, H., Sekiya, M., Tomita, S., Okazaki, H., Tamura, Y., Yahagi, N., Iizuka, Y., Harada, K., Gotoda, T., Shimano, H., Yamada, N. and Ishibashi, S. (2003). Early embryonic lethality caused by targeted disruption of the HMG-CoA reductase gene. *J. Biol. Chem*. 278, 42936-42941.

Omkumar, R.V., Darnay, B.G. and Rodwell, V.W. (1994). Modulation of Syrian hamster 3-hydroxy-3-methylglutaryl-CoA reductase activity by phosphorylation. Role of serine 871. *J. Biol. Chem*. 269, 6810-6814.

Paleolog, E.M. (2002). Angiogenesis in rheumatoid arthritis. *Arthritis Res*. 4, S81-S90.

Park, H,J., Kong, D., Iruela-Arispe, L., Begley, U., Tang, D. and Galper, J.B. (2002). 3-Hydroxy-3-methylglutaryl coenzyme A reductase inhibitors interfere with angiogenesis by inhibiting the geranylgeranylation of RhoA. *Circ. Res*. 91,143-150.

Perel, P., Roberts, I., Bouamra, O., Woodford, M., Mooney, J. and Lecky, F. (2009). Intracranial bleeding in patients with traumatic brain injury: A prognostic study. *BMC Emerg Med*. 9, 15.

Peterson, R.T., Shaw, S.Y., Peterson, T.A., Milan, D.J., Zhong, T.P., Schreiber, S.L., MacRae, C.A. and Fishman, M.C. (2004). Chemical suppression of a genetic mutation in a zebrafish model of aortic coarctation. *Nat. Biotechnol*. 22, 595-599.

Peterson, Y. K., Kelly, P., Weinbaum, C. A. and Casey, P. J. (2006). A novel protein geranylgeranyltransferase- I inhibitor with high potency, selectivity, and cellular activity. *J. Biol. Chem*. 281, 12445–12450.

Plummer, N.W., Gallione, C.J., Srinivasan, S., Zawistowski, J.S., Louis, D.N. and Marchuk, D.A. (2004). Loss of p53 sensitizes mice with a mutation in Ccm1 (KRIT1) to development of cerebral vascular malformations. *Am. J. Pathol*. 165, 1509–1518.

Prawan, A., Kundu, J.K. and Surh, Y.J. (2005). Molecular basis of heme oxygenase-1 induction: Implications for chemoprevention and chemoprotection. *Antioxid. Redox. Signal*. 7, 1688-1703.

Qureshi, A.I., Bliwise, D.L., Bliwise, N.G., Akbar, M.S., Uzen, G. and Frankel, M.R. (1999). Rate of 24-hour blood pressure decline and mortality after spontaneous intracerebral hemorrhage: a retrospective analysis with a random effects regression model. *Crit. Care Med*. 27, 480–485.

Qureshi, A.I., Mohammad, Y.M., Yahia, A.M., Suarez, J.I., Siddiqui, A.M., Kirmani, J.F., Suri, M.F., Kolb, J. and Zaidat, O.O. (2005). A prospective multicenter study to evaluate the feasibility and safety of aggressive antihypertensive treatment in patients with acute intracerebral hemorrhage. *J. Intensive Care Med*. 20, 34-42.

Ramchandran, R., Mehta, D., Vogel, S.M., Mirza, M.K., Kouklis, P. and Malik, A.B. (2008). Critical role of Cdc42 in mediating endothelial barrier protection in vivo. *Am. J. Physiol. Lung Cell Mol. Physiol*. 295, 363–369.

Rink, E. and Wullimann, M. F. (2002). Development of the catecholaminergic system in the early zebrafish brain: an immunohistochemical study. *Brain Res. Dev. Brain Res*. 137, 89-100.

Roberts, P. J., Mitin, N., Keller, P. J., Chenette, E. J., Madigan, J. P., Currin, R. O., Cox, A. D., Wilson, O., Kirschmeier, P. and Der, C. J. (2008). Rho family GTPase modification and dependence on CAAX motif-signaled posttranslational modification. *J. Biol. Chem*. 283, 25150-25163.

Rosenberg, G.A., Mun-Bryce, S., Wesley, M. and Kornfeld, M. (1990). Collagenase-induced intracerebral hemorrhage in rats. *Stroke*. 21, 801-807.

Rosenberg, G.A., Estrada, E.Y. and Dencoff, J.E. (1992). Matrix metalloproteinases and TIMPs are associated with blood-brain barrier opening after reperfusion in rat brain. *Stroke*. 29, 2189-2195.

Sahni, R. and Weinberger, J. (2007). Management of intracerebral hemorrhage. *Vasc. Health Risk. Manag.* 3, 701-709.

Sahoo, T., Johnson, E.W., Thomas, J.W., Kuehl, P.M., Jones, T.L., Dokken, C.G., Touchman, J.W., Gallione, C.J., Lee-Lin, S.Q., Kosofsky, B., Kurth, J.H., Louis, D.N., Mettler, G., Morrison, L., Gil-Nagel, A., Rich, S.S., Zabramski, J.M.,

Boguski, M.S., Green, E.D. and Marchuk, D.A. (1999). Mutations in the gene encoding KRIT1, a Krev-1/rap1a binding protein, cause cerebral cavernous malformations (CCM1). *Hum. Mol. Genet*. 8, 2325-2333.

Saint-Amant, L. and Drapeau, P. (2000). Motoneuron ac-tivity patterns related to the earliest behavior ofthe zebrafish embryo. *J. Neurosci*. 20, 3964–3972.

Santoro, M.M., Pesce, G. and Stainier D.Y. (2009). Characterization of vascular mural cells during zebrafish development. *Mech. Dev*. 126, 638-649.

Santos, A.C. and Lehmann, R., 2004. Isoprenoids control germ cell migration downstream of HMGCoA reductase. *Dev. Cell*. 6, 283–293.

Sato, R., Goldstein, J.L. and Brown, M.S. (1993). Replacement of serine-871 of hamster 3-hydroxy-3-methylglutaryl-CoA reductase prevents phosphorylation by AMP-activated kinase and blocks inhibition of sterol synthesis induced by ATP depletion. *Proc. Natl. Acad. Sci. U S A*. 90, 9261-9265.

Seiler, C., Abrams, J. and Pack, M. (2010). Characterization of zebrafish intestinal smooth muscle development using a novel sm22α-b promoter. *Dev. Dyn*. 239, 2806-2812.

Serebriiskii, I., Estojak, J., Sonoda, G., Testa, J.R. and Golemis, E.A. (1997). Association of Krev-1/rap1a with Krit1, a novel ankyrin repeat-containing protein encoded by a gene mapping to 7q21-22. *Oncogene*. 15, 1043-1049.

Shen, M., Yu, H., Li, Y., Li, P., Pan, P., Zhou, S., Zhang, L., Li, S., Lee, S.M. and Hou, T. (2013). Discovery of Rho-kinase inhibitors by docking-based virtual screening. *Mol. Biosyst*. 9, 1511-1521.

Sirtori, C.R. (1993). Tissue selectivity of hydroxymethylglutaryl coenzyme A (HMG CoA) reductase inhibitors. *Pharmacol. Ther*. 60, 431–459.

Skalnik, D.G., Narita, H., Kent, C. and Simoni, R.D. (1988). The membrane domain of 3-hydroxy-3-methylglutaryl-coenzyme A reductase confers endoplasmic reticulum localization and sterol-regulated degradation onto beta-galactosidase. *J. Biol. Chem*. 263, 6836-6841.

Sluimer, J.C. and Daemen, M.J. (2009). Novel concepts in atherogenesis: angiogenesis and hypoxia in atherosclerosis. *J. Pathol*. 218, 7-29.

Spence, J.D. (2012). Statins do not cause intracerebral hemorrhage. *Neurology*. 79, 1076-1077.

Spindler, V., Schlegel, N. and Waschke, J.(2010). Role of GTPases in control of microvascular permeability. *Cardiovasc. Res*. 87, 243–253.

Stainier, D.Y., Fouquet, B., Chen, J.N., Warren, K.S., Weinstein, B.M., Meiler, S.E., Mohideen, M.A., Neuhauss, S.C., Solnica-Krezel, L., Schier, A.F., Zwartkruis, F., Stemple, D.L., Malicki, J., Driever, W. and Fishman, M.C. (1996). Mutations

affecting the formation and function of the cardiovascular system in the zebrafish embryo. *Development*. 123, 285-292.

Steiner, T., Vincent, C., Morris, S., Davis, S., Vallejo-Torres, L. and Christensen, M.C. (2011). Neurosurgical outcomes after intracerebral hemorrhage: results of the Factor Seven for Acute Hemorrhagic Stroke Trial (FAST). *J. Stroke Cerebrovasc. Dis.* 20, 287-294.

Strieter, R.M., Burdick, M.D., Mestas, J., Gomperts, B., Keane, M.P. and Belperio, J.A. (2006). Cancer CXC chemokine networks and tumour angiogenesis. *Eur. J. Cancer*. 42, 768–778.

Sutherland, G.R. and Auer, R.N. (2006). Primary intracerebal hemorrhage. *J. Clin. Neuroscience*. 13, 511–517.

Thelen, K.M., Rentsch, K.M., Gutteck, U., Heverin, M., Olin, M., Andersson, U., von Eckardstein, A., Björkhem, I. and Lütjohann, D. (2005). Brain cholesterol synthesis in mice is affected by high dose of simvastatin but not of pravastatin. *J. Pharmacol. Exp. Ther*. 316, 1146-1152.

Thorpe, J.L., Doitsidou, M., Ho, S.Y., Raz, E. and Farber, S.A. (2004). Germ cell migration in zebrafish is dependent on HMG-CoA reductase activity and prenylation. *Dev. Cell*. 6, 295–302.

Traver, D., Paw, B. H., Poss, K. D., Penberthy, W. T., Lin, S. and Zon, L. I. (2003). Transplantation and in vivo imaging of multilineage engraftment inzebrafish bloodless mutants. *Nat. Immunol*. 4, 1238-1246.

Tsukita, S., Furuse, M. and Itoh, M. (2001). Multifunctional strands in tight junctions. *Nat. Rev. Mol. Cell Biol*. 2, 285-293.

Van Doren, M., Broihier, H.T., Moore, L.A. and Lehmann, R. (1998). HMG-CoA reductase guides migrating primordial germ cells. *Nature*. 396, 466-469.

Vaughan, C.J. and Delanty, N. (1999). Neuroprotective properties of statins in cerebral ischemia and stroke. *Stroke*. 30, 1969-1973.

Verlaan, D.J., Laurent, S.B., Sure, U., Bertalanffy, H., Andermann, E., Andermann, F., Rouleau, G.A. and Siegel, A.M. (2004). CCM1 mutation screen of sporadic cases with cerebral cavernous malformations. *Neurology*. 62, 1213-1215.

Versmissen, J., Oosterveer, D.M., Yazdanpanah, M., Defesche, J.C., Basart, D.C., Liem, A.H., Heeringa, J., Witteman, J.C., Lansberg, P.J., Kastelein, J.J. and Sijbrands, E.J. (2008). Efficacy of statins in familial hypercholesterolaemia: a long term cohort study. *BMJ*. 337, a2423.

Voss, K., Stahl, S., Schleider, E., Ullrich, S., Nickel, J., Mueller, T.D. and Felbor, U. (2007). CCM3 interacts with CCM2 indicating common pathogenesis for cerebral cavernous malformations. *Neurogenetics*. 8, 249-256.

Wagner, K.R., Xi, G., Hua, Y., Kleinholz, M., de Courten-Myers, G.M. and Myers, R.E. (1998). Early metabolic alterations in edematous perihematomal brain regions following experimental intracerebral hemorrhage. *J. Neurosurg*. 88, 1058–1065.

Wagner, K.R., Sharp, F.R., Ardizzone, T.D., Lu, A. and Clark, J.F. (2003). Heme and iron metabolism: role in cerebral hemorrhage. *J. Cereb. Blood Flow Metab*. 23, 629-652.

Wagner, K.R., Xi, G., Hua, Y., Kleinholz, M., de Courten-Myers, G.M., Myers, R.E., Broderick, J.P. and Brott, T.G. (1996). Lobar intracerebral hemorrhage model in pigs: rapid edema development in perihematomal white matter. *Stroke*. 27, 490–497.

Wang, C., Tao, W., Wang, Y., Bikow, J., Lu, B., Keating, A., Verma, S., Parker, T.G., Han, R. and Wen, X.Y. (2010). Rosuvastatin, identified from a zebrafish chemical genetic screen for antiangiogenic compounds, suppresses the growth of prostate cancer. *Eur. Urol*. 58, 418-426.

Wasserman, J.K. and Schlichter, L.C. (2007a). Neuron death and inflammation ina rat model of intracerebral hemorrhage: effects of delayed minocyclinetreatment. *Brain Res*. 1136, 208–218.

Weinstein, B.M., Stemple, D.L., Driever, W. and Fishman, M.C. (2005). Gridlock, a localized heritable vascular patterning defect in the zebrafish. *Nat. Med*. 1, 1143-1147.

Weis, M., Heeschen, C., Glassford, A.J. and Cooke, J.P. (2002). Statins have biphasic effects on angiogenesis. *Circ. Res*. 105,739–745.

Weitz-Schmidt, G. (2002). Statins as anti-inflammatory agents. *Trends Pharmacol. Sci*. 23**,** 482–486.

Westover, M,B,, Bianchi, M,T., Eckman, M.H. and Greenberg, S.M. (2011). Statin use following intracerebral hemorrhage: a decision analysis. *Arch. Neurol*. 68, 573-579.

Whitehead, K.J., Chan, A.C., Navankasattusas, S., Koh, W., London, N.R., Ling, J., Mayo, A.H., Drakos, S.G., Marchuk, D.A., Davis, G.E. and Li, D.Y. (2009). The cerebral cavernous malformation signalling pathway promotes vascular integrity via Rho GTPases. *Nat. Med*. 15,177-184.

Wu, S.C., Shiang, J.C., Lin, S.L., Wu, T.L., Huang, W.C., Chiou, K.R. and Liu, C.P. (2005). Efficacy and safety of statins in hypercholesterolemia with emphasis on lipoproteins. *Heart Vessels*. 20, 217-223.

Wu, Y., Wang, J., Scott, P.G. and Tredget, E.E. (2007). Bone marrow-derived stem cells in wound healing: a review. *Wound Repair Regen*. 15, S18-S26.

Xi, Y., Yu, M., Godoy, R., Hatch, G., Poitras, L. and Ekker, M. (2011). Transgenic zebrafish expressing green fluorescent protein in dopaminergic neurons of the ventral diencephalon. *Dev Dyn*. 240, 2539-2547.

Xie, J., Farage, E., Sugimoto, M. and Anand-Apte, B. (2010). A novel transgenic zebrafish model for blood-brain and blood-retinal barrier development. *BMC Dev. Biol*. 10, 76.

Ye, J., Rawson, R.B., Komuro, R., Chen, X., Davé, U.P., Prywes, R., Brown, M.S. and Goldstein, J.L. (2000). ER stress induces cleavage of membrane-bound ATF6 by the same proteases that process SREBPs. *Mol. Cell*. 6, 1355-1364.

Yi, P., Han, Z., Li, X. and Olson, E.N. (2006). The mevalonate pathway controls heart formation in Drosophila by isoprenylation of Ggamma1. *Science*. 313, 1301-1303.

Yoo, S. K.,Deng, Q.,Cavnar, P. J.,Wu, Y. I., Hahn, K. M. and Huttenlocher, A. (2010). Differential regulation of protrusion and polarity by PI3K during neutrophil motility in live zebrafish. *Dev. Cell*. 18, 226–236.

Yoruk, B., Gillers, B.S., Chi, N.C. and Scott, I.C. (2012) Ccm3 functions in a manner distinct from Ccm1 and Ccm2 in a zebrafish model of CCM vascular disease. *Dev. Biol*. 362, 121-131.

Yu, Y.L., Kumana, C.R., Lauder, I.J., Cheung, Y.K., Chan, F.L., Kou, M., Chang, C.M., Cheung, R.T. and Fong, K.Y. (1992). Treatment of acute cerebral hemorrhage with intravenous glycerol: a double-blind, placebo-controlled, randomized trial. *Stroke*. 23, 967–971.

Zelzer, E. and Shilo, B.Z. (2000). Cell fate choices in Drosophila tracheal morphogenesis. *Bioessays* 22, 219–226.

Zeng, L., Carter, A.D. and Childs, S.J. (2009). miR-145 directs intestinal maturation in zebrafish. *Proc. Natl. Acad. Sci. USA*. 106, 17793-17798.

Zhao, T., Zondervan-van der Linde, H., Severijnen, L.A., Oostra, B.A., Willemsen, R. and Bonifati, V. (2012). Dopaminergic neuronal loss and dopamine-dependent locomotor defects in Fbxo7-deficient zebrafish. *PLoS One*. 7, e48911.

Zhao, X., Sun, G., Zhang, J., Strong, R., Song, W., Gonzales, N., Grotta, J.C. and Aronowski , J. (2007). Hematoma resolution as a target for intracerebral hemorrhage treatment: role for peroxisome proliferator-activated receptor gamma in microglia/macrophages. *Ann. Neurol*. 61, 352-362.

Zhong, T.P., Rosenberg, M., Mohideen, M.A., Weinstein, B. and Fishman, M.C. (2010). gridlock, an HLH gene required for assembly of the aorta in zebrafish. *Science*. 287, 1820-1824.